TABLE OF CONTENTS

LIST OF FIGURES

LIST OF TABLES

CHAPTER 1

INTRODUCTION

CHAPTER 1

INTRODUCTION

1.1. Overview

Ice accretion normally occurs when rain falls from an elevated above-freezing air layer into a colder, sub-freezing air layer near the ground. This causes the liquid precipitation (or drizzle) to freeze on contact with surfaces whose temperature is at or below 0°C. Prolonged or heavy freezing rain events could result in several-centimeters-thick ice layers on vegetation, buildings, vehicles, power lines, towers, and other manmade structures. Open structures that are not properly designed to withstand increased ice and wind loads may fail. Excessive ice loads may lead to mechanical damage to power network equipment, especially ground wires, phase conductor and towers. In many cold climate regions, overhead transmission lines and substations are subjected to ice and snow accumulation due to different events such as freezing rain and drizzle, in-cloud icing, icing fog and wet snow [1 – 6]. In addition to mechanical issues, ice accretion may disrupt the electrical performance of power networks. The electrical problems are mostly related to the flashover of insulators under icing conditions, sometimes leading to power outages. Insulator flashovers and consequent power outages under the influence of contaminated ice or snow have been reported in North America [8 – 10], Europe [11, 12] and Asia [13, 14].

Outdoor insulation design with regard to pollution and icing performance is a critical factor for the reliability of power networks. The majority of transmission line failures are caused by environmental conditions such as lightning, pollution and/or ice. This is the reason why researchers around the world commenced serious field and laboratory investigations when the consequences of these phenomena came to light. Reports and observations have shown that the number of faults increases after ice accretion and during the melting phase following a rise in ice surface temperature.

A good deal of laboratory research has been conducted in this respect [e.g. 3, 15 – 17]. As a general rule, these reports and studies indicate that the thickness and type of ice, the level of contamination and the rise in air temperature have significant effects on the withstand voltage of ice-covered insulators. Researchers do agree that ice surface flashover is caused mainly by the combination of several phenomena, including [3, 18, 19 and 30]:

- Decrease in effective leakage distance caused by ice bridging;
- Presence of a pollution layer at the surface of the ice;
- Increase in surface conductivity caused by the presence of a water film resulting from various factors, such as wet ice accretion process, condensation, heating effect of leakage current, partial arcs, rise in air temperature, or sunshine;
- Formation of air gaps caused by the heating effect of partial arcs, a rise in air temperature, or ice shedding.

Ice accretion along energized insulators may not be uniform [29]. The parts of the insulator that are free of ice are referred to as air gaps. It is generally agreed that the

presence of a water film on the ice surface is necessary for flashover to occur. The high conductivity of the water film (caused by the rejection of impurities from the solid part toward the liquid portion of drops or droplets during solidification, and by pollution of the water and ice surface from corona discharge by-products [4, 19]) leads to voltage drops essentially across the air gaps. The initiation of corona discharges leading to the development of a partial discharge (violet arc) in these zones causes a substantial increase in leakage current. Under sufficient electrical stress, an arc will propagate along the ice surface, eventually forming a white arc. When the white arc reaches a certain length, flashover occurs along the entire length of the insulator.

1.2. Problem description

Up to now, research in this area has mainly focused on the experimental determination of the critical flashover voltage [8, 14 – 18], establishment of standard test methods [20] to evaluate the performance of insulator under icing conditions, and development of mathematical models simulating this phenomenon [21- 24]. Understanding the fundamental aspects of flashover on ice-covered insulators, that is, the mechanisms involved in the propagation of electrical arc on an ice surface, are important for accurate modeling and better design of insulators destined to cold climate regions.

Some work has been done on characterizing discharge over ice surfaces [19, 25], but there is still no complete physical understanding of the mechanisms and nature of these discharges. Although some theories have been proposed to describe the mechanisms

involved in the development of electric discharge along an ice-covered insulator surface [19, 26, 27], understanding of the related physical processes is still deficient. This situation is mostly related to the complexity arising from the presence of ice surface which interacts with arc initiation and propagation, contrary to air gap discharges. In the case of ice-covered insulators, the mechanisms are even more complex due to the presence of several interfaces (resulting from water film formation) e.g. ice-water, water-air, ice-insulator, and other parameters such as water conductivity. When covered with a water film the ice surface acts like an electrolyte. The resistance of the electrolyte around the arc root is reduced due to the Wien effect, e.g. influence of electric field on ion mobility, and heating [28]. The heating of the electrolyte is associated with the current flowing through it and the arc voltage drop. The diffusion of heat through the electrolyte and the arc root propagation velocity over its surface are further factors that render a rigorous analysis complicated. Most of these studies were performed on small physical ice surface models under conditions, which were sometimes different from those observed on ice-covered insulators in the field [25, 26]. Furthermore, these studies focused on the formation and propagation of the streamer only, in which there is no significant thermal ionization.

This study was motivated by the need to understand the physical processes involved in the flashover of ice-covered insulator, and was carried out under a grant from NSERC/Hydro-Quebec/UQAC Industrial Chair on Atmospheric Icing of Power Network Equipment (CIGELE) and Canada Research Chair on Engineering of Power Network Atmospheric Icing (INGIVRE) at Université du Québec à Chicoutimi.

1.3. Research objectives

The general objective of this research is to investigate the physical mechanisms involved in the propagation of electric arcs on the surface of ice.

The specific objectives are:

a) **Experimental observation of the characteristics of arcs propagating over an ice surface**

Measuring different parameters of arcs over an ice surface, such as channel radius and propagation velocities, and studying the propagation pattern and arc foot geometry are the specific objectives of this part of the study. These investigations may provide background information for understanding the entire flashover process phenomenon.

b) **Describing the formation and propagation mechanisms of "violet arcs" and "white arcs" on the surface of ice**

The aim of this section is to describe the mechanisms and conditions governing the formation of violet arcs, and the transition from violet arc to white arc. Another important aspect would be identifying the dominant ionization process that could explain the velocity of propagation and the temperature of arc at this stage.

c) **The effect of polarity on the propagation of discharges**

Significant differences in behavior between positive and negative arcs during discharge propagation have been observed. The root structure, current profile, propagation

pattern and velocity should be studied with the aim of proposing mechanisms enabling description of the differences between positive and negative polarities.

d) **Investigating the effects of various macroscopic parameters (e.g. applied water conductivity, water film thickness, and humidity) on the different stages of flashover**

Several factors may influence arc propagation. According to the previous researches and initial observations, water film conductivity and thickness, and relative air humidity were found to have the greatest influence, and hence were selected for study as experimental parameters.

e) **Describing the final jump (last stage in the flashover process) and associated mechanisms**

At a critical arc length the speed of arc propagation increases. This suggests a change in the propagation mechanism at that stage. Measuring the speed of arc, determining its critical length, and suggesting a theory that could describe the ionization process and propagation speed are the specific objectives for this stage.

It should be stated that this research focuses on the propagation of dc arcs. However, where possible, experiments using ac voltage were conducted to observe the phenomenon. But, the effect of arc decays and re-ignitions as ac voltage goes through zero is not in the scope of this study (which was the main reason for concentration on dc

voltages). Moreover, this study is limited to the propagation of a single arc in the presence of only one air gap.

1.4. Methodology

The present investigation was motivated by the need to understand the physical processes involved in flashover of ice-covered insulators. One of the main causes for the currently limited fundamental insight in the physics of this phenomenon is that only a few diagnostics are applicable. This is due to the complex discharge geometry, fast-occurring phenomena, and limitation of presence of high voltage. It became clear at the beginning that, because of the complex nature of the problem, explaining the flashover process physically is a demanding task. The best approach considered was building simplified models so that the principal physical mechanisms could be determined and studied in a controlled manner.

To be able to observe the phenomenon with optical recording devices, a flat ice surface was selected. An air gap was created between the high voltage electrode and ice surface. Optical parameters were observed using one or a combination of the following equipment: ultra-high-speed video camera, image intensifier, and PMT. Voltage and current measurements were also made and synchronized with optical recordings through a data acquisition system (DAQ). Generally, the following analyses were carried out on experimental results:

A. Propagation velocity measurement

At different stages of propagation, discharge velocity was measured from the video recording calibrated to give real dimensional values of distances.

B. Current profile analysis

Arc current, either measured from a shunt resistance or current monitoring probe, were recorded through the DAQ. Analysis of this current consists in detecting current jumps and variations in the slopes of current-time profiles.

C. Propagation pattern analysis

In this time-consuming part, the pattern of arc propagation was attentively tracked from the video recording images. The presence of discharges, shape of arc foot and arc channel radius were also observed.

D. Arc luminosity

The variations in discharge luminosity during propagation and at different locations along the arc channel and foot were analyzed from the PMT output, or simply from the comparison of brightness in the video images.

The above analyses were also accomplished by studying the effects of voltage polarity, setup orientation, water film thickness and conductivity, and relative humidity.

The above-described experimental method was designed to obtain the required information about the entire flashover phenomenon. This permits us to propose hypotheses that could explain the observations and give fundamental insight into the mechanisms of arc propagation over ice surfaces.

1.5. Statement of originality and contribution to knowledge

To the best of our knowledge, no fundamental work has yet been done on the process of arc propagation over a one-meter ice surface. Previous researches [19, 25, 26] were conducted on small setups (a few centimeters) that are not representative of full-scale insulators and in which thermal ionization does not play a significant part. Those investigations concentrated on the initiation and propagation of streamers. Moreover, the flashover phenomenon has been observed with streak and framing cameras, which only captures visible light. Employing a photomultiplier tube (PMT), which operates in the 185 nm to 900 nm range, only produces an electrical output signal corresponding to the intensity of light. It could not be used to observe the whole arc channel with spatial resolution (as opposed to video cameras).

This study is the first to use an ultra-high-speed camera (above 20,000 fps and up to 675,000 fps) on a large-scale ice surface. Moreover, employing an image intensifier along with an ultraviolet (UV) band-pass filter enabled us to observe UV activity during the discharge propagation.

Besides the originality of employing high-technology equipment, this work is the first research to emphasize close-up observations of arc root and channel, as well as the propagation pattern of discharge. Based on the new findings, this fundamental work proposes physical mechanisms contributing to arc propagation along an ice surface and involving forces and ionization activities.

1.6. Thesis outline

This dissertation is structured as follows:

Chapter one, herein, provides general information about the problems resulting from ice accretion on power network equipment. It defines general processes occurring during the flashover of ice-covered insulators, and explains the necessity and motivation for the present research. The general and specific objectives are clarified and the methodology selected to achieve the objectives is explained.

In Chapter 2, a survey of related literature will be presented. Distinct results on the mechanisms of discharge propagation over an electrolyte and ice surface will be reviewed.

Chapter 3 introduces the available equipments and describes the experimental procedure for performing the experiments in details.

Chapters 4 and 5 present the experimental results. Chapter 4 describes the general findings from analyzing the optical and electrical studies. Chapter 5 deals specifically with the effects of water film thickness and conductivity, and relative humidity.

Chapter 6 discusses arc propagation mechanism based on the experimental results presented in the two preceding chapters.

The general conclusions derived from the results and discussions covered in the previous chapters will be presented in the seventh chapter of this thesis. It will also include the areas of research that we recommend exploring for continuity and progress following the research described herein.

CHAPTER 2

LITERATURE REVIEW

CHAPTER 2

LITERATURE REVIEW

2.1. Introduction

At temperatures close to zero, when a thin water film forms on it, an ice surface acts like an electrolyte [31, 32 and 33]. This fact is the motivation to firstly start with reviewing the literature in the more studied subject of arc propagation along an electrolyte surface. Most of these studies were aimed at understanding contamination flashover using simple physical models. Through different approaches, several theories have been proposed to try and explain the researcher's observations. The first part of this chapter reviews the most important results obtained from these investigations. In the second section, research works dealing with discharge propagation over an ice surface are presented. Due to the importance of water molecules in discharge propagation, the last section of this chapter will focus on the effect of humidity on discharge propagation.

2.2. Mechanisms of discharge propagation over an electrolyte surface

The pioneering work of Hampton [34] can be considered as the first attempt to describe flashover propagation, although his work was based on the quantitative theory developed by Obenaus in 1958 [35], followed by Neumarker in 1959 [36]. Hampton [34] showed that as surge current heats up the pollution layer, its resistance falls in the normal manner of an electrolyte. Further heating boils off water in the layer, but the overall resistance does not change markedly until a saturated electrolyte has been formed, since a decrease in the thickness of electrolyte is offset by an increase in conductivity. When the electrolyte is saturated, further loss of water results in a rapid increase in resistance. He noted that the growth of a discharge on a polluted surface usually took several voltage cycles to build up into flashover, and that this growth was markedly affected by the current going through zero at each half cycle. Hence, with the aim of reducing the number of variables affecting discharge propagation, he used a direct-current supply for his work. He also confined his investigation to the behavior of an arc discharge rooted on the surface of a column of electrolyte having a constant resistance per unit length to overcome the complexities induced by the varying resistance of a wet polluted layer. These requirements were met by using as a resistance a jet of water flowing from a nozzle. A uniform flow of water was ensured by a constant-head tank and the resistivity of the water was adjusted by mixing in a small portion of saturated salt solution. The resistance of the water column was maintained at the required value by injecting salt solution at a controlled rate into the water flowing to the nozzle. Hampton concluded that if the voltage gradient along the discharge

falls below the gradient along the resistive column, flashover will occur. He also hypothesized that when an arc propagates along the surface of a water column, the arc burns in an atmosphere of steam instead of air. This statement was based on the measurement of the voltage gradient in the column of an arc burning in atmosphere of steam as a function of current, compared to a similar arc burning in air.

Wilkins and Al-Baghdadi [37] suggested that the arc moves to a position where the rate of energy expenditure is a maximum. Furthermore, a mechanism for arc propagation entitled "discharge elongation by ionization and successive root formation" was proposed [37]. The theory suggests that extension is produced by new ionization paths created at the tip of the discharge (Figure 1). They also showed that the voltage gradient in a discharge along a strip of electrolyte is close to the value for a static discharge in air at the same current. They also verified their proposed mechanism of arc propagation by measuring the transient voltage distribution along the electrolyte strip during flashover. They noticed that even after the discharge tip is well beyond a particular probe, there exists a potential difference between this probe and the first probe. This indicates that there is current flowing in the pollution layer behind the discharge root, supporting the theory of elongation by ionization and successive root formation. The current flows into the electrolyte ahead of the discharge tip and also behind the tip, the latter current dying away after the tip has passed a particular point. This was in contrast to what should be expected from the previous theories, which assume that the current enters the electrolyte via a discrete discharge root.

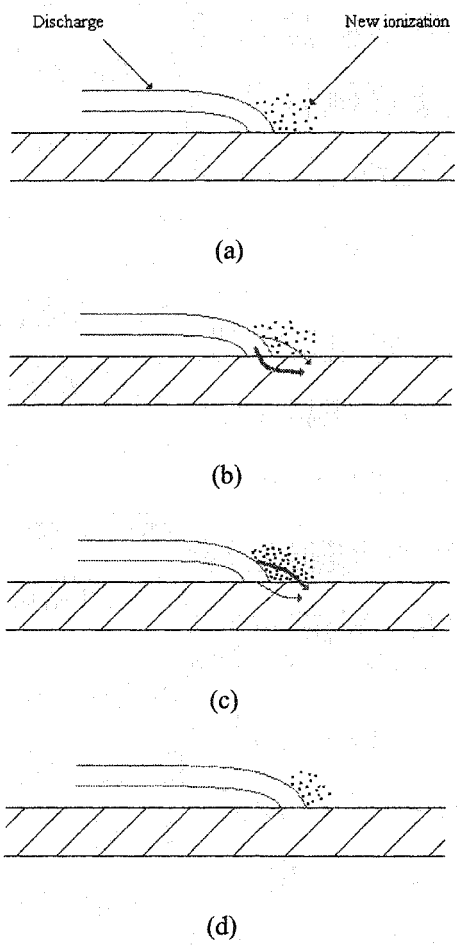

Figure 2.1. Proposed mechanism of elongation [37]:
(a) Ionization in front of discharge tip

(b) Possible current paths

(c) Current distribution after increasing the ionization

(d) Elongation the discharge to the new location

Using high-speed photography, Claverie [43] stated that the progression of arc on polluted insulators is surely due to thermal phenomena. In the meantime, Jolly [38] published a paper in which the different possible forces, including electrostatic attraction, electromagnetic force, thermal buoyancy force and steam pressure, which may be the cause of "pulling" the discharge across the surface, were evaluated. He concluded that,

contamination flashover is essentially an electrical breakdown process caused by the field concentration at the discharge tip. The current flow lines in the contaminant layer converge at the discharge root, producing a high local electric field. If this local field is high enough, the air in front of the discharge tip will be ionized, extending the discharge. Ionization by electron impact may be aided by thermal and photoelectric ionization processes. His main reason for this conclusion was the velocities of 3000-5000 m/s, which could be the result of the drifts of the electrons in an electric field [38]; but he also mentioned that when flashover occurs slowly, over several half cycles, thermal and electrostatic forces might also be involved.

Rahal and Huraux [39] stated two requirements for propagation of a discharge at the surface of an electrolyte. First, the electrical condition (applied voltage and discharge current) should be satisfied to sustain the discharge, and second, a physical mechanism that pulls the discharge and leads to flashover. They showed experimentally that, the physical mechanism is electrostatic force acting on the discharge column.

Sudarshan and Dougal [40] suggested that the major difference between breakdown near or at an insulator surface with breakdown in air must eventually be traced to a modification in the rate coefficient, which describes the ionization growth. They also stated that charge accumulation on an insulator surface modifies the electric field distribution in the gap, which in turn influences the initiation and propagation of a discharge.

Li [41] showed that the electric field stress at the arc root is too low to cause air breakdown. He suggested that flashover is caused by the high temperature ionization of salt

in the arc column and completed by the migration of positive and negative ions under the effects of the electric field.

Allen [42] demonstrated that the ionization close to the insulator is enhanced by electron emission from the surface by photons from the avalanches in the gas. The relatively high propagation velocity of streamers along an insulating surface rather than in air supports his arguments. However, he stated that the dependence of the streamer propagation velocity on the material suggests that this mechanism is a function of the insulating material nature [42].

Matsuo et al [44] used an electrolyte solution to simulate the surface of wet polluted insulators under impulse voltage. They found that the propagation velocity of discharge increases with the of photoemission intensity from the tip of the local discharge. They mentioned that the influence of air pressure and the applied voltage waveform on the velocity is very small.

Boudjella et al [46] preformed experiments using a cell of two polluted water channels. They observed that putting a metallic sphere in one channel influences the discharge propagation direction. They deduced that in addition to the gradient of potential and current in pollution, the electric field strength around the discharge tip has an effect on the discharge development direction.

Bruggeman et al [45] studied experimentally electrical breakdown between a metal pin and a water-surface electrode. They observed a glow-to-spark transition when the pin is cathode, and when the metal pin is anode, a streamer-to-spark like transition occurred.

Another interpretation for the propagation mechanism on an electrolyte surface was proposed by Mercure et al [47]. They showed that current gradient (dJ/dt) in the arc is much larger on the forward side of the arc root, in the direction of propagation of the arc, than in the opposite direction. A large temperature gradient is associated with this large gradient of current; therefore, as the heat flux depends on the temperature gradient, forward heat conduction could be expected. It will results in an expansion in the forward direction of the boundary of the electrically conducting plasma.

The electric field required for sustained positive corona streamer propagation shows a strong linear dependence on the water vapor partial pressure [48]. Yamashita et al [49] performed experiments using several photomultipliers to observe the propagation of local discharge on an electrolyte surface. They showed that the velocity of the local discharge is determined by the intensity of the photo-emission, and is independent of the length of the water channel and applied voltage when the resistance per unit length of water channel is the same.

Matsumoto et al [50] conducted streak photography and spectroscopic measurement for a partial arc on a contaminated surface containing NaCl. They measured the arc diameter as a function of current. It was also revealed that the light emitted from the arc contains strong Na emissions.

Employing Schlieren photography, Boylett and Maclean [51] revealed a complex discharge structure and the presence of a strong liquid wave disturbance accompanying discharge propagation across the surface of an electrolyte. They also showed that the speed of propagation of the discharges increases with voltage and with distance travelled, and that

this speed is influenced by resistive gradients in the electrolyte. They found that the shape and speed of discharge are strongly polarity dependent. For a given starting condition, the discharge is observed to propagate ten times faster under positive voltage.

In another work [52], Jolly and Poole studied experimentally contamination flashover under dc applied voltage. They found that polarity influenced the flashover voltage, with flashover occurring more readily for negative polarity. They stated that this difference is attributed to cathode spot phenomena and electrochemical effects.

Rumeli [53] noticed differences in dc flashover of a water jet regarding polarity. He mentioned that this difference could be explained by the dependency of the discharge-voltage-gradient-current characteristic upon polarity.

Flazi et al [54] commented on Hampton's criterion and Wilkins' criterion using multidirectional and circular-sector setups. They proposed that flashover is possible if the electric field distribution along the leakage distance is sufficient for discharge evolution by progressive breakdown between the discharge and the electrolyte.

The effect of thermal forces on the propagation of the arc was proposed by [55]. They noted a difference in the propagation pattern in three cases of horizontal, vertical and VEE string orientation.

Johnson et al [56] reported similar effects. Using a high-speed camera with 1000 fps recording speed, they observed that the surge-to-flashover transition mechanism of the horizontal strings was quite different from that of the vertical strings. As the skirt side arcs reached the upper edge of the insulator, they did not immediately flash over to the caps, but instead extended into the air for several inches and then looped back to terminate on the top

surface of the insulator at various points. In some cases these long arcs would withdraw to their initial position for a few cycles and then develop into another arc terminating on the top surface. With sufficient voltage the arcs eventually terminated on the caps, completing the flashover circuit.

Deviations from Ohm's law in electrolytic conductors were discovered by Wien [57]; for liquid electrolytes. He showed that the conductance increases with the intensity of the field. This increase has been shown in general to arise from two different effects: e.g., a destruction of the "ionic atmosphere" and a modification of the dissociation kinetics [58]. In weak electrolytes the latter effect is rather more important; a theory which has been developed by Onsager. [59]

The effect of an external electric field on the electrolytic dissociation was computed kinetically from the equations for Brownian motion in the combined Coulomb and external fields [59]. The result was an increase of the dissociation constant, which is proportional to the absolute value of the field intensity, and inversely proportional to the dielectric constant.

Cserfalvi and Mezei [60] tried to measure the cathode drop potential originating from metal salts in the electrolyte cathode as a function of different discharge parameters. The observed dependence of the cathode drop on pH was explained only as being due to the self-sustaining discharge processes taking place at the plasma-solution interface. In a steady state of glow discharge, the bombardment of positive ions accelerated by the electric field of the cathode dark space produces cathode sputtering and secondary electron emissions from the cathode. These electrons, gaining an available kinetic energy from the

field, are able to excite and ionize the neutral atoms. During these ionization collisions, positive ions and new electrons are generated and, finally, multiplication of charge carriers occurs in the cathode dark space. Supposing that for each of the (K-1) electrons formed in the plasma, γ electrons are released at the cathode by various mechanisms, for the discharge to be self-sustaining the usual condition must be satisfied (if $K >> 1$):

$$K\gamma = 1$$

where K is the multiplication factor in the gas phase, and γ is the secondary electron emission coefficient of the cathode. Since in electrolyte-cathode discharge the acidification of the solution changes the cathode material, the observed dependence of the cathode drop on the pH can be attributed to a change in the value of γ. If acidification causes an increase of γ, this can lead to a decrease of the cathode fall through a higher output of charge multiplication. The cathode fall and γ are interdependent. [60]

Emissions from an atmospheric pressure glow discharge, with alkali metal chloride solution as the cathode, were studied by Maksimov et al [61]. The relation between the discharge emission and the cathode sputtering process leading to the transfer of solution components to the plasma zone was also analyzed. They concluded that plasma radiation from an electrolyte cathode glow discharge is closely related to cathode sputtering, the process of transferring solution components to the plasma. This process not only supplies the gas phase with water and solutes, it also initiates redox processes affecting the properties of plasma and its emission spectrum.

As suggested by Park et al [62], it is metal cations that are transferred to the gas phase from solution; in the dark cathode space, they undergo three-body recombination

with electrons followed by the electron impact excitation of the atoms produced. In view of the fact that the potential drop at an electrolyte cathode can be as great as a few hundred volts [63], the transfer of positive ions from the solution to the plasma zone seems to be improbable. At the same time, it is evident that the appearance of atoms in the plasma zone is due to cathode sputtering. By analogy with classical cathode sputtering, it should be expected that the components of solution, primarily neutral species, will appear in the gas phase.

The spectral lines arise mainly from the elements dissolved originally (Ca, Na, and K) and spiked (Cu, Pb) in tap water and can be attributed to the effect of cathode sputtering during discharge. The emission mechanism has been extensively investigated [60, 64]. When the discharge is operating, the positive metal ions are released from the electrolyte cathode surface due to cathode sputtering. These positive metal ions cannot pass through the negative space charge near the cathode dark space, but escape from the cathode surface and diffuse into the negative glow only if they are recombining (becoming neutral) in the cathode dark space. The recombination of the positive metal ions takes place via a three-body collision involving one positive metal ion and two electrons. The neutral metal atoms produced in this way diffuse into the negative glow, where they are excited by electron collisions [62].

2.3. Discharge propagation on an ice surface

Khalifa and Morris [15] explained the flashover of ice-covered insulators based on the cumulative heating effects of leakage currents. Due to the non-uniform conductance of the leakage paths in the ice, the temperature rises in some localized zones where the current density is highest. The rise in temperature at such zones increases the ice conductivity and thus further increases the current density and the rate of heat development.

To the best of our knowledge, the study of basic phenomena occurring during the flashover of ice-covered insulators was pioneered by Farzaneh et al [17, 18] while studying the different parameters affecting the performance of insulators under icing conditions. These authors distinguished the different stages, such as the appearance of water film on the ice surface, the initiation of corona discharges, development of local arcs, increase of leakage current, and finally flashover. These processes appear in a single arc at a speed sufficiently slow to allow detailed observation, unlike contamination flashover, which tends to have multiple dry band and arc development paths. Most of the other studies were carried out to determine the withstand voltages, critical conditions for arc propagation, and modeling of arc on ice surfaces. They investigated several factors and parameters related to the icing processes and environmental conditions influencing the flashover voltage of ice-covered insulators. They showed that wet-grown ice deposits are more dangerous than ice grown in a dry regime. They found that the maximum withstand voltage of one to four ice-covered insulators varied linearly as a function of dry-arcing distance. They also reported that, as the wind velocity increased, the ice distribution became less uniform, leakage

distance increased, and the maximum withstand voltage gradient increased as well. For a post-insulator, they showed that maximum withstand voltage gradient decreases with an increase of ice thickness up to three cm and then remains constant.

Farzaneh and Drapeau [17] revealed that the gradient of maximum withstand voltage of the tested post-insulator decreases with an increase in spray water conductivity, σ, up to value of 80 μS/cm. At relatively high values of water conductivity, because of high corona discharge activity during the icing period, there was almost no ice deposited on the top shed of the insulator (HV side).

Farzaneh et al [19] carried out several experiments using high-speed streak photography to observe streamer propagation on an ice surface. They measured the streamer inception voltage and propagation velocity considering parameters such as freezing water conductivity and HV electrode radius. They concluded that in the presence of an ice surface, discharge is initiated in fields with lower intensity than in air alone, and also that streamers propagate with higher velocities than in air [19]. They suggested enhanced electric fields caused by the permittivity of the surface, accumulated charges on the ice surface, and release of electrons from the surface due to photo-ionization as the possible mechanisms affecting streamer propagation on ice surface, compared to air. These investigations were performed using ordinary ice and small inter-electrode distances, which are not representative of actual outdoor insulators covered with atmospheric ice. Also, these studies focused on streamer formation and propagation only, in which thermal ionization is not significant.

Contrary to mechanical effects, the physics, thermodynamics and electrochemistry aspects of the flashover process on ice-covered insulators is a complex topic, and some aspects of the phenomenon are not yet fully understood. Some tentative explanations have been reported in the scientific literature in this field [3, 18]. Basic studies are essential to the elucidation of the mechanisms involved in the initiation of discharges, and their transition to arc propagation.

However, researchers do agree that ice surface flashover is caused mainly by the combination of several phenomena, including [3, 18 and 19]:

- Decrease in "effective" leakage distance caused by ice bridging;
- Presence of a pollution layer on the surface of the ice layer;
- Increase in surface conductivity caused by the presence of a water film resulting from various factors, such as wet ice accretion process, condensation, heating effect of leakage current, partial arcs, rise in air temperature and/or sunshine;
- Formation of air gaps caused by the heating effect of partial arcs, a rise in air temperature and/or ice shedding.

Ice accretion along energized insulators may not be uniform. The parts of the insulator that are free of ice are referred to as air gaps. It is generally agreed that the presence of a water film on the ice surface is necessary for flashover to occur. The high conductivity of the water film (caused by the rejection of impurities from the solid part toward the liquid portion of drops or droplets during solidification, and by pollution of the water and ice surface from the by-products of corona discharge [4, 19]) leads to voltage

drops essentially across the air gaps. The initiation of corona discharges leading to the development of a partial discharge (violet arc) in these zones causes a substantial increase in leakage current. Under sufficient electrical stress, an arc will propagate along the ice surface, eventually forming a white arc. When the white arc reaches a critical length, the whole insulator suddenly undergoes complete flashover.

As the discharge in the air gap is a rather well-understood phenomenon, some authors have tried to compare insulating material surface discharge characteristics to those in air. The presence of an insulating surface has two main effects on corona and breakdown: a) it causes a distortion of the electric field, which lowers the discharge inception voltage and causes the discharge trajectory to become attached to the insulator; (b) it modifies the effective ionization and attachment rates which affect the propagation characteristics of the discharge (propagation speed, charge, current, etc.)[19].

In the case of ice, there are major differences compared to the other surfaces: (a) the bi-state conductivity of ice surface, and (b) the presence of a liquid or liquid-like film at the air/ice interface at subfreezing temperatures [19].

Concerning the performance of ice-covered insulators under dc voltage, several investigations have been conducted on:

- The effects of atmospheric pressure and applied water conductivity on the dc flashover voltage [65, 66];
- The influence of ambient temperature and applied voltage type [67];
- The influence of insulator length on flashover voltage[68]; and
- The effect of pollution severity [69].

Some experimental studies were also performed to measure voltage drops and arc characteristics (voltage gradient versus current, namely E-I curve) on ice surfaces [70]. These studies provided substantial information used in the development of mathematical models [24, 71 and 72].

However, few publications are available on the fundamental physical phenomena occurring inside a discharge channel propagating over an ice surface [19, 26, 27 and 73]. Most of these studies were performed on small physical ice surface models under experimental conditions which were sometimes different from those observed on ice-covered insulators.

2.4. Effect of voltage polarity

Regarding the effect of voltage polarity on discharge propagation, experimental research resulted in finding the differences in arc constants and voltage-current characteristics for positive and negative cases [71]:

$E= 84.6I^{-0.772}$ for negative arcs

$E= 208.9I^{-0.449}$ for positive arcs

The other difference was found to be the electrode voltage drop value for positive and negative polarities. For negative and positive arcs, the measured values of electrode voltage drop are 526 V and 799 V, respectively [71].

2.5. The effect of humidity

It has been well established that the flashover voltages of air gaps subjected to positive lightning impulse increase linearly with humidity at a rate of 1 % / (g/m^3) over a wide range of humidity [74]. Kuffel [75] first noted that the enhanced electrical behavior of air by water vapor is comparable to electro-negative gases, and is qualitatively due to the loss of free electrons by attachment and absorption of photons by water vapor.

Air humidity could affect the flashover process in two ways [76]: first, it may influence the fundamental physical process, which can be referred to as the direct effect of humidity. Second, it may influence the field distribution, thus influencing the outcome of flashover. This can be referred to as the indirect effect. The flashover voltage of air gaps increases linearly with increasing humidity due to the direct effect of humidity. When a dielectric surface is involved, an additional change in flashover voltage caused by the indirect humidity effect would be superimposed on the linear component [76].

The electric field necessary for stable streamer propagation increases linearly with humidity, from about 4 kV/cm in dry air to about 5.5 kV/cm at 20 g/m^3 [77]. The size of corona streamers is also reduced as humidity increases [77].

The leader gradient is inversely proportional to the square root of the charge per unit length, which decreases with increasing humidity [77]. In fact, both streamer and leader gradient increase with humidity; leading to an increase in the breakdown voltage. The influence of humidity on the breakdown parameters is a consequence of a modification in the leader advancement and sudden restrikes, enhancing the overall leader velocity [78].

It is also believed that humidity affects the flashover voltage in the presence of a tangential dielectric by creating a thin layer of water on the surface, which is more easily ionized. The higher the humidity, the thicker the layer on the surface and the easier it is for field-emitted electrons to produce secondary electrons [79].

2.6. Conclusions

During the arc propagation over an electrolyte surface, the following mechanisms were found to have a greater influence in the related literature: electrical field concentration, thermal buoyancy, heat conduction, photo ionization, charge accumulation on the surface and secondary electron emission.

Previous research on initiation and propagation of discharge over an ice surface provided valuable information on the mechanisms of streamer propagation in the presence of an ice surface. The necessary electric field for streamer initiation and the velocity of propagation were calculated and hypotheses were proposed to explain the observations. However, these studies were performed on small physical ice surface models and were limited to streamer formation and propagation, in which thermal ionization is not significant.

CHAPTER 3

FACILITIES AND PROCEDURES

CHAPTER 3

FACILITIES AND PROCEDURES

3.1. Introduction

The proposed research was carried out using the following methods that were chosen based on previous models (different geometries of ice samples: triangular [83- 85], cylindrical [24, 82], and rod-rod or rod-plane system in a small Plexiglas mould [19, 67, 86 and 87]), which have been demonstrated to be effective and successful in CIGELE's research laboratory.

In order to achieve the objectives, simultaneous optical, electrical and environmental condition measurements were performed. However, the data from electrical and optical measurement categories were synchronized through a data acquisition (DAQ) system.

Discharge current and applied voltage are the important parameters in the electrical measurement categories. Leakage current measurements, which can provide more insight on the initiation and propagation of discharge, were done using Pearson coil and/or shunt resistance via the DAQ system. The monitored environmental conditions were ambient humidity and temperature, and thickness of water film on the ice surface.

Optical measurements were performed using different instruments, which will be introduced in Section 3.2. These measurements aimed to observe and determine ionization activity in visible and ultraviolet regions, the shape of arc root, propagation velocity, discharge channel diameter, and propagation pattern. With its high rate of frames per second, the high-speed camera enables us to observe different stages of arc propagation on the ice surface. These data were used to develop and validate the proposed theories.

Because discharge paths are usually randomly distributed along the ice surface and are unlikely to develop within camera range, care has to be taken. To meet the proposed objectives, a simple time-saving test setup was chosen, in which the arc starts at one end and the path of arc propagation can be easily recorded with camera. Discharge luminosity could be investigated by PMT. Simultaneously, the leakage current and applied voltage were monitored.

3.2. Test facilities

Experimentally, such fast physical processes require specialized and sophisticated instrumentation. The equipment and instruments used for the experiments of this research are listed hereafter.

3.2.1. High-voltage equipment

High voltage was supplied by a 240 kVA single-phase test voltage transformer, with a 120 kV short-circuit impedance of 5%. The output voltage is adjusted from 0 to 120 kV through a regulator, consisting of an SCR control type feedback thyristor with a dynamic

voltage drop of the source below 5% when the load current is 0.5 A. Voltage is increased either manually or automatically at a fairly constant rate of about 3.9 kV/s.

Whenever needed DC voltage is supplied using the above transformer connected to a rectifier module, comprising a half-wave rectifier and a smoothing capacitor (15.2 μF). Positive and negative DC voltages are obtained by inverting the diode direction in the rectifier. Using the automatic control, DC voltage increases at a constant rate of about 5.5 kV/s. A high voltage SF_6 bushing conducts the applied voltage through the walls of the climate chamber.

3.2.2. Current and voltage measurement devices

In AC experiments, the applied voltage was measured using a capacitive voltage divider. Current measurements were carried out using a current transformer (Pearson™ current monitor: Model 110) with sensitivity of 0.1 V/A and usable rise time of 20 ns.

In DC experiments, voltage measurements were performed using a resistive voltage divider. The leakage current was measured using a 10 Ω shunt resistance between the ground electrode of the test setup and ground terminal of the HV system.

3.2.3. Climate chamber

The climate chamber is a uniquely designed 6 m (W) × 6 m (L) × 4 m (H) room equipped with an HV SF_6 composite bushing. The temperature inside the room can be adjusted to values as low as -30 ±0.2° C.

3.2.4. High-speed camera

The FASTCAM SA1 (Photron Co.) high speed camera has a recording speed of 5400 full frames per second (fps) with a 1024 x 1024 pixel resolution, and maximum recording rate of 675,000 fps at reduced resolution. It is controlled either by a PC through the Gigabit Ethernet port, or by an RS-422 remote control keypad with built-in 5" LCD monitor for complete camera set-up and operation.

The Photron FASTCAM Viewer (PFV) is a Windows-based application program that makes it possible to control Photron's FASTCAM series high-speed video cameras from a PC, including operations such as camera setup, framing and downloading. It also enables the user to select the playback rate, step through video one frame at a time, and selectively save video sequences in a variety of compressed and uncompressed formats.

3.2.5. Image intensifier

The UV camera intensifier amplifies the light in an extended spectral range (from UV to NIR) for display on the phosphor screen. The available UV Camera Intensifier (Invisible® Vision UVi, model: 1850-10-S20-P46) has a wavelength response range between 200-800 nm with a decay of 1us and can be gated as low as 10 ns. It is equipped with a 105mm/F4.5 UV lens. This intensifier is optimized for use with high-speed video cameras.

The UVi can be programmed through its integral menu driven LCD display/control panel or via its USB interface and software synchronized with an external TTL or video signal, offering multiple, digitally programmed gain, delays and exposures (10 ns in 10 ns

steps) at input trigger rates greater than 100,000 per second and up to 20,000,000 per second in burst mode.

When needed, a UV band pass filter can be used in front of the intensifier to block all the light except ultraviolet region. The available filter is a U-340 2" square band pass filter from Edmund Optics with a center wavelength of 340 nm and Full Width-Half Max FWHM (nm) of 85 nm.

3.2.6. PMT

The CIGELE laboratory has a photomultiplier tube (R928P from Hamamatsu Photonics) with a wavelength range of 185-900 nm and peak sensitivity of 400 nm. It is used to detect ionization activity within the above wavelength range. Furthermore, while operating in photon-counting mode, the electrical output signal may be used to assess the intensity of photoemission from the discharge channel.

3.2.7. Corona detection camera

Corocam 504 is a video camera with a combined output for ultraviolet and visible light. The spectrum range of the UV channel is between 240 and 280 nm, with a 30 Hz standard video frame rate.

3.2.8. Data acquisition system

To establish synchronization between electrical and optical measurements and also enable data storage with a high sampling rate, the following data acquisition (DAQ) system was used. The test signals were connected to a measuring set through a conditioning box

providing protection and insulation. A DAQ card from National Instruments (PCI-6035E, 200 kS/s, 16-Bit, 16-Analog-Input Multifunction DAQ) and LabVIEW software as a user-interface are used to acquire and store the signals from different devices.

3.3. Procedure

Because discharge inception at the HV electrode is usually randomly distributed and unlikely to develop at a specific predetermined point, measures had to be taken to ensure discharge inception recording. The rod-plane arrangement constitutes one of the basic configurations for investigating discharge inception in high-voltage studies [80, 81]. The rod simulates the tip of an icicle or a high-voltage conductor, from which the discharge initiates. A distance between the rod electrode and the ice surface simulates the "air gap" formed during ice accumulation on energized insulators. Real line or post-insulators covered with ice or a cylindrical test setup, which could be used to simulate the real case [82], are not suitable choices for this study due to the random propagation pattern of discharges, which may not be in the viewing field of observation devices. A simplified physical geometry was chosen to perform the experiments. A flat plane ice surface ensures the propagation of discharge in two dimensions, in front of an optical observation device (e.g. PMT, cameras...).

Figure 3.1 shows a schematic diagram of the physical setup and equipment.

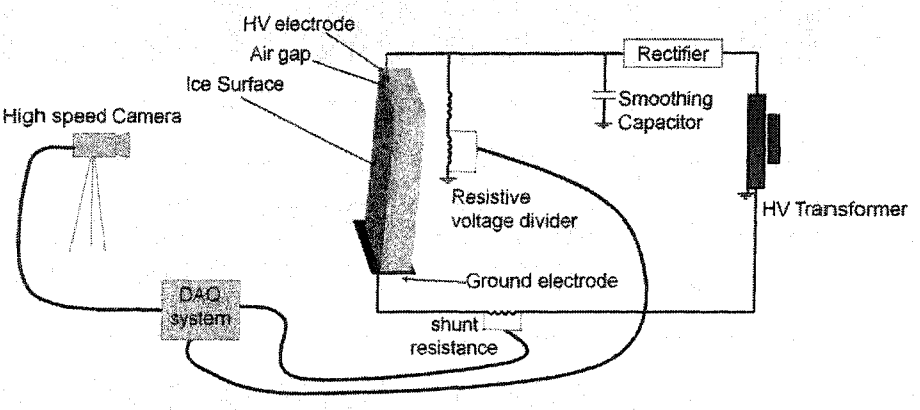

Figure 3.1. A schematic diagram of physical setup and equipment.

3.3.1. Physical test setup preparation

A simplified physical geometry was chosen for the experiments. Two types of moulds were used depending on whether it is necessary to remove the ice or not. The first one was a rectangular mould made from Plexiglas and the second was a plastic-covered cardboard box to avoid water infiltration and from which the ice could be removed.

The overall dimensions of the moulds were different, depending on the type of experiment they were used for. However, wherever not specified, the mould dimensions were 140 cm (L) × 15 cm (W) × 5 cm (D).

Ice making proceeded as follows: First, the mould was filled up in several stages with distilled water and put into a cold chamber to freeze completely. Then a narrow band about 5 cm wide and 3 cm deep was made along the ice. This strip was filled up in 3 stages with salty water to achieve a predetermined level of conductivity. The strip simulates a long icicle that bridges the insulator sheds. After each stage it is returned to the cold chamber to let the layer freeze. Finally, an air gap of about 6 cm was made at one end, and the ground

electrode is placed at the other end (Figure 3.2). Voltage was then applied to this setup, which guides the arc to propagate along the central area of higher conductivity. The HV electrode was a stainless-steel hemisphere 2 cm in diameter. The ground electrode was a metallic plate placed at the other end of the specimen, as shown in Figure 3.2.

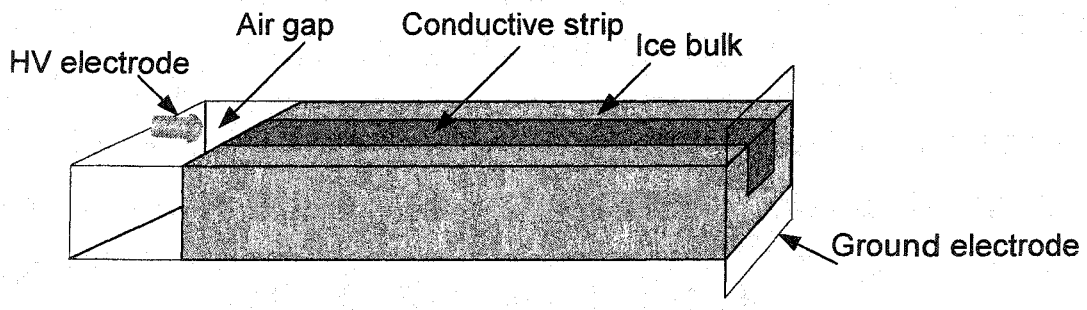

Figure 3.2. Ice geometry (model *a*)

Another test setup, which will be referred as model (b), was also used. In this configuration, instead of a conductive strip, a conductive layer was formed (Figure 3.3). The ice mass was built up in several steps with de-ionized water to achieve the flattest surface possible. This ice serves to protect the Plexiglas mould from being heated by discharge activity, and also as a base for the conductive layer, as the final goal is to cause an arc to propagate along the surface of the conductive layer. Then, a thin 3 cm conductive ice layer was formed on top of the ice. This layer was constructed in three steps with freezing water of predetermined conductivity, adjusted by adding sodium chloride (NaCl) to the de-ionized water. In between steps, the model was returned to the cold chamber to let the layer freeze. Ice construction using model (b) is simpler and faster than with model (a). The inconvenience is that the arc may come in contact with the Plexiglas mould and

damage it. However, whenever if the ice is to be removed from the mould, this is not an issue.

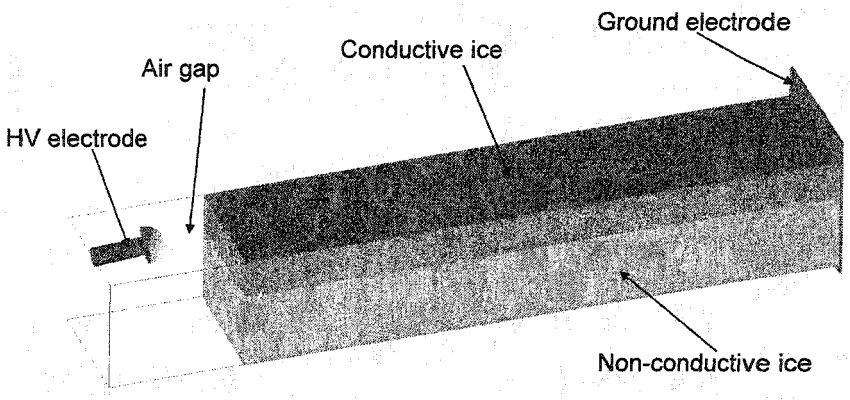

Figure 3.3. Ice geometry (model *b*)

3.3.2. Setup alignments

To study the effects of the direction of discharge propagation, vertical and horizontal setups were tested. In vertical alignment, the setup was arranged in two different positions, as shown in Figure 3.4 a and b. In position (a), the air gap, where the arc is initiated, was located at the top, whereas in the position (b), the air gap was located at the bottom of the setup. This permits to study the possible effect of upward thermal forces on the arc channel.

In other test categories, the ice setup was removed from the mould and placed horizontally, conducting layer upward, on two post insulators as support. This arrangement was especially used to study the effect of water film thickness. The preparation procedure for this configuration is detailed in Section 3.3.5.

The viewing angle of the camera was also varied. To examine the arc foot in high resolution, a side view of the ice setup was used to gain a better view of the area of contact between the arc and ice surface. However, to observe the propagation pattern and ionization regions over the surface, a front view was used.

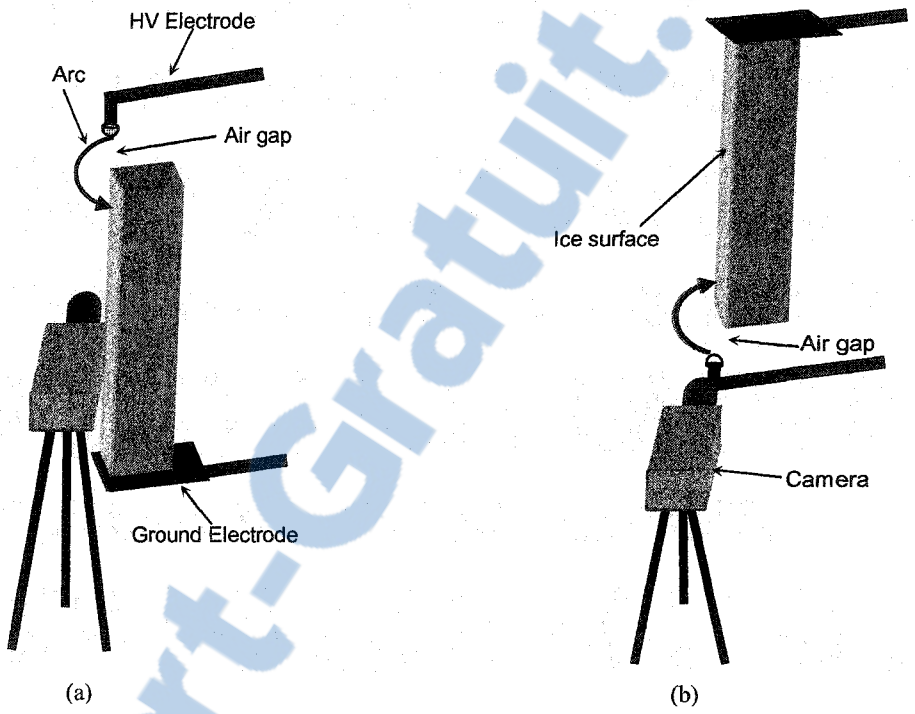

Figure 3.4. Two different setup arrangements in vertical position

3.3.3. Voltage application

AC voltage was applied from the output of test transformer to the HV electrode for each setup. The ground electrodes of the setups were connected directly to a shunt resistance for current measurement, and then to the laboratory grounding system. AC current measurements were also performed using a CT (Pearson coil at the ground electrode). The required voltage was set through the voltage regulation system. Then the

transformer was energized, and the voltage increased from 0 to the preset value (automatically at a constant rate of about 3.9 kV/s).

DC voltage was provided using the rectifier module described in Section 3.2.1. Positive and negative DC voltages are achieved by inverting the diode direction in the rectifier. A partial arc with the positive voltage on the HV electrode is denoted as a positive arc, and vice versa. Current measurements are taken at the ground electrode. Thus, in the case of DC-positive, measurements represent the cathode current, and anode current for DC-negative.

3.3.4. Effects of humidity on test procedure

To study the effect of humidity, two types of experiments were performed. Moist air was produced by a water spray system using a nozzle. The device consists of a water nozzle into which a high-pressure airstream is inserted. Water flows from the nozzle and the airstream causes the water to break up into tiny droplets. This creates a fine mist at the outlet of the spray system. Using this method in the climate chamber, the relative humidity can be increased up to 95%. A dehumidifier was then used to bring the humidity level down to about 40%.

3.3.5. Water film thickness test procedure

The ice setup was removed from the mould and placed horizontally, conducting layer upward, supported by two post insulators. The ice was exposed to ambient

temperature from 1 to 120 minutes, depending on the experiment type, to ensure the formation of a thin water film on the surface. The ice setup was positioned sideways to the camera to closely observe the contact of the arc with the ice surface. Then the voltage was applied. The HV electrode tip was inclined 45 degrees from horizontal at a distance of 35 mm from the ice surface. The ground electrode consisted of a metal plate placed at the other end of the specimen, as shown in Figure 3.5.

Special positioning of the HV electrode in these types of experiments was selected from experimental viewpoint. When the ice is subjected to ambient temperature for a relatively long time, melting and water dripping occurs. If the EV electrode is placed in line with the ice surface it may cause the discharge to initiate and propagate over the sides and bottom surface of setup, which is not desirable. Using this special configuration in which the HV electrode is placed above the surface eliminates this contingency.

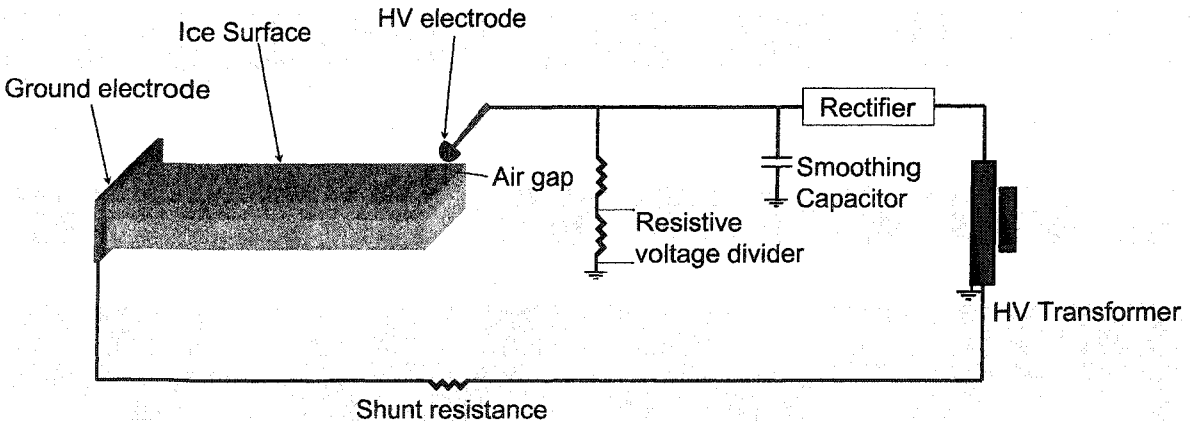

Figure 3.5. Setup arrangement to study the effect of water film

3.3.6. Water film thickness measurement procedure

The thickness of the water film was measured by applying a DC voltage of about 8 kV using two metal plates at the ends of the sample, and measuring the leakage current simultaneously. This voltage value was selected as a trade off between two restrictions. It should be high enough to produce a readable current. It should be low enough not to disturb the thickness of the film. The applied voltage was removed rapidly in order to avoid excessive water melting due to Joule heating. The procedure for measuring the thickness of the water film is detailed in Chapter 5.

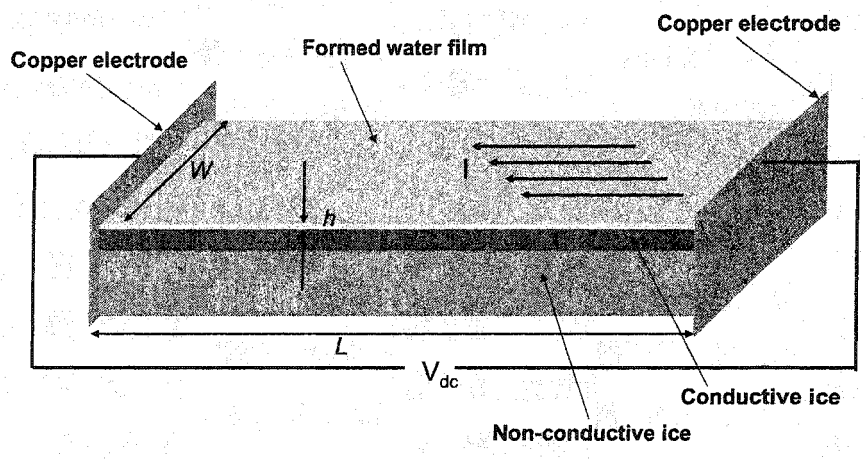

Figure 3.6. Water film thickness measurement
W, L are ice width and length, h is the water film thickness and I is the measured current

3.3.7. Synchronization between electrical and optical measurements

As mentioned above, synchronization between electrical (current and voltage) and optical observation devices (PMT, cameras) was achieved through the DAQ system.

The camera was set to "trigger-end" mode (working until receiving a trigger signal which stops the recording). Current, voltage and the trigger output from the camera were

collected via a data acquisition system. Knowing the recording speed of the camera, this method enables synchronizing electrical measurements with camera frames.

CHAPTER 4

EXPERIMENTAL RESULTS ON ARC PROPAGATION FEATURES

CHAPTER 4

EXPERIMENTAL RESULTS ON ARC PROPAGATION FEATURES

4.1. Introduction

For an arc propagating over an ice surface, one end of the discharge is located over a water film. As water has a significantly smaller secondary emission coefficient than most metals [88], it consequently has significantly different electrode properties. In our case, another difference from other surface discharges is the variation of surface conductivity during discharge propagation. This is due to melting ice by Joule effect, which causes the surface conductivity to increase during discharge progression.

In this chapter, using the methodology described in Chapter 3, the process of arc propagation over an ice surface will be studied. The experiments were conducted in such a way as to extract as much optical and electrical information as possible.

DC discharge over an ice surface was observed closely to study the glow-to-arc transition, discharge velocity, arc channel diameter, and arc foot shape and structure. Discharge propagation patterns were also observed with high-speed imaging. The effect of voltage polarity on the propagation pattern and physical structure of arc foot and column were also examined. Several tests were performed under AC voltage to observe the

propagation pattern and differences in the positive and negative half cycles. Discharge light in the ultraviolet region was captured to get the information about the ionization activity.

4.2. Glow to arc transition threshold

Formation of the white arc begins with a remarkable change in color of the discharge: thin filamentary violet partial discharges suddenly transform into a thick white channel. The white arc observed here is distinct from those found in most other arcing and flashover processes, including contamination and cold fog. The arc-root radius at the point of contact between the arc and the ice surface establishes the contact resistance between the arc and ice layer [89]. This transition is also associated with an increase in the arc current level and its rate of variation. From the data recorded from leakage current measurements through the data acquisition system, the threshold current I_C was measured at 20 mA, as was the case in a previous study [90]. This threshold level does not change with freezing water conductivity, ambient temperature or ice length. Regardless of the above-mentioned parameters, if the desired conditions (increase in surface conductivity resulting from the formation of water a film, and/or from applied voltage) are reached, this transition will take place around this threshold level. This transition level is also associated with an increase in the leakage current variation rate, as shown in Figure 4.1.

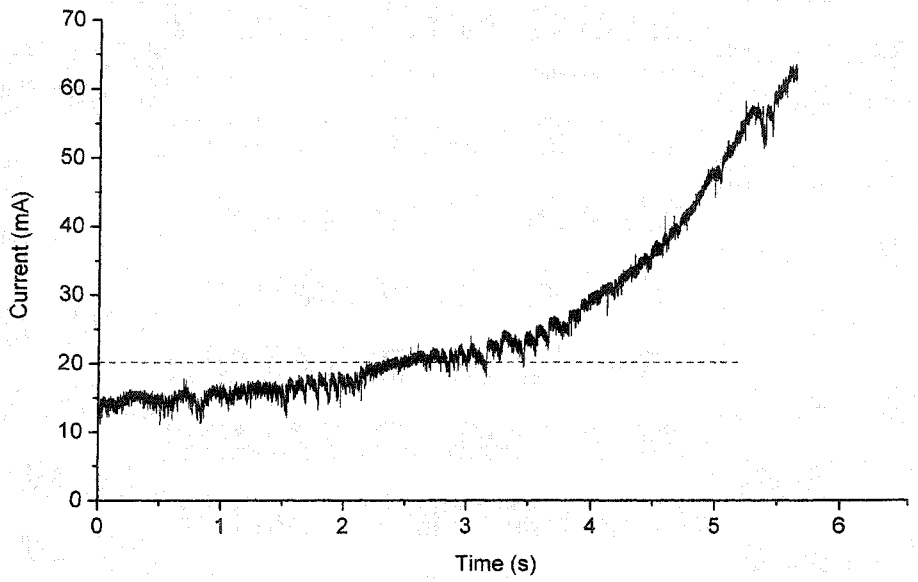

Figure 4.1. Leakage current during the glow to arc transition

4.3. Arc radius variation along the arc channel

To observe the arc foot in high resolution, a side view of the ice setup was taken by the camera, to better see the contact surface of the arc with ice. The setup was arranged in two different positions, as shown in Figure 4.2. In position (a), the air gap where the arc is initiated was located at the top of the setup, whereas in position (b) the air gap was located at the bottom.

It was observed that the arc radius is not uniform, as it appears to increase from the bottom to the top. This observation is more obvious in position (b), where the arc starts from the positive electrode in the lower end, bridges the air gap, and propagates upward along the ice surface to the negative electrode. Figure 4.3 illustrates this observation.

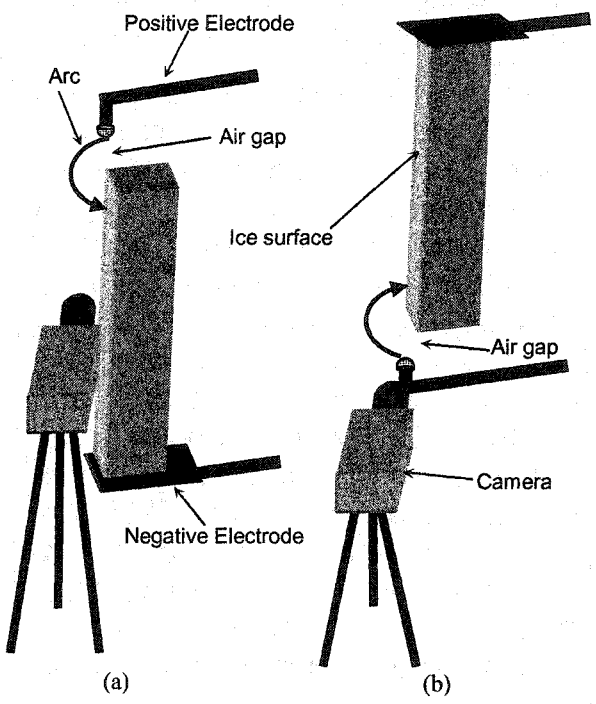

Figure 4.2. Two different setup arrangements

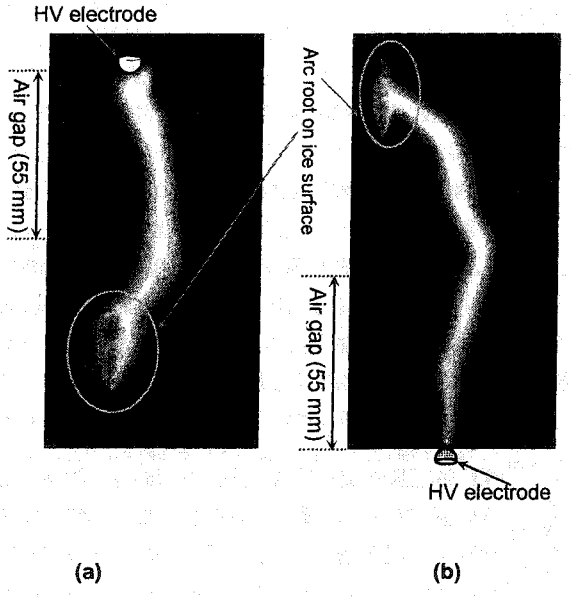

Figure 4.3. Arc channel corresponding to positions a and b

4.4. Arc radius and leakage current

The radius of arc depends not only on environmental conditions such as temperature, humidity and pressure, but also greatly on the leakage current [91]. The arc radius is not uniform along the column. However, for the purpose of calculating the residual resistance of the ice layer and establishing thermodynamic equations for modeling the arc propagation, it is a major parameter that has to be measured accurately.

Before the formation of the white arc, the discharges appear as thin filaments whose radius is difficult to estimate. In the occurrence of the white arc, two distinct regions may be distinguished: its interior is a very bright core surrounded with an envelope that is not as bright as the core.

The diameters of the central core of light and the zone of weak surrounding ionization were measured from the high-speed camera pictures, as shown in Figure 4.4, for leakage currents up to 500 mA. The results represent the average diameters along the channel.

These data suggest the existence of a mathematical relation between arc propagation velocity and leakage current. According to Wilkins' empirical model [92], the arc radius could be calculated as a function of leakage current:

$$r(t) = \sqrt{\frac{I_{arc}(t)}{k\,\pi}} \qquad (4\text{-}1)$$

where r is the arc radius in mm , I is the arc current in amps and k is a constant. Using regression analysis on the experimental results for the central core, the constant k is calculated

to be 0.778. This value differs from what was found in [85]. This difference is due to using a camera with higher resolution than what was used.

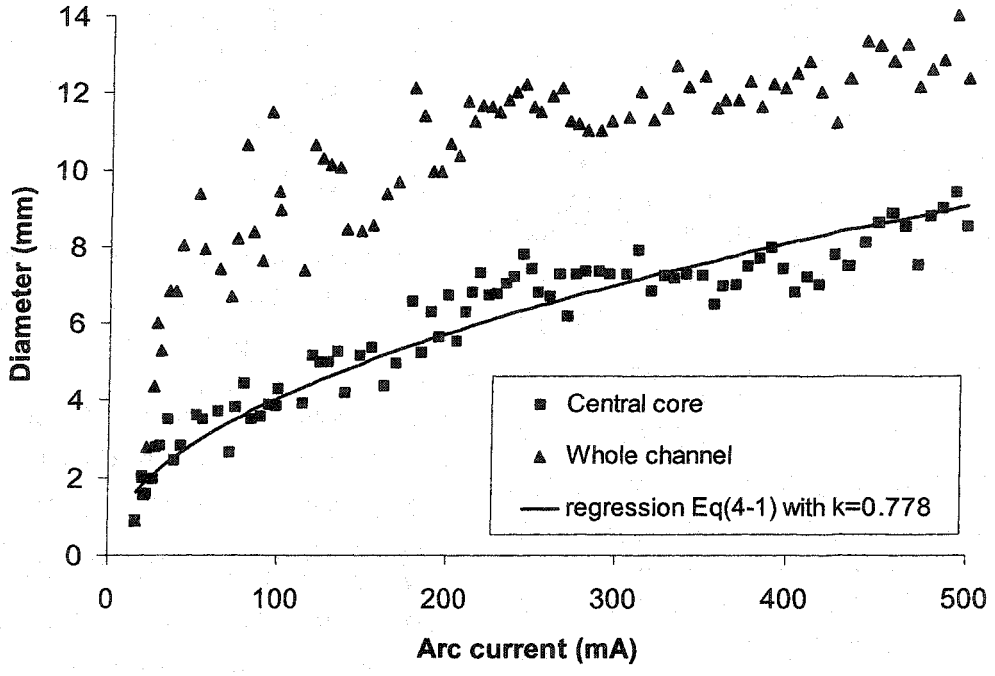

Figure 4.4. Arc diameter as a function of leakage current

4.5. Arc propagation features

The natural tendency of the unconfined arc, responding to convective forces, is to rise and burn over a much longer path [93]. The temporal behavior of the arc current often shows some repetitive features. For low-current arcs, convective influences will lead to a relatively low-frequency repetition of arc excursions and reconnections (see Figure 4.5). Normally two prominent frequencies can be identified in the current as well as in the video recordings. The lower frequency corresponds to the saw-tooth-like shape related to the overall convective change of arc length, whilst the other frequency component relates to the

faster and shorter excursions and reconnections superimposed on the slower overall rises and reconnections of the arc. Lower frequencies appear at higher current levels, where the convection can create longer arches.

It was also observed that the arc obviously does not propagate in complete contact with the surface. The arc channel is completely formed in the air, and only the arc foot is in contact with the ice surface. This observation is contrary to the results of Mercure *et al.* [47] and Boylett [94] for arc propagation over an electrolyte. These authors stated that the arc column remains in electrical contact with the surface of the electrolyte. However, the shape of contact surface is not circular. The arc foot appears branched, each branch carrying part of the arc channel current to the ice surface (Figure 4.6). In some cases, the arc foot spreads over a fairly long region, of about 5 cm, parallel to the ice surface with several streamers, as shown in Figure 4.7(a). Sometimes, one of these streamers carries more current and propagates as a secondary arc branch, making another independent foot contact with the ice several centimeters ahead of the main arc foot, as depicted in Figure 4.7(b).

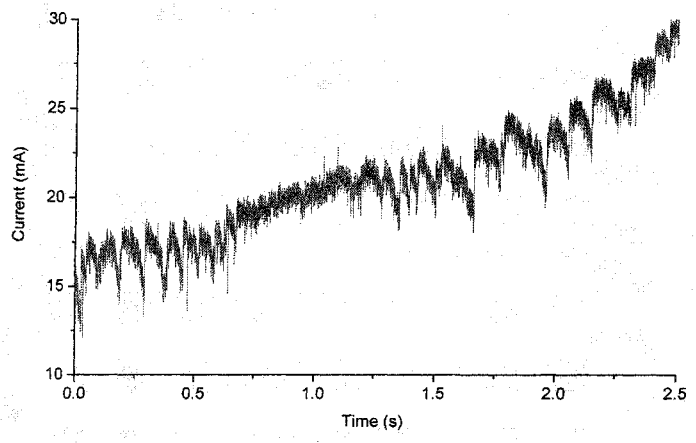

Figure 4.5. Arc current saw-tooth-like shape

Along about the first two centimeters of the arc channel, the arc is straight. Beyond that, perturbations begin to develop, as seen in Figure 4.8. Knowing the time frame interval and the number of frames, it was calculated that these perturbations moved downstream at about the free-stream flow velocity. It appears that a laminar-to-turbulent transition occurred at a distance of approximately 2 cm along the column. The perturbations are thought to be due to turbulent eddies.

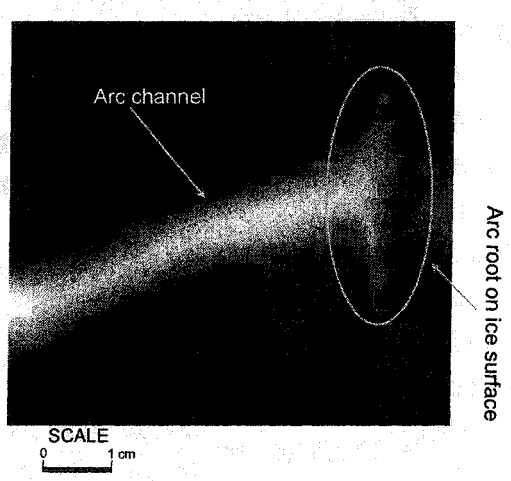

Figure 4.6. Branched arc channel in contact with the ice surface

Considering the arc propagation pattern, as seen from different frames in Figure 4.9, the arc is initiated across the air gap and propagates with a moving foot on the ice surface. The arc lengthens not only because of longitudinal propagation along the ice, but also due to bowing of the hot channel resulting from buoyancy force. Arc elongation is associated with a decrease in leakage current. The channel will lengthen up to a critical value. Beyond this value, the input power will be enough to heat it up and maintain the conductivity of plasma. At this moment, another discharge will appear at a shorter distance from the ice

surface, and will convert the current to the new path. This pattern corresponds to each saw-tooth-like repetition of measured leakage shown in Figure 4.5.

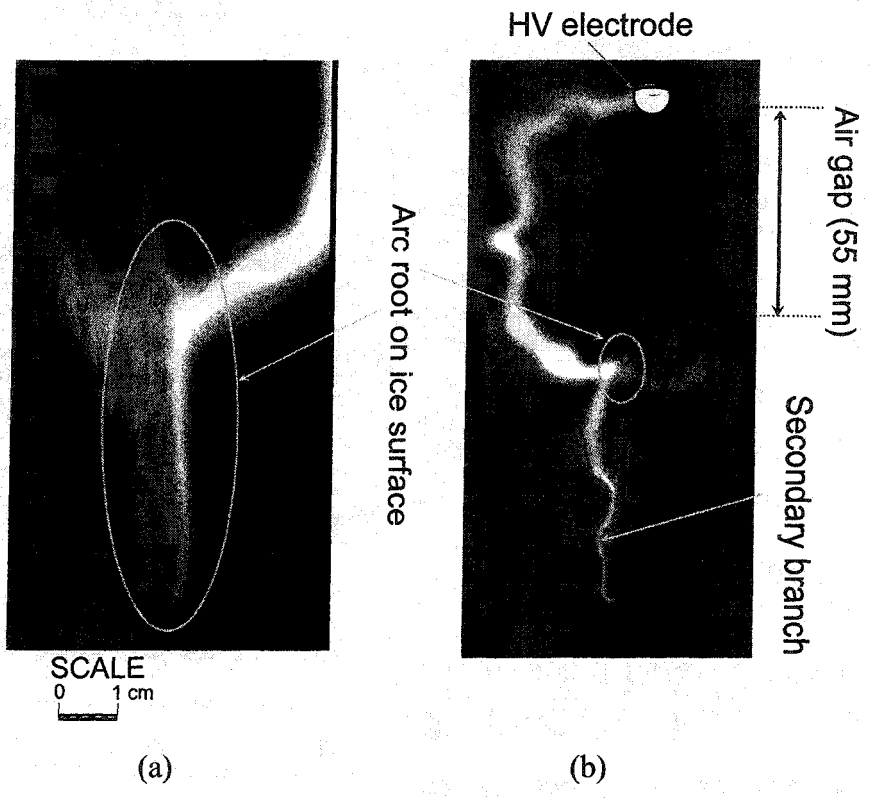

Figure 4.7. (a) Widespread branched arc channel (b) secondary arc foot

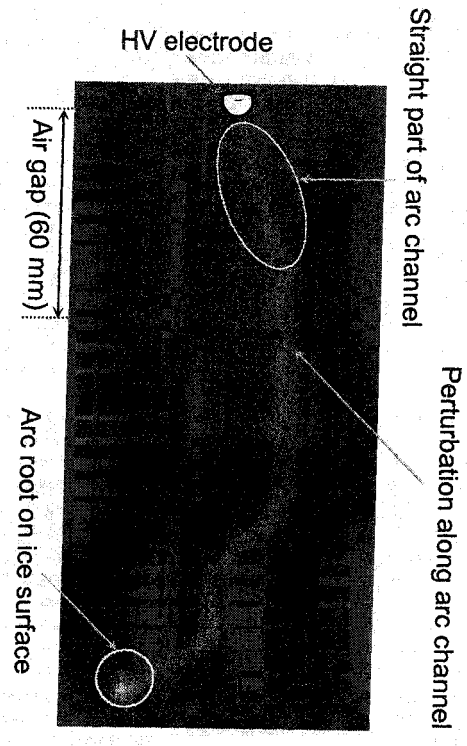

Figure 4.8. Arc channel side view:
the first 2 cm of the arc from the upper electrode are straight; the rest of channel shows distortion

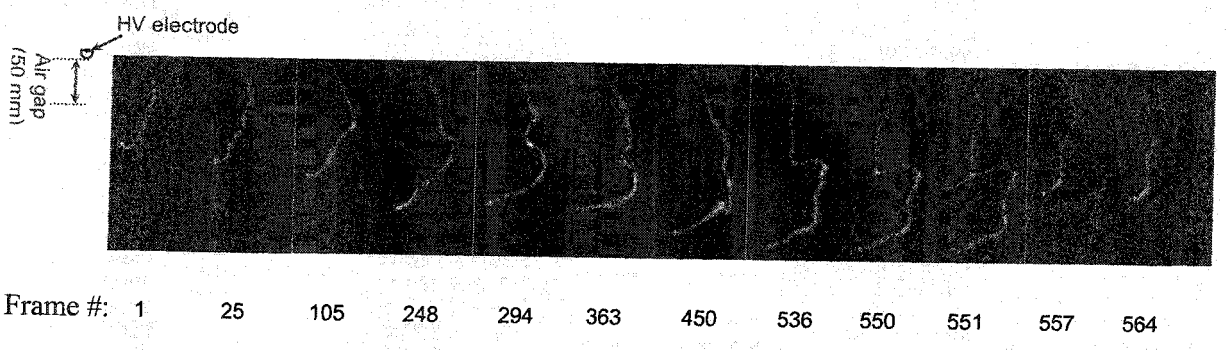

Figure 4.9. Arc propagation pattern at 4000 frames per second

4.6. Major and minor collapses

From the video recordings and current monitoring and measurements, it was found that the temporal behavior of the DC arc often shows repetitive sequences. Even though in this case (compared to AC arc), the alternating cycling of the voltage will not result in extinction and re-ignition of the arc, some kind of arc decay is observed during its development. From this viewpoint, it looks similar to a gliding arc climbing a Jacob's ladder. The arc can be said to exhibit an expected randomness, but with some patterns related to the current level and ice surface conductivity.

As shown in Figure 4.1, the leakage current recorded during a flashover process is increasing. This is mainly due to the increase in ice surface conductivity and the concomitant decrease in residual resistance. The variation in residual resistance can be calculated from the rate of increase of leakage current. However, this increase is not permanent, and will stabilize at a certain value depending on water conductivity, ambient temperature, and ice length and thickness.

Basically, the arc will propagate as long as its power input is increasing. From the simultaneous observation of current signals and the video images, two different cases may be identified. The natural tendency of an unconfined arc, responding to convective forces, is to rise and burn over a much longer path [93]. However, if this increase in length is associated with an increase in current, concomitantly the arc will move along the ice surface toward the other electrode. The second case happens when the current is decreasing during the arc elongation. In this situation, the arc root not only will not propagate on the

ice, but will apparently stretch upward into the air due to rising hot gas by natural convection and to buoyancy forces.

During the arc excursions and reconnections, two types of arc collapse were identified. The first one, which we call "minor or partial collapse", as in [97], occurs when two points along the arc come into contact with each other. Electrically, this jointing of the arc along its column causes short-circuiting of an arc fraction and a decrease in arc resistance. It is also associated with a sudden rise in leakage current (as shown in Figure 4.10 b). The second, called "major collapse" [97], happens when the arc length exceeds its critical value, as the current can no longer flow into the former arc path, and the distance between the electrodes and the ice is bridged by a new shorter path. This collapse often causes a larger increase in the current waveform, compared to minor collapses (see Figure 4.10-a). It has been found that sudden current increases often reach more than 20% of initial value prior to collapse. The longer the arc length is before collapsing, the greater the sudden rise in the arc current.

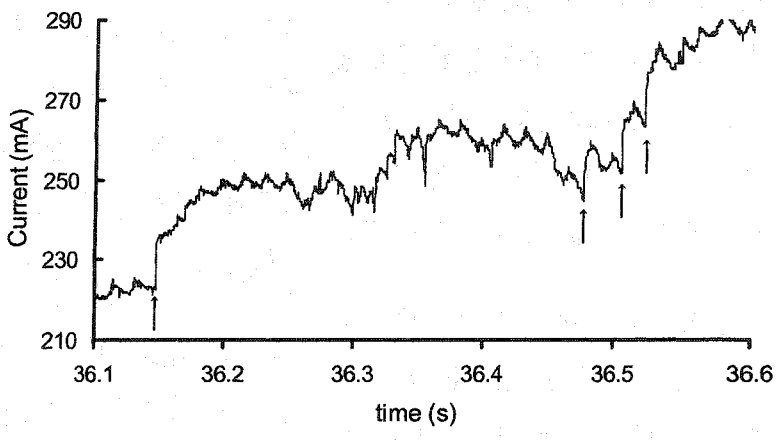

(a)

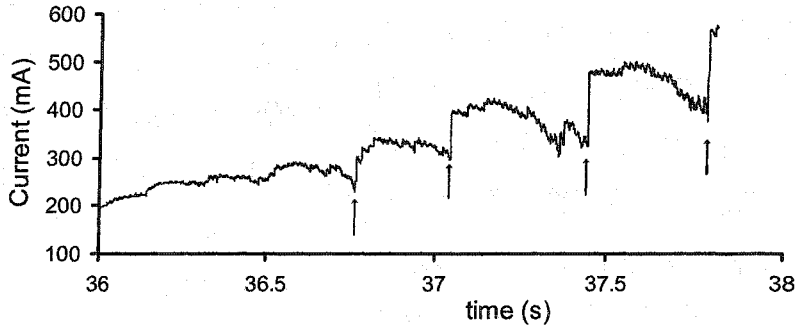

(b)

Figure 4.10. Leakage current, (a) four major arc collapses associated with four current jumps are indicated (b) minor arc collapses

4.6.1. DC-positive

Close examination of major arc collapse using high-speed photography showed that when the wetted ice surface acts like an extended cathode (i.e. dc-positive), the following sequence of events occurs and was identical for all the observed cases. Firstly the outer arc sheath bended toward the ice surface, creating a curved shape, while the arc column core diameter did not change significantly, as seen in Figure 4.11-b. This sheath expansion continued until it reached a specific length between the sheath and the ice surface (Figure

4.11-c). The development speed of the sheath increased as it approached the surface. At this stage, a very thin bright filament discharge initiated from the arc core and moved toward the ice surface (Figure 4.11-d). Upon contacting the surface, the root spread over a relatively large area (about a few centimeters long). This instant also corresponded to a sudden jump in the leakage current signal. The diameter of this new discharge increased rapidly (Figure 4.11-e), whereas the diffused root shrank. Over a short period, the total current diverted from the previous channel to this newly formed discharge. The arc channel diameter increased to a value proportional to the total flowing current. As the arc started to decay from its initial path, its high luminosity decreased, followed by a decrease in diameter and defragmentation (Figure 4.11-f). It should be noted that after the current was diverted to the new path, the remnants of the arc persisted for some time (Figure 4.11-g and -h). At higher current levels, the effect was even more pronounced, i.e. an arc carrying a current of 120 mA took about 13 ms to disappear completely, while these times were 30 ms for 300 mA, and 45 ms for 400 mA.

Concerning the minor collapse, where two points along the arc came into contact, similar steps were observed. It should be stated that the minor collapses usually take place when the arc column drifts up due to buoyancy forces and this connection of two points makes the arc shorter. The interesting feature found in all the recorded cases is that the new discharge path always initiated from a point closer to the HV electrode, which in this case acted as the anode (Figure 4.12-b). The voltage drop along the arc column means that the new streams originated from a point in the arc that had a higher voltage compared to the

other points, i.e. the final destination of the new discharge. This aspect will be discussed in greater detail in Chapter 6.

Furthermore, in the minor collapse, unlike the bending and extending of the sheath in the major collapse, the new discharge initiated from a point on the arc channel without any visible bending of the sheath or core toward the destination point, as clearly seen in Figure 4.12-b. This thin filamentary streamer could propagate several tens of centimeters to reach another point (Figure 4.12-d). The propagation speed was reduced significantly when approaching the sheath of the arc at the destination point. Following the connection of this streamer to the arc channel core, the total current diverted to this shorter path and the former channel decayed slowly (Figure 4.12-e to h).

These types of decay could be observed in all of the configurations. In Figure 4.13 and Figure 4.14, minor and major collapses could be observed where the setup is vertical and the air gap is placed at the top of the setup. Note the hot gas remnants along the former arc path.

As the arc starts decaying from its initial path, its high luminosity is reduced, which is followed by a decrease in diameter and defragmentation. It should be noted that after the current is diverted to a new path, the remnants of the arc persist for some time. At higher current levels, the effect is even more pronounced, e.g. an arc carrying a current of 120 mA takes about 13 ms to completely disappear. It takes 30 ms for a 300 mA arc current and 45 ms for a 400 mA arc current to extinguish. It is noteworthy that prior to decay, the arc maintains its luminosity despite the decrease in current and diversion to a new channel. This suggests that the column had been hot enough for thermal ionization to take place.

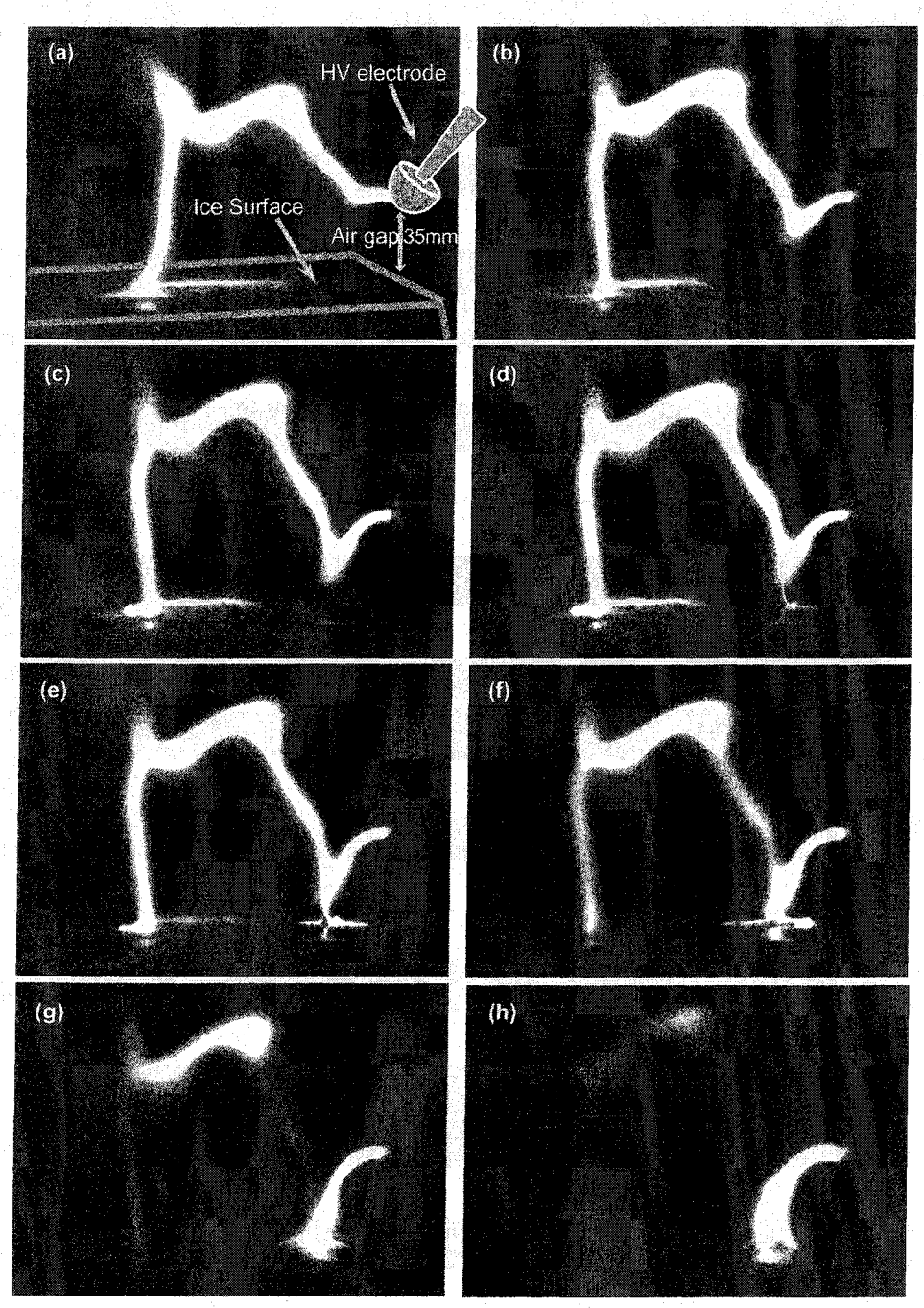

Figure 4.11. Major collapse under DC+:
(a) arc column prior to the collapse t = 0; (b) bending of the arc sheath toward the ice surface t = 18 ms; (c) arc position before the formation of streamer t = 23 ms; (d) the instant of streamer connection with the ice surface t = 23.25 ms; (e) increasing diameter of the new discharge t = 23.75 ms; (f) total transfer of current to the new path t = 26.25 ms; (g) decay of the old channel t = 31.25 ms; (h) t = 47 ms

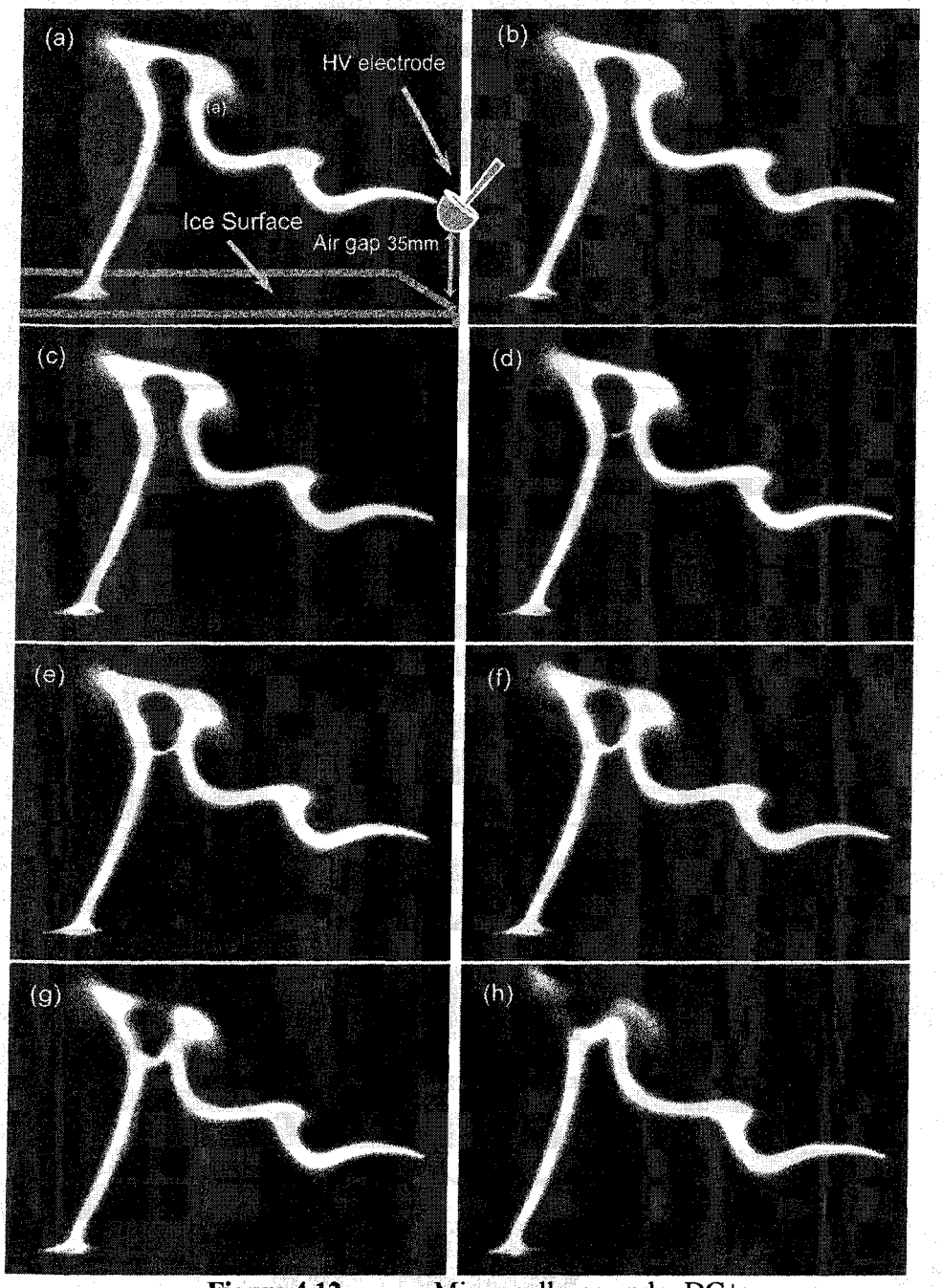

Figure 4.12. Minor collapse under DC+:
(a) the arc column prior to the collapse t = 0; (b) formation of a positive streamer from a point closer to the HV electrode t = 0.75 ms; (c) streamer propagation in-between the columns t = 1 ms; (d) the streamer tip reaches the sheath t = 1.25 ms; (e) streamer connection to the arc core t = 1.75 ms; (f) transfer of current to the new path t = 3.25 ms; (g) decay of the old channel t = 5.5 ms; (h) t = 15.75 ms

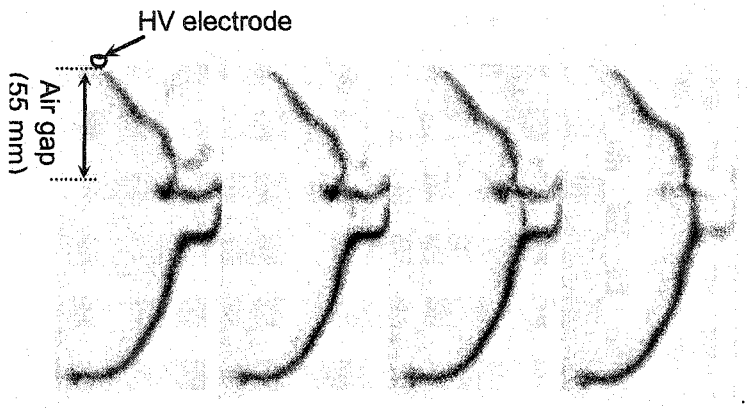

Figure 4.13. Minor collapse in vertical position

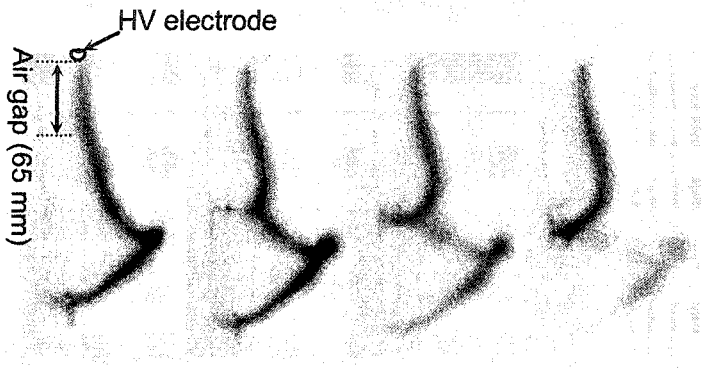

Figure 4.14. Major arc collapse (Notice hot gas remnants along former arc path.)

4.6.2. DC-negative

When the ice surface acted like an anode, i.e. DC-negative voltage, the arc propagated differently than observed in the previous case. The arc sheath did not indicate any considerable curvature toward the surface, contrarily to DC-positive (Figure 4.15-a).

Suddenly, a very thin bright filament initiated somewhere along the ice surface and moved rapidly toward the arc column (Figure 4.15-b). During the propagation, the root on the surface looked as if it was branched at times. This new discharge usually followed a

slightly curved path toward the arc channel, with the curvature away from the HV electrode, as shown in Figure 4.15-c. The average speed of propagation was relatively low compared to DC-positive. Furthermore, contrary to DC-positive, the propagation velocity decreased near the arc sheath. In the close vicinity of the sheath (Figure 4.15-d) it propagated very slowly, penetrating the sheath and finally forming a bright channel from the ice surface to the luminous arc core (Figure 4.15-f). The variation of propagation velocity from the inception of the new discharge to the instant of connection to the arc sheath is depicted in Figure 4.16. The formation of this new luminous path led to the following events, similarly to the positive arc. Current diverted to this new column and the old channel decayed slowly according to its current intensity before extinction.

The discharge propagation was tracked until it made contact with the sheath of the arc channel. After this moment, the cover surrounded the discharge tip and the location of the tip could not be determined precisely. Hence, the last point in Figure 4.16 corresponds to an instant similar to that observed in Figure 4.15-d, when the discharge tip joins the arc sheath.

Using the curve-fitting method and the sum of two exponential functions on the measured points, the following constants were obtained:

$$L = Ae^{Bt} + Be^{Ct} \qquad (4\text{-}2)$$

where L is the discharge length in cm, t is time in seconds and A, B, C and D are constants calculated from curve fitting with 95% confidence, as follows:

A = 3.328, B = 38.52, C = -3.356 and D = -2251. This function is also depicted in Figure 4.16. The velocity of the discharge development was calculated from the derivative

of the above function. It may be seen that the maximum velocity of about 80 m/s corresponds to the inception of the discharge from the surface, and decreases rapidly as it progresses to reach a velocity less than 2 m/s near the arc sheath.

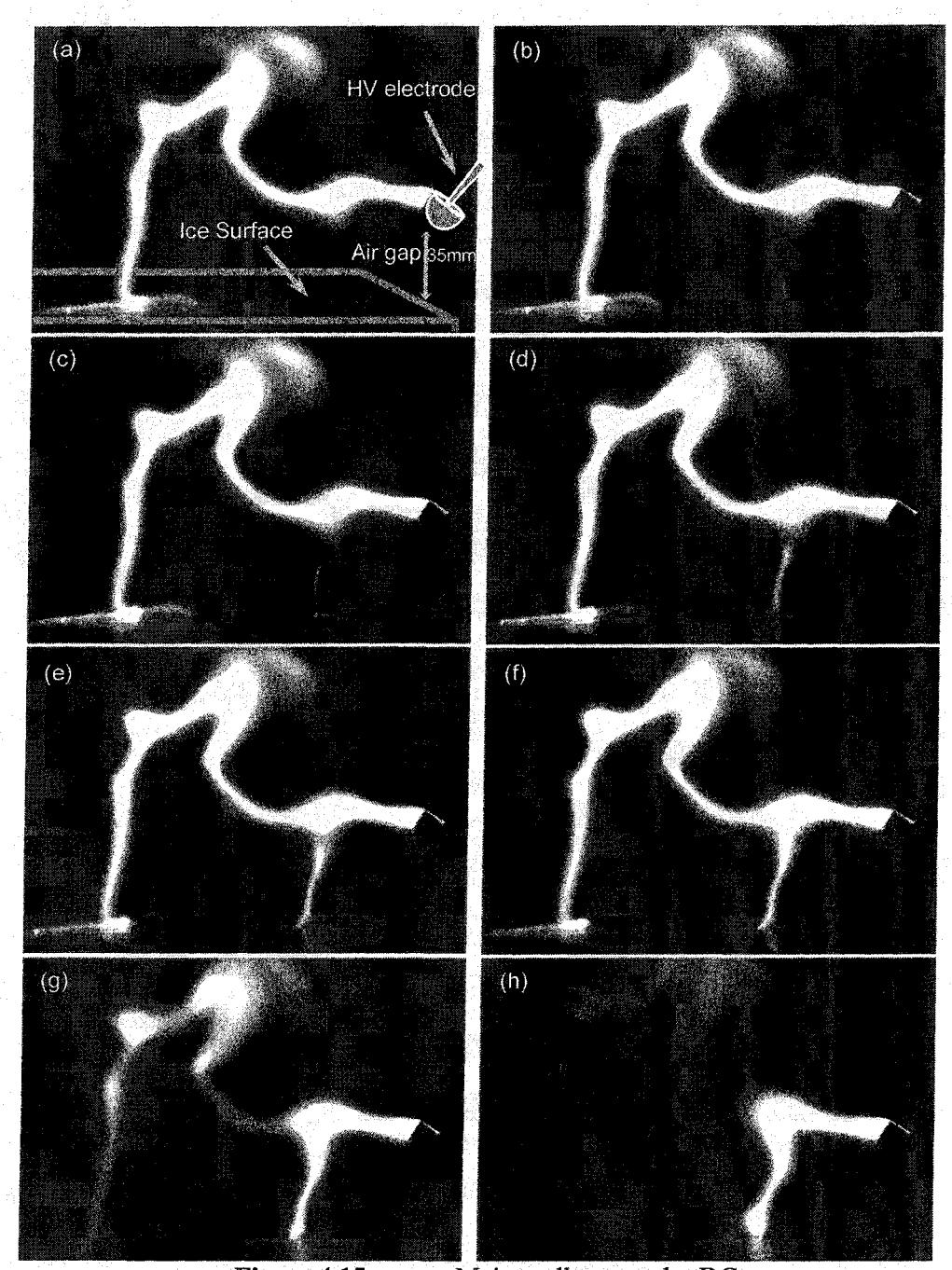

Figure 4.15. Major collapse under DC-:
(a) the arc column prior to the collapse t = 0; (b) initiation of a filamentary streamer from the ice surface t = 0.25 ms; (c) streamer propagation toward the arc channel t = 0.5 ms; (d) the instant of streamer connection to the arc sheath t = 3.25 ms; (e) slow propagation of the streamer in the sheath region t = 6.75 ms; (f) connection to the core t = 7.7 ms; (g) decay of the old channel t = 11.25 ms; (h) t = 20.5 ms.

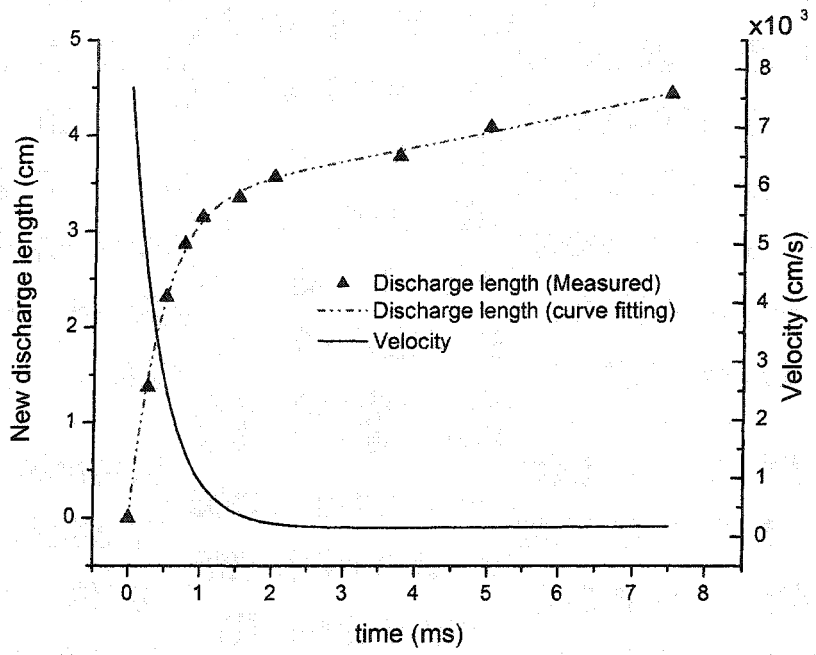

Figure 4.16. Discharge length during a major collapse under DC-negative, and estimated velocity of propagation

Concerning the minor collapse of negative arcs, almost the same steps as in DC-positive were observed. But contrary to DC-positive, the new discharge path always initiated from a point midway along the arc toward a point closer to the HV electrode (Figure 4.17).

4.6.3. Physical appearance of the channel and contact surface

It is believed that flashover occurs when the local discharge continues to propagate, depending on the conditions at the discharge tip [95]. Therefore, to clarify the local discharge propagation mechanism, it is important to know the electrode voltage drop, the current density at the tip, and the contact surface between the arc root and electrolyte

surface. Probe measurements [71] have shown that, on the ice surface, the cathode and anode voltage drops are approximately 799 and 526 volts, respectively.

Video records show that the positive arc appears brighter and thinner than the negative arc. In the positive arc, the discharge tips are much branched (Figure 4.18) and close examination revealed cathode-spot-like structures. Mainly, these cathode spots are at the tips of subsidiary branches. The spots are sometimes observed beneath the main column. These observations substantiate the conclusion that the discharge current enters the ice surface at more than one contact point.

Contrarily, the images of negative arcs reveal few branches (Figure 4.19). Several bright spots are often observed at the thick tip of the arc. The negative arc root appears as a diffused luminous region of greater diameter than the arc channel (Figure 4.19). A very small dark region can also be seen between the tip and the ice surface. Additional filamentary thin discharges are frequently seen beneath the main arc column.

Contrary to positive arc, these filaments, as well as their corresponding bright spots in negative arc, float away from the surface, appearing as suspended strings without any support at the top (Figure 4.20). Another important feature was that the central part of a negative arc drifts up much faster than that of a positive arc.

It was also observed that the arc column shape appeared to be more convolved for positive arcs. A similar result [96] was obtained for partial arcs on electrolyte surfaces from interferometry techniques, indicating turbulent-type airflow for positive arcs and laminar-type for negative arcs.

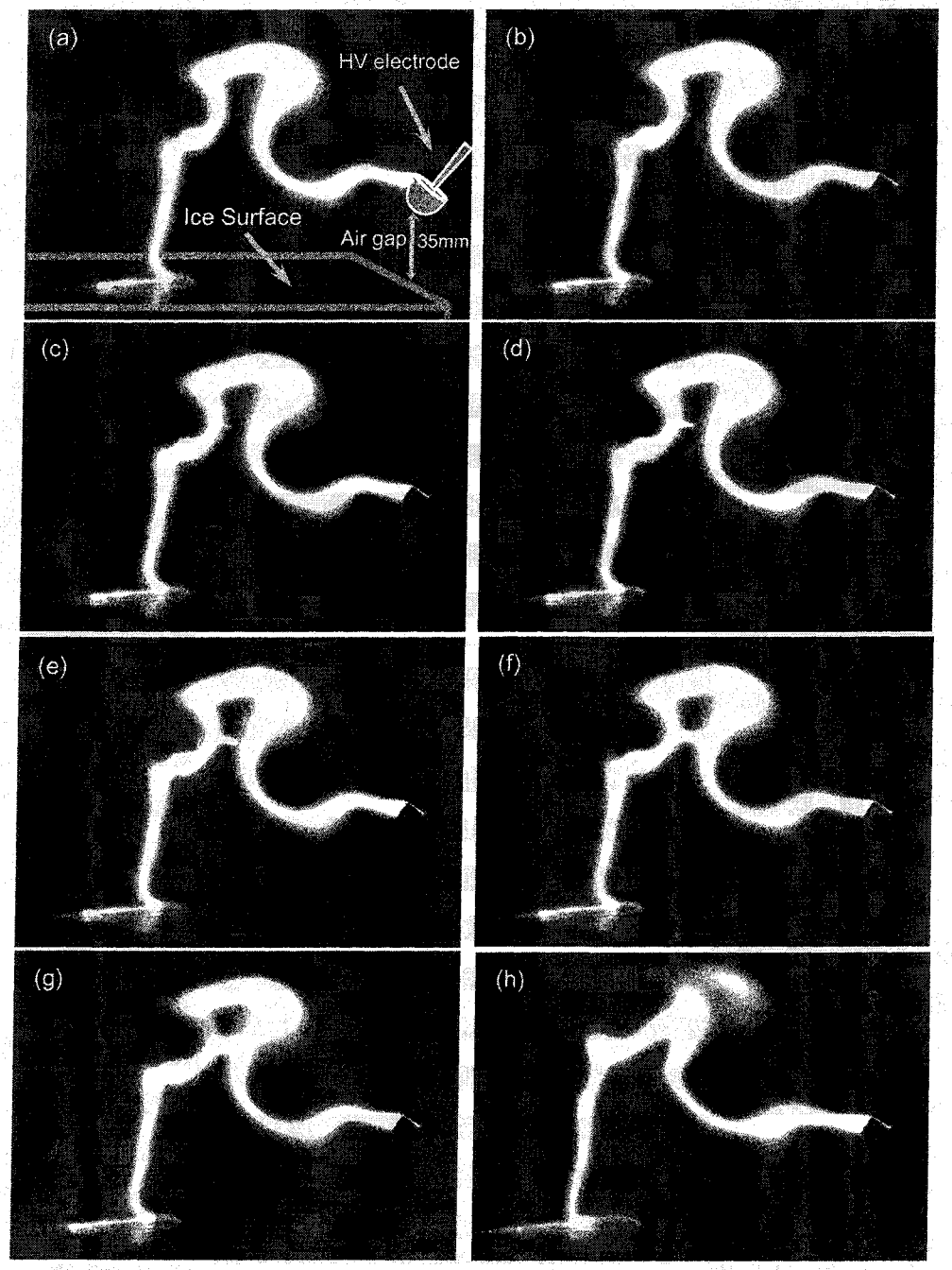

Figure 4.17. Minor collapse under DC-:
(a) the arc column prior to the collapse t = 0; (b) formation of a positive streamer from a point closer to the HV electrode t = 1 ms; (c) streamer propagation in-between the columns t = 1.5 ms; (d) the streamer tip reaches the sheath t = 2.25 ms; (e) streamer connection to the arc core t = 2.75 ms; (f) transfer of current to the new path t = 3.25 ms; (g) decay of the old channel t = 6.75ms; (h) t = 25 ms.

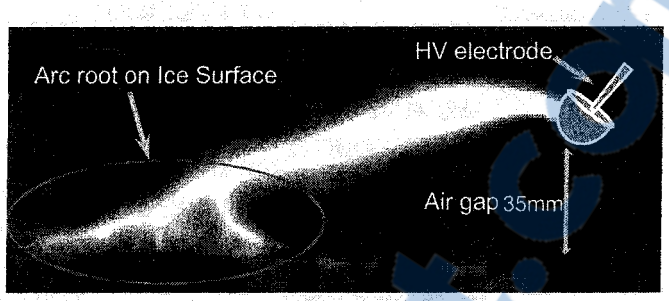

Figure 4.18. Arc root under dc positive voltage

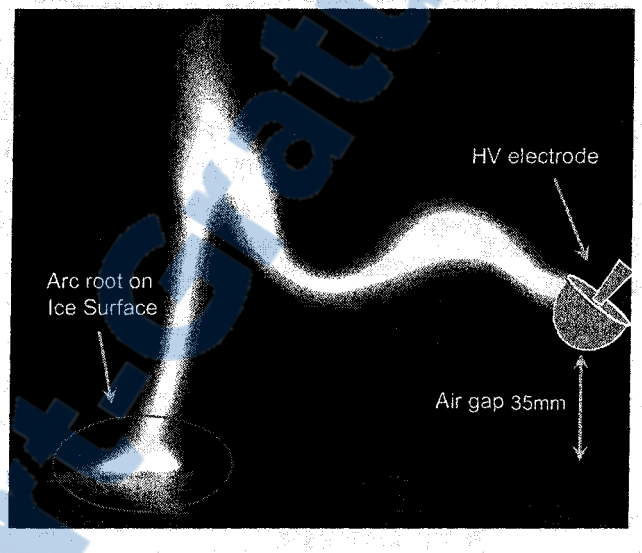

Figure 4.19. Arc root under dc negative voltage (Reflections from the ice surface are seen in the side view)

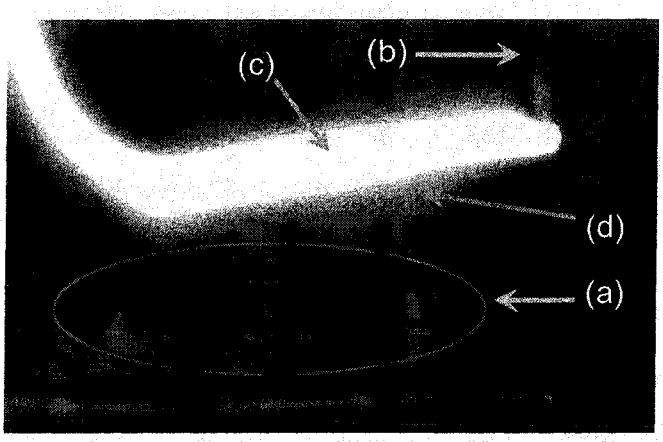

Figure 4.20. (a) Discharge activity beneath the negative arc column (b) high-voltage electrode (c) arc core (d) arc sheath

4.6.4. Anode and cathode current jumps

In all the experiments, the current was measured at the ground electrode. During the propagation of the positive arc, with the HV electrode connected to DC-positive, the current was measured at the cathode and at the anode in the case of the negative arc. Anode and cathode current waveforms look dissimilar when observed simultaneously through the video recordings of collapses. Figure 4.21 and Figure 4.22 show the recorded leakage current corresponding to major collapses in DC-positive and DC-negative, respectively. Figure 4.21 shows that, for the positive arc, the current does not change significantly before contact (point b) then it suddenly rises; but in the case of negative arc, the current jump-starts upon the appearance of filamentary streamers on the ice surface (point (a) in Figure 4.22). Details concerning this observation are given in Chapter 6.

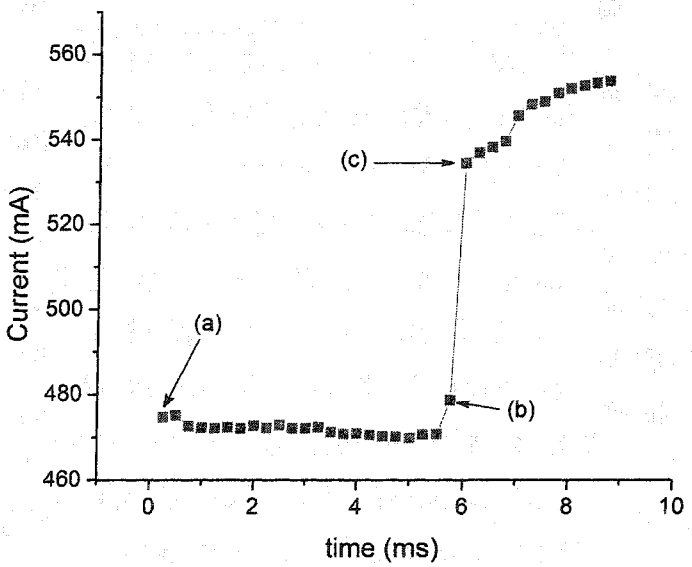

Figure 4.21. Cathode current during a major collapse under DC-positive: (a) start of sheath bending; (b) streamer formation from the arc column; (c) contact with the ice surface.

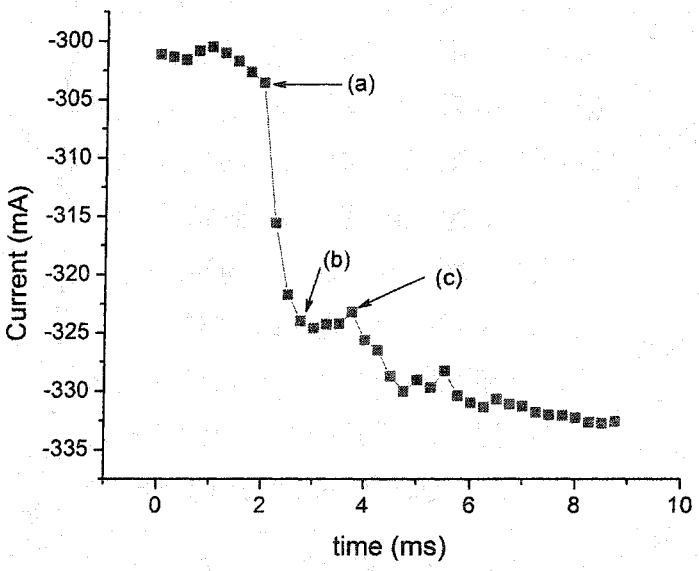

Figure 4.22. Anode current during a major collapse under DC-negative: (a) formation of positive streamer on the ice surface; (b) the instant of streamer connection to the arc sheath; (c) streamer connection to the core.

4.7. Effect of propagation direction on velocity

During the early stages of arc propagation on the ice, the arc velocity was also measured with the two configurations described in Section 3.3.2. The results showed that when the air gap is located at the bottom of the ice sample (test position *b*), the arc propagates faster compared to when the air gap is at the top (test position *a)*. Also in test position *a*, the arc propagation velocity decreases with increasing current. These two observations reveal the significant effect of the buoyancy force on the arc channel. It may be concluded that this force is comparable to the force responsible for arc elongation along the ice surface.

4.8. V-I characteristics of DC-positive arc on ice surfaces

The arc voltage is a function of the arc current and arc length. It is often customary to express the voltage gradient E of the arc in terms of current I and constants A and n as [24, 71]:

$$E = AI^{-n} \qquad (4\text{-}3)$$

So that the arc voltage V_a is:

$$V_a = EL_{arc} \qquad (4\text{-}4)$$

where L_{arc} is the arc length.

For DC+ arcs on an ice surface, the constants A and n were calculated to be 208.9 and 0.449, respectively [71].

In the developed model [71] of arc on an ice surface, we have:

$$V = V_e + V_a + IR_{res} \qquad (4\text{-}5)$$

where V is the applied voltage, V_e is the electrode voltage drop, I is the leakage current, and R_{res} is the residual resistance of unbridged ice. The electrode voltage drop V_e for DC+ was determined to be 799 V [71].

Three different measurement samples were considered in one of the experiments with an applied voltage of V=97,500 V. In the first position, an arc length of L_{arc1} = 33.6 cm and a leakage current of I_1 = 110 mA were recorded; the voltage gradient, E_1 = 560 V/cm, and the arc voltage, $V_{arc\ 1}$= 18,829 V, were calculated from (4-3) and (4-4), respectively, while the residual resistance $R_{res1} \approx 708$ kΩ, was computed from (4-5).

Departing from this point, the arc grew in 12 ms to a critical length of L_{arc2} = 45 cm with a leakage current of I_2= 92 mA. The main point is that between these two positions, the arc grew in the air while the arc root stayed at the same location on the ice. Due to the short time duration (12 ms) and to the overall variation of leakage current versus time, which had already stabilized, the residual resistance could be considered to be unchanged, $R_{res2} \approx 708$ kΩ. This assumption will be verified later. From (4-5), we obtained V_{arc2} = 31,571 V, which yields the gradient of E_2 = 701 V/cm.

To validate the assumption of constant residual resistance, if we follow the arc development, it displays a major collapse after the second position leading to a shorter arc length of L_{arc3} = 32 cm and a current increase to I_3 = 111 mA. Applying the same procedure as for the first point yields E_3 = 558 V/cm and V_{arc3}= 17,859 V, leading to $R_{res1} \approx 710$ kΩ, which confirms our assumption.

A contradiction arises from the result of voltage gradient for the second point. For an arc current of I_2 = 92 mA, according to (1) and the determined arc constants [71], a voltage gradient of E_2 = 607 V/cm should be expected. However, the experiments resulted in a value of E_2 = 701 V/cm, which is about 15% higher than the calculated voltage gradient. The measured and calculated points are presented in Figure 4.23.

This condition is more pronounced at higher current levels where the discrepancy is even more than 15%. The reason behind this observation is that the arc constant values determined in [71] were measured using a 280 mm-long ice sample. Moreover, it was mentioned in that study that the arc was normally formed across the air gap and near the ice surface.

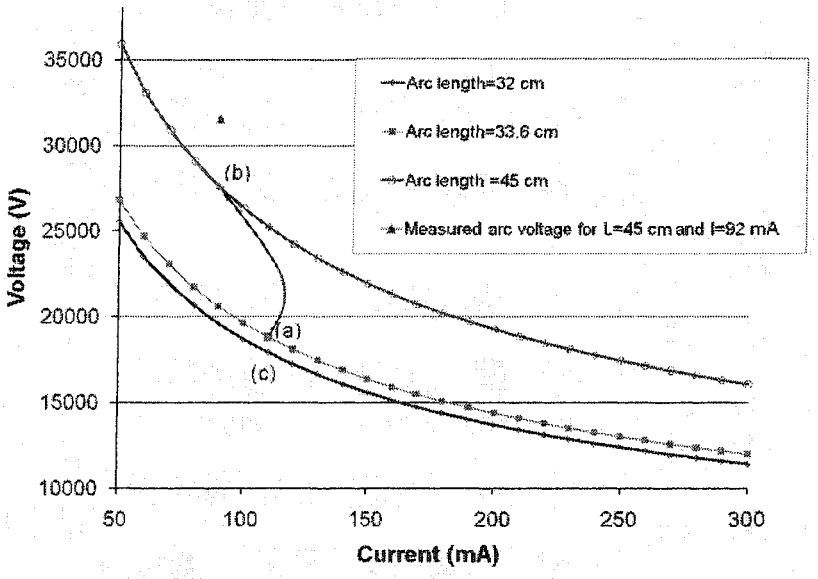

Figure 4.23. V-I characteristics used for calculations

From the physical viewpoint it may be explained as follows. The length of the arc increases together with its voltage; its power increases up to the maximum value depending

on the source. During this quasi-equilibrium stage, the gas temperature does not change significantly. The non-equilibrium stage starts when the length of arc exceeds a critical value. Heat losses from the plasma column begin to exceed the energy supplied by the source, and the plasma cannot be sustained in quasi-equilibrium state. Then, the plasma rapidly cools down while conductivity is sustained by high electron temperature. After departure from non-equilibrium discharge, a new breakdown takes place at the shortest distance between the arc channel and the ice surface. The cycle then repeats.

From the above discussion it is clear that the measured results were applicable only for the quasi-equilibrium stage and for the critical length, which is in the non-equilibrium stage. The arc column has a lower conductivity and consequently a higher voltage gradient.

The arc can be viewed as a series of static arcs with different lengths, as shown in Figure 4.24. The actual or dynamic V-I characteristic is superimposed and the arc will thus operate at the successive connection points, a, b, c... If the arc were to stall at connection point e for example, it would be stable and sustained. The arc, however, continues to evolve and eventually reaches a length such that the two characteristics become tangential (connection point f in Figure 4.24) and ceases to evolve further because the power input is now constant or decreasing. Arc instability and collapse follows and a new channel forms at a shorter distance.

To overcome the problem, it is suggested to use a mean gradient curve for a normal arc in quasi-equilibrium stage, and a critical gradient curve for the critical arc length as reported in [97] and as shown in Figure 4.25. Even from the experimental measurement points in [71], one could draw such an upper envelope for this critical gradient. If the

gradient drops below values given by these curves, the arc decays and extinction follows. The derivation and use of such curves in the mathematical model still needs further investigation.

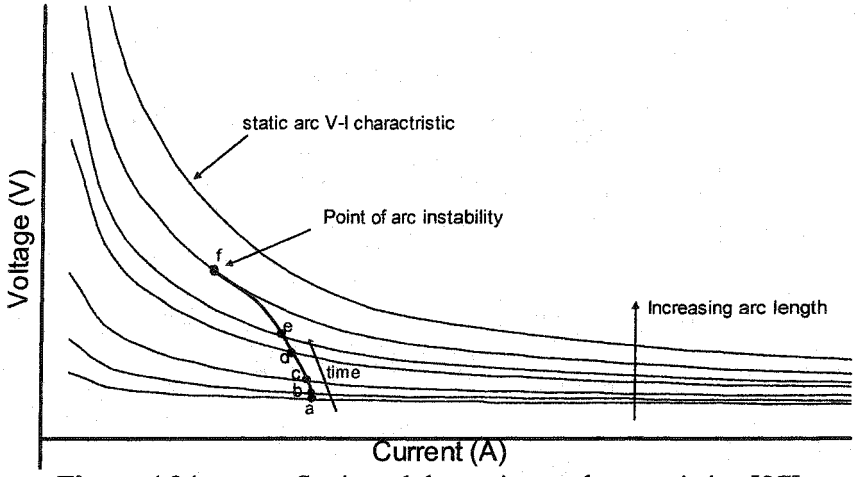

Figure 4.24. Static and dynamic arc characteristics [97]

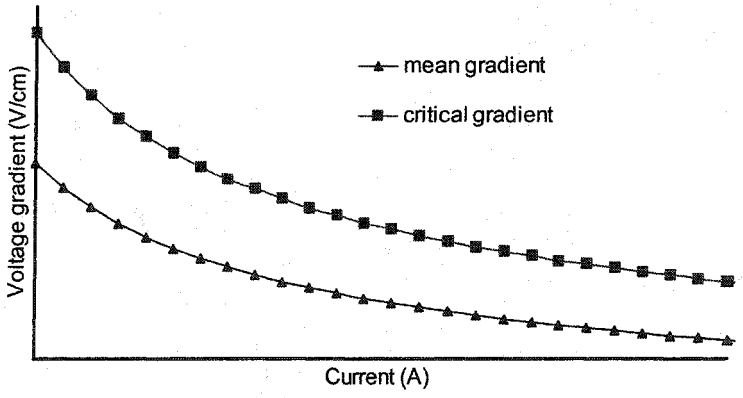

Figure 4.25. Arc voltage gradient versus current [97]

4.9. AC discharge propagation

Using the methodology described in Chapter 3, several tests were conducted and arc velocities in two distinguishable stages were derived using our existing high-speed camera and AC excitation.

In the first stage, the arc extended relatively slowly, with a velocity of about 10 m/s. When the arc length reached about 60% of the inter-electrode length, arc propagation velocity increased suddenly to a relatively large value until completion of the flashover. Velocity in this stage was more than 1000 m/s.

This process has also been observed with ultraviolet image intensifiers, which are used to count photons. Our observations show that during the propagation of white arc on the ice surface, there is a region at the tip of arc which emits a lot of ultraviolet in the view field of Corocam (between 240 and 280 nm). The length of this zone, because of the limitations of the camera (resolution), cannot be measured exactly, but it varies between 5 and 20 cm during the propagation.

Regarding this characteristic, we used a configuration consisting of an image intensifier in front of a very high-speed camera. Only the ultraviolet light is captured using a high-pass or UV band-pass filter in front of the intensifier. This will allow us to study the streamer propagation, and to propose and verify a theory describing the extension of arc, and also the transition from corona to arc.

4.9.1. Subsidiary discharge along AC arcs

The initiation of a local arc across the air gap and the early stages of discharge development on the ice surface were carefully observed using the ultra-high-speed camera with an image intensifier and UV filter. It was observed that once the discharge was initiated along the air gap, it appeared as a bright common root (stem) emitting high-intensity light in the UV region. The discharge decayed as the current passed through zero twice every half cycle. After each re-ignition, the discharge appeared again along the air gap and propagated over the ice surface. At early stages, the arc length increased by a small value at each re-ignition. Also, the discharge tip emitted more light in the ultraviolet region as compared to the discharge channel. This could be related to the fact that ionization of the channel is mostly due to thermal ionization, which emits the light in the visible region, whereas the ionization occurring at the tip of the discharge is collision ionization. These findings are in accordance with the characteristics of leaders in long air gap discharge [98].

It was observed that besides the main channel, there were some subsidiary discharge regions, which also emitted high intensity light (Figure 4.26). These regions appeared as distinct luminous spots starting about 5 cm away from the discharge root, separated from one another by about 2 cm, and having the same alternating luminosity as the ac voltage source. During the development of the arc, UV activity in these areas was found to increase. Moreover, it was found that the speed of the main discharge underwent rapid and stepwise changes when approaching these areas. Hence, it may be concluded that ionization in these zones creates a space charge zone that governs and accelerates the growth of the main discharge.

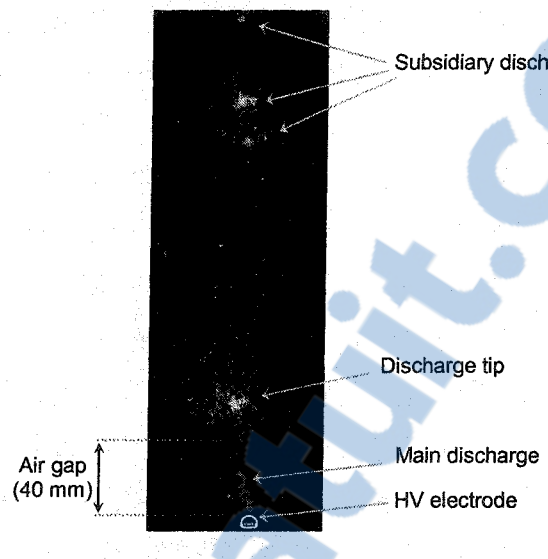

Figure 4.26. UV photograph of main and subsidiary discharge zones

4.9.2. Final jump

The arc propagation velocity was also studied using the high-speed camera in the visible range. At the early stages, the arc almost re-ignites to the same length after each alternation of ac voltage. When the arc develops on the ice surface and the arc length increases; the speed of propagation increases as well.

The final jump, the last stage of the flashover process, is characterized by a rapid increase in current, a brighter arc channel, and a greater propagation velocity, eventually leading to a short-circuit.

It was observed that, in the half-cycle before the one in which flashover occurs; the arc length reaches a considerable portion of the inter-electrode distance. However, because of the large variations of the observed cases, it is not possible to determine an exact lower

limit for this arc length, e.g. 50-60% of inter-electrode distance [85]. In some cases, values as low as 35% have been observed.

Even in the last half-cycle before the start of the final jump, the arc velocity increases compared to the previous half-cycle, e.g. for an arc which took 4.44 ms to elongate to 40 cm in the previous half-cycle, in the last half-cycle it will just take 2.67 ms to cover the same distance. It was observed that in this stage the discharge paths are exactly the same for both half-cycles, which shows that the previous discharge prepared a well-ionized and hot enough plasma trace for faster propagation in the next re-ignition.

We should also pay attention to the differences between the afore-mentioned final jump in the case of flashover on ice surfaces, and the final jump introduced by the authors for the final stage of spark breakdown of long gaps [98]. In the case of long gap breakdown, at the beginning of the final jump, the axial leader has an average velocity of about 1.4 cm/μs, which increases to a few m/μs during development of the final jump, when the leader reaches the other electrode [98]. In this case, for flashover on ice surfaces, the velocity of the arc does not exceed a few thousand m/s even before the flashover. The final jump for long gaps starts when the first streamers of the leader corona reach the other electrode [98], but the mechanism and nature of the final jump for flashover on ice should be different, considering the great difference between their propagation velocities.

Figure 4.27 shows the arc propagation, which eventually causes a complete flashover. In this case the applied voltage was 90 kV and the conductivity of the water used to form the ice was 400 μS/cm.

Figure 4.28 shows the temporal variation of the arc length, as well as the applied voltage and leakage current in the half-cycle in which flashover takes place. The applied voltage was 60 kV and the conductivity of the water used to form the conductive band was 500 μS/cm.

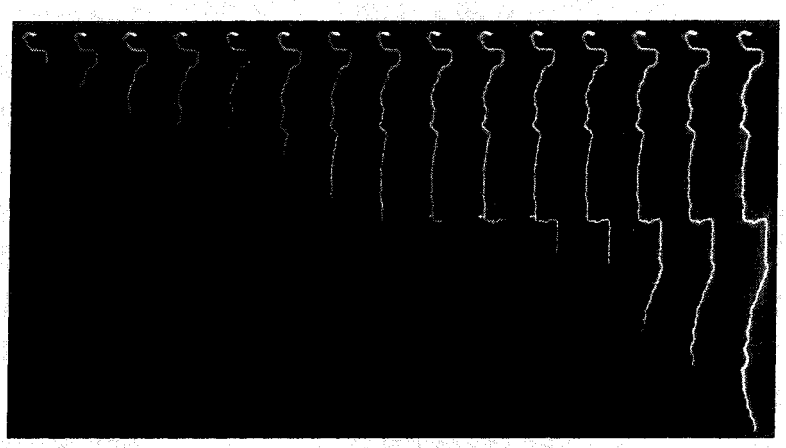

Figure 4.27. Photographs of the flashover process.
From left to right: Frames #1, 5, 7, 10, 17, 18, 19, 20, 25, 32, 33, 34, 35, 36 and 38. Recorded speed: 18,000 frames per second

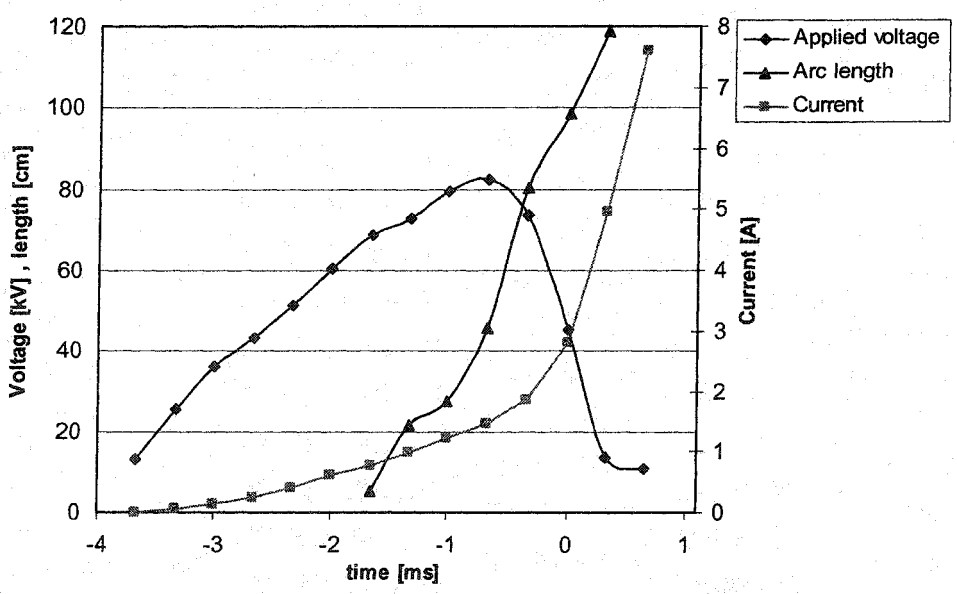

Figure 4.28. Simultaneous presentation of applied voltage, leakage current and arc root location in the last half-cycle before flashover

4.9.3. Effect of applied water conductivity

The effect of the conductivity of the water used to form the conductive band was also considered. Five different conductivities were selected: 200, 300, 400, 500 and 700 μS/cm.

The applied voltage was 90 kV in all the cases. At a conductivity of 200 μS/cm no flashover was observed, the conductive band melted completely, and the discharge activity stopped. At 700 μS/cm, the current in the propagation phase of the arc was so high that the transformer breaker was tripped. Therefore, for two of our cases no results are available. Figure 4.29 shows the effect of conductivity on arc propagation velocity before complete flashover. As seen, the higher the conductivity of water, the faster the arc propagates along the ice surface.

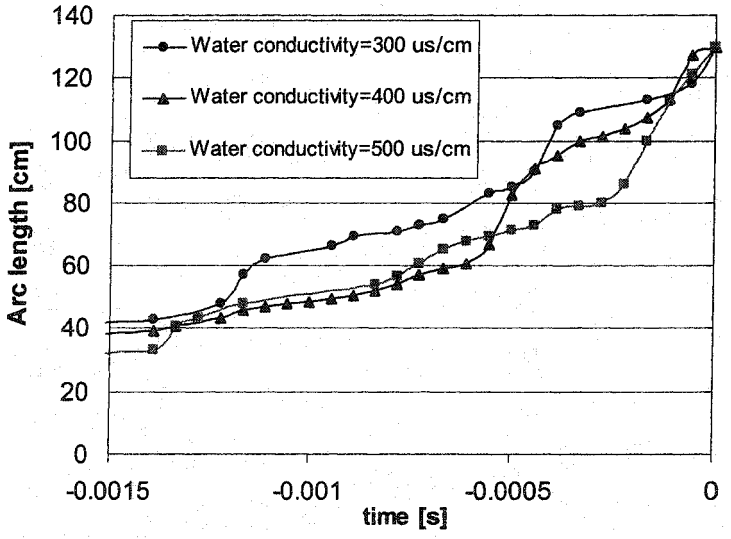

Figure 4.29. Effect of applied water conductivity on arc velocity

4.10. Conclusion

Different features of arc propagation over an ice surface were experimentally studied. A transition level in the current profile from glow to arc discharge was obtained. Arc channel radius versus current was measured and a mathematical relation was established. Arc foot geometry was found to be different under positive and negative polarities. Repetitive patterns in current profiles were observed. Using synchronic observations of measured current with video recordings, the arc decays were found to be responsible for this saw-tooth-like shape in the current profile. During the observation of the ultraviolet emissions ahead of the principal discharge, some bright spots with high ionization activity were detected. The effect of buoyancy forces on the propagation pattern of the arc, and the variation of arc diameter along the channel were studied.

CHAPTER 5

EFFECT OF WATER FILM AND AIR HUMIDITY

CHAPTER 5

EFFECT OF WATER FILM AND AIR HUMIDITY

5.1. Introduction

It is well known that the presence of a water film on the ice surface accreted on an insulator string is one of the main conditions for flashover to occur. This water film could be the result of various factors, such as wet ice accretion process, condensation, heating effect of leakage current, partial arcs, rise in air temperature or sunshine. The high conductivity of the water film originates from the rejection of impurities from the solid part toward the liquid portion of drops or droplets during solidification, and by pollution of the water and ice surface by the by-products of corona discharge. There is a large difference in surface conductivity of ice between dry and wet conditions, which makes the mechanisms of ice-covered surface flashover more complex than the same phenomenon on other surface materials.

In this chapter, using a simple ice setup in a horizontal position, the thickness of the water film will be measured and the effect of water film thickness and applied water conductivity on discharge initiation and propagation will be studied.

Another important parameter of discharge propagation over an ice surface is the relative humidity of ambient air, as in the case of air gap breakdown. Beyond the effect of water molecules in the air, which change the corona activity in the air discharges, they could also modify the ice surface parameters. In this chapter, the results of experiments on the effect of humidity on discharge initiation and propagation will also be described.

5.2. Effects of water film

Several tests were performed using different ice sample lengths, different water conductivities for ice construction, and different exposure times to ambient temperature, to create different thicknesses of water film.

According to the methodology exposed in Chapter 3, the resistance of the water film on the ice surface was measured. Figure 5.1-a, shows a sample test that illustrates the leakage current variation during voltage application. In this experiment, the voltage was increased to about 8 kV and kept constant for about 4 seconds, then the voltage supply was disconnected and the capacitors were discharged with a time constant depending on the capacitance, discharge resistance and setup resistance.

The resistance of the water film is also shown in Figure 5.1-b, as calculated from the ratio of applied voltage to the measured leakage current.

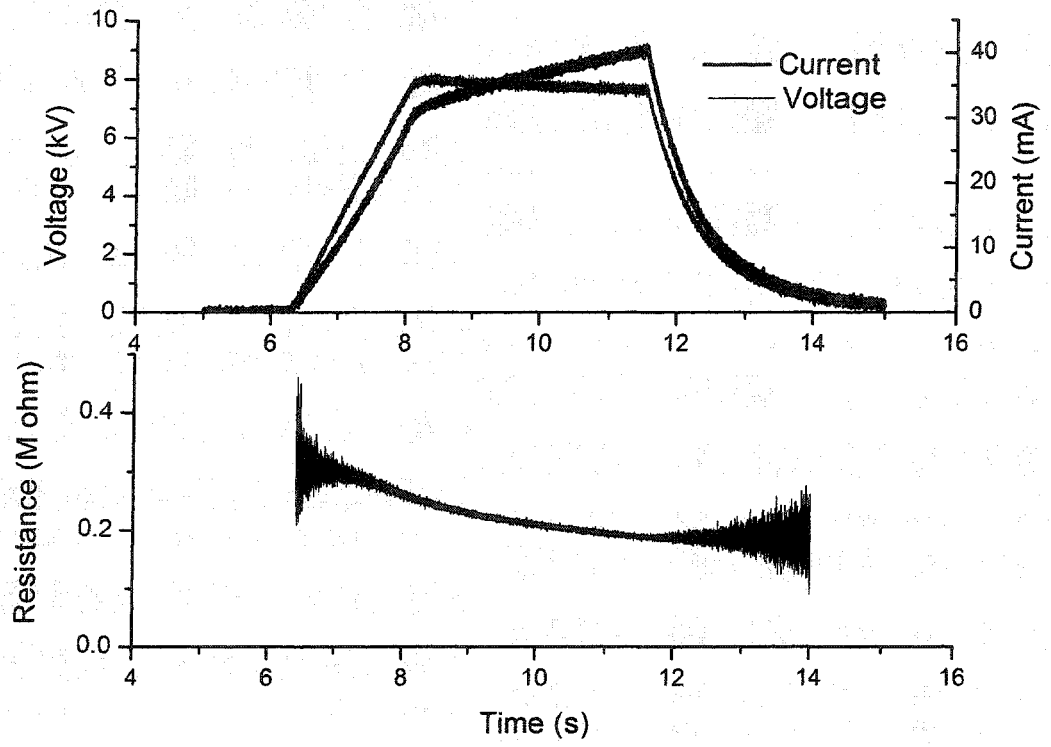

Figure 5.1. Variation of (a) leakage current and (b) resistance

The above experiment only served to illustrate the voltage application method, the rate of variation of resistance versus the elapsed time, and the intensity of flowing leakage current. In the following tests, the applied voltage was used to create a small leakage current, then rapidly removed to prevent excessive ice melting. The first readable resistance value was used to express the resistance of the water film built up on the sample.

Considering the ice geometry, the water film resistance could be calculated from the following relationship:

$$R = \frac{1}{\sigma}\frac{L}{Wh} \qquad (5\text{-}1)$$

Where R is the water film resistance, σ is the applied water conductivity, L and W are ice setup length and width respectively, and h is the thickness of the water film formed on the ice surface.

Table 5.1 shows the results of several tests with different ice lengths, different water conductivities, and different exposure times to ambient temperature (20° C).

In Figure 5.2, the water film thickness versus exposure time is represented for each experiment, as calculated from Equation (5-1). An exponential function was used to interpolate the resulting data. As shown, the correlation coefficient (R^2) is close to 1, thus this function could be used as the best fit for approximating water film thickness in the subsequent tests, in which the water film will not be measured because of the possible Joule effect from leakage current flowing through the surface.

5.2.1. Effect of residual resistance on discharge initiation

In what follows, the term "initiation current" will be used as the value of leakage current at the instant of arc inception. A linear correlation between the initiation current and the inverse of resistance of the water film was found. Figure 5.3 summarizes the results of measured initiation current versus different values of $1/R_{res}$. Note the linear relationship with a correlation coefficient (R^2) of 0.977.

Table 5.1. Measurement results for ice surface resistance

Water conductivity (μS/cm)	Ice length (cm)	Ice width (cm)	Exposure time (min)	Measured resistance (M Ω)
80	43	25	10	7.68
80	43	25	60	0.82
80	43	25	110	0.20
80	58	25	83	0.79
80	58	25	103	0.26
250	58	25	34	0.88
250	58	25	45	0.43
250	43	25	70	0.33
250	43	25	20	1.01
150	58	25	80	0.32
150	58	25	1	2.18
150	43	25	25	1.15

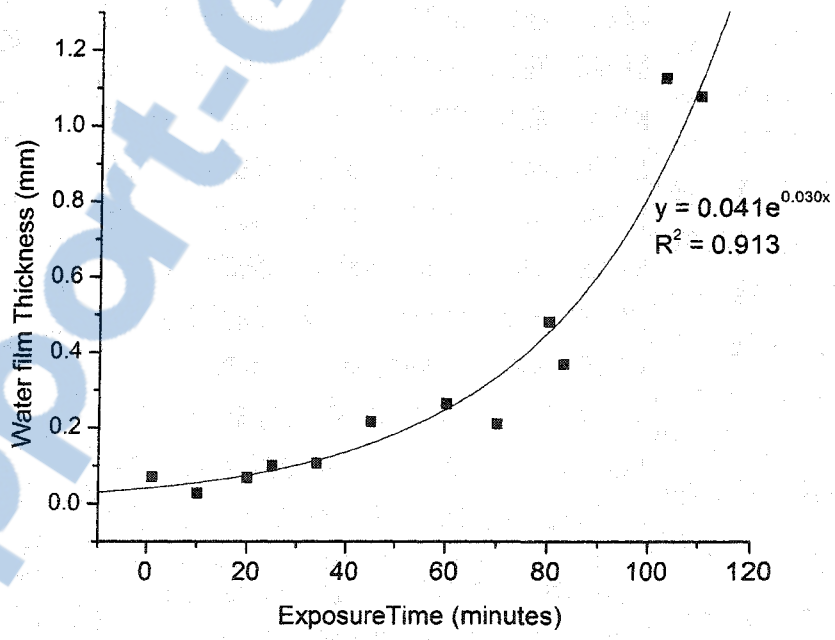

Figure 5.2. Water film thickness versus exposure time to ambient temperature (measured value and fitted curve)

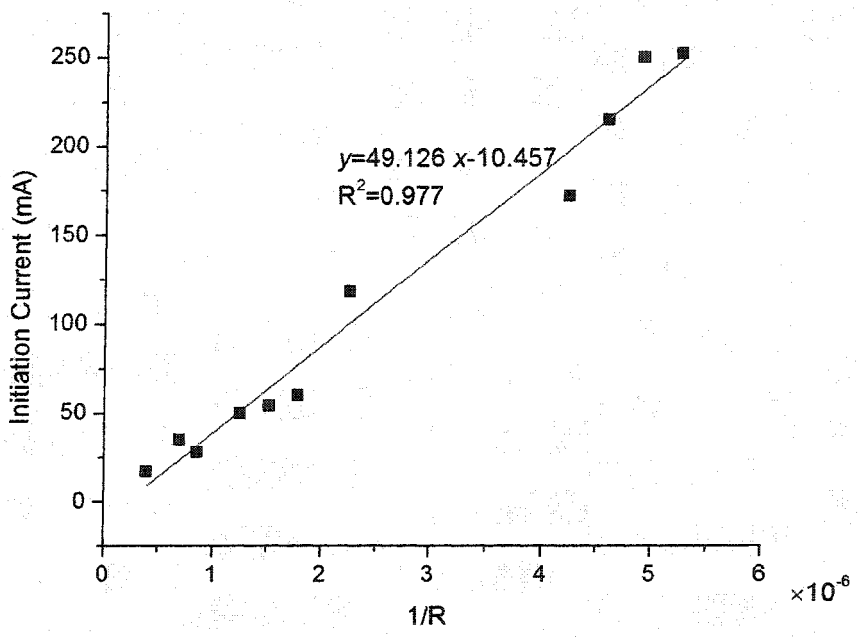

Figure 5.3. Measured initiation current versus different values of $1/R_{res}$

5.2.2. The effect of water film thickness on leakage current variation

To study the effect of the initial water film thickness on the rate of leakage current variation, the following experience was carried out. Two ice setups with identical dimensions were selected. Water with a conductivity of 150 μS/cm was used to form both ice samples. The first sample was exposed to ambient temperature for about 80 minutes, while the exposure time for second setup was 2 minutes. Figure 5.4 shows the variation of leakage current for these two samples. The current in the first sample starts from about 250 mA while for the second setup, the initial current was 27 mA. Note that the rate of leakage current increase following discharge initiation is different due to the different thicknesses of water film prior to voltage application. The next step was to examine whether or not this difference in the initial condition (water film thickness before voltage application) affects

the rate of current variation in the future stages. To this end, the leakage current curve for the second setup (2-minute exposure time) was shifted leftward to coincide with the other curve at 250 mA (Figure 5.5). Figure 5.5 shows that the rate of leakage current increase after 250 mA is nearly the same in these two cases.

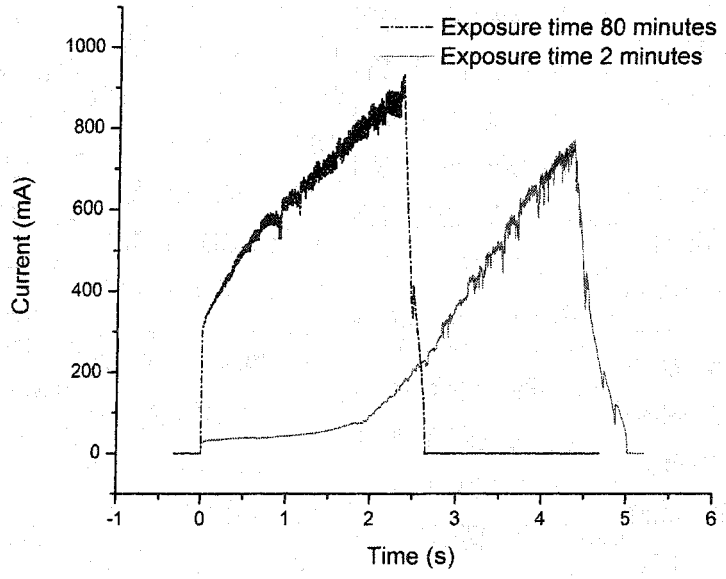

Figure 5.4. Leakage current variation for two different initial water film thicknesses

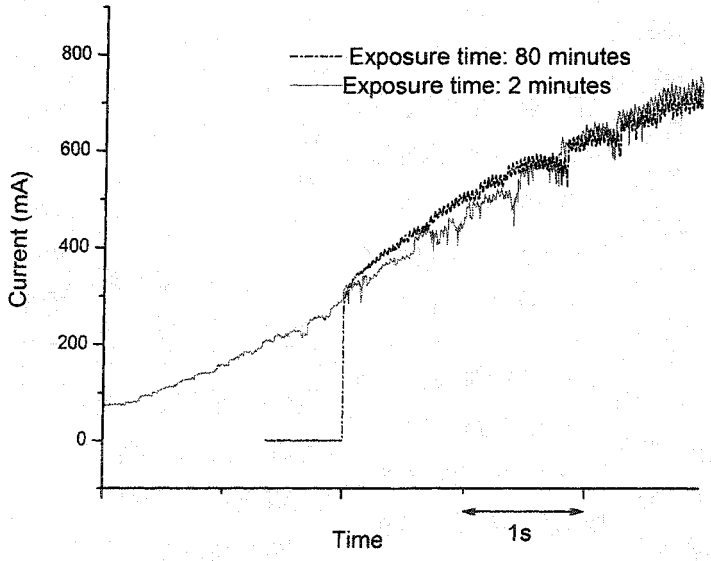

Figure 5.5. Shifted curves corresponding to Figure 5.4

5.2.3. Effect of water conductivity

Comparisons between the tests performed with different initial water film thicknesses and different conductivities are depicted in Figure 5.6. Note that the rate of increase of leakage current (particularly beyond 50 mA) depends only on the conductivity of water and does not depend on the initial conditions or ice length. Figure 5.6 shows that, for the same water conductivity, the current-time curves increase at the same rate. Three experiments with an applied water conductivity of 80 μS/cm show a current increase rate of about 100 mA/s, this rate is about 275 mA/s for 150 μS/cm, and 350 mA/s for 250 μS/cm.

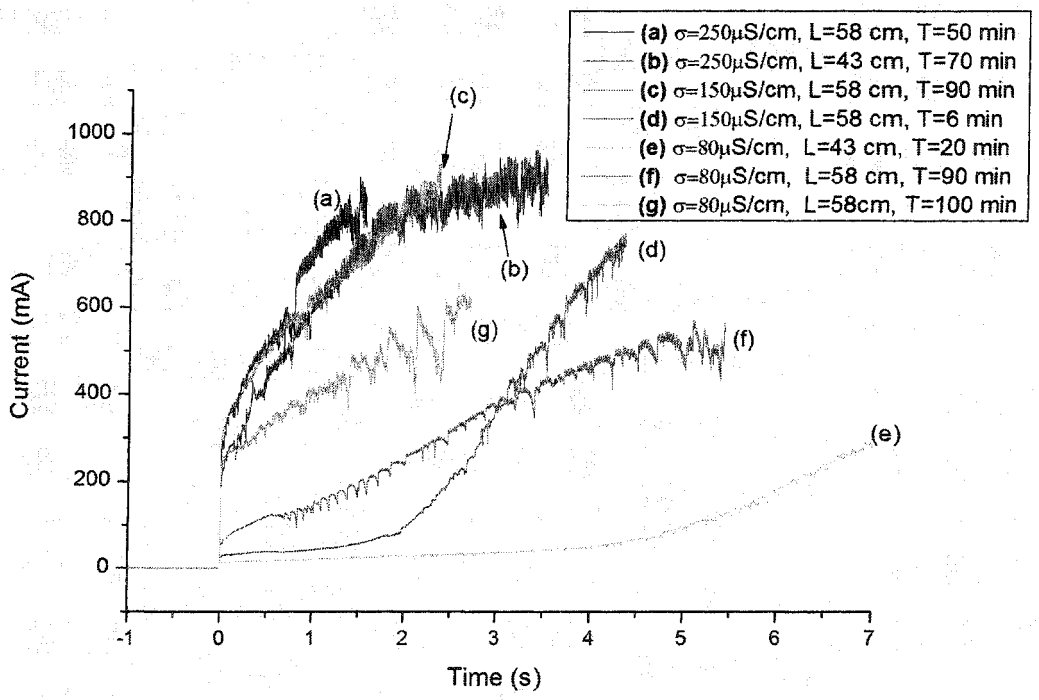

Figure 5.6. Leakage current variation for different tests
(σ is the conductivity of applied water, L is the ice length and T is the time that the setup has been exposed to ambient temperature)

5.3. Humidity effect

To study the effect of humidity, three different sets of tests were performed. Using a dehumidifier, the humidity of the test room was decreased to about 40 %, which is referred to as the "low humidity" condition hereafter. The air humidity for the "normal humidity" condition varied between 58 - 67 %. The "high humidity" condition was that obtained using a spray system. Humid air was produced by a water spray system using a nozzle, into which a high-pressure airstream was inserted. Water flows from the nozzle and the airstream causes the water to break up into tiny droplets, in the form of a fine mist. Using this method in the climate chamber, the relative humidity was increased up to 95 %.

Two categories of experiments were performed in order to study the humidity effect: inception and propagation of discharge. In the first category the emphasis was laid on the effect of humidity on the discharge inception voltage, while in the second type, special attention was paid to the discharge propagation characteristics (velocity, luminosity, discharge diameter and contact surface shape).

5.3.1. Effect of humidity on visible discharge initiation

The applied voltage was increased at a rate of about 5.5 kV/s until the first visible discharge was detected. This voltage was considered the inception voltage. For each test, two identical ice samples were chosen. The first one was used for water film thickness measurements and the second served as the test specimen. Using this method, it was

possible to measure water film thickness without disturbing the specimen used for studying discharge inception and propagation.

For three different humidity levels, a series of experiments were performed. Figure 5.7 shows the comparison of the results. Each data is the average of at least 3 tests performed in the same conditions. These results indicate that increasing the humidity from low (≈40%) to normal (58-67 %) level will cause an average increase of about 3 % in the discharge inception voltage. Comparing the inception voltages under normal and high humidity conditions (≈95%) also shows that increasing the humidity level will cause an increase in the inception voltage.

Another effect of humidity was found during water film measurements. Ice surface measurements were performed on three identical ice samples which were exposed to ambient temperature for the same time period. Figure 5.8 shows the results for two different tests (A) and (B), with different time exposures to ambient temperature, 5 and 60 minutes respectively. This figure shows that in test (B) the humidity level did not considerably change the resistance, whereas in test (A) the high humidity air considerably reduced the surface resistance. The reason is illustrated in Figure 5.9, where the measured water film thickness is shown. These results show that increasing the humidity from normal to high will cause the water film thickness to increase by about 0.08 mm. This increase of the water film thickness could considerably change the resistance of test (A), in which the water film thickness in the absence of humidity was a low value.

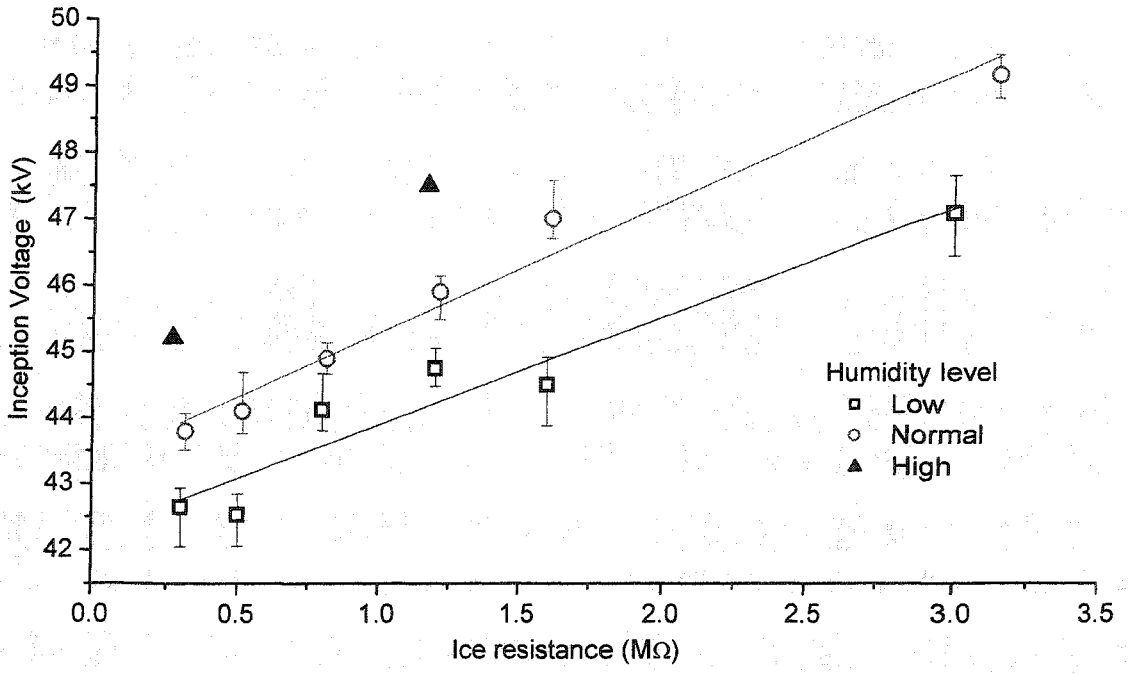

Figure 5.7. Inception voltage for different air humidity levels

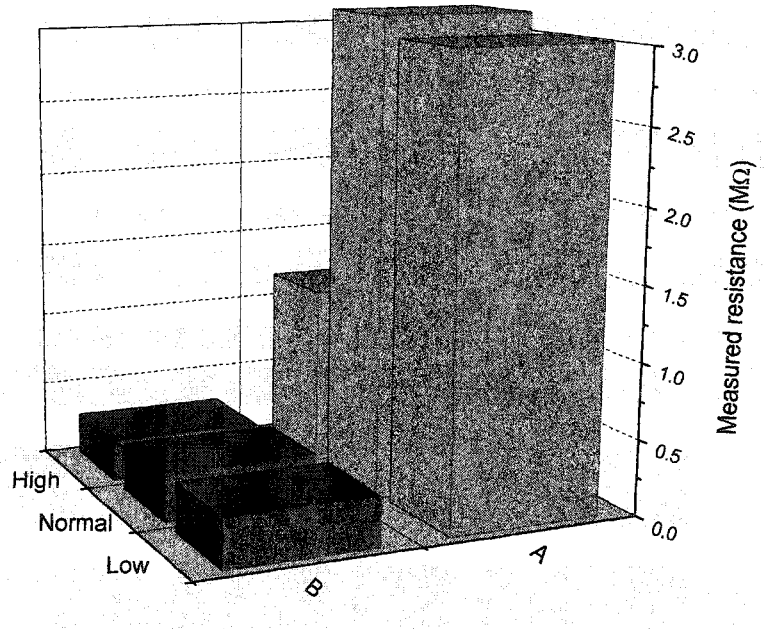

Figure 5.8. Measured resistances for three humidity levels using two different exposure times (A) 5 minutes (B) 60 minutes

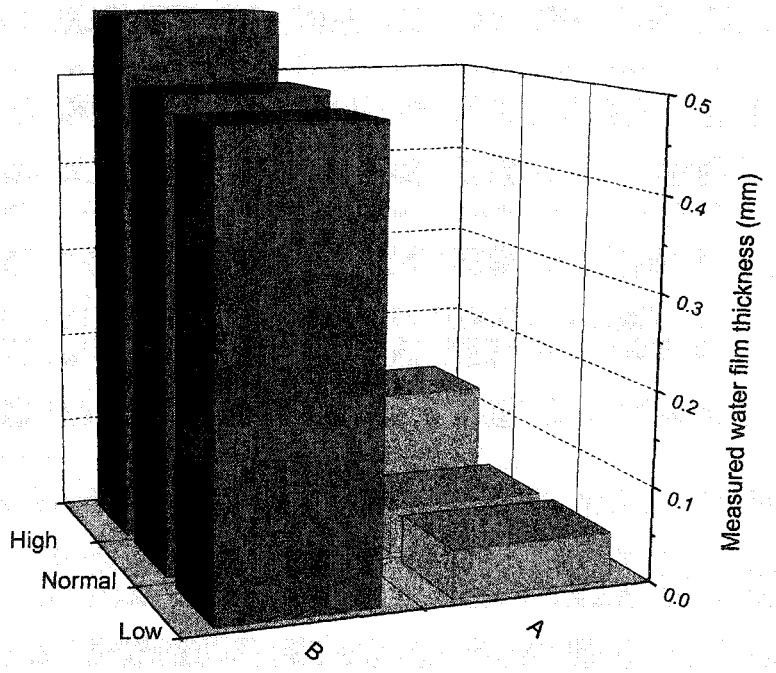

Figure 5.9. Calculated water film thickness for three humidity levels using two different exposure times (A) 5 minutes (B) 60 minutes

5.3.2. Effect of humidity on discharge propagation

During the discharge propagation, time lags were observed when the arc root seemed to stay still in its position for a few tenths of a second before suddenly continuing its forward motion. In all the experiments, this sudden elongation of discharge, similar to lightning flash restrikes, was observed. However, the frequency of restrike repetition and elongation do not show any correlation with ambient air humidity.

From video recordings taken in the same conditions, it was also observed that increasing the humidity level reduces the luminosity of discharge. The same results have been obtained from the Photomultiplier Tube (PMT) output signal. The PMT was placed at the same distance of 1m from the starting edge of the ice surface for all the humidity tests.

The output signal showed an overall reduction of about 21 % when humidity was increased from low to high air humidity conditions.

Regarding the humidity effect on the discharge elongation, it was observed that under the same applied voltage, the overall propagation velocity decreased with increasing humidity. Moreover, higher voltages were needed for supporting the development of discharge in high humidity.

5.4. Conclusion

In this chapter, using a simple method, the thickness of the water film on an ice surface was measured. The thickness of the water film was found to be a determinant factor of discharge initiation and initial current level. Conductivity of applied water for ice formation was found to be the decisive factor for the rate of current increase.

It was found that for a given ice surface resistance, increasing the air humidity will cause the discharge inception voltage to increase. The higher the humidity level is, the lower is discharge propagation velocity and luminosity. Increasing the humidity level can considerably change the thickness of the water film, which results in a notable decrease in ice surface resistance.

CHAPTER 6

INVOLVED MECHANISMS IN ARC PROPAGATION OVER AN ICE SURFACE

CHAPTER 6

INVOLVED MECHANISMS IN ARC PROPAGATION OVER AN ICE SURFACE

6.1. Introduction

As previously noted, discharge propagation mechanisms over an ice surface differ from that of a discharge propagating over a dielectric material, or of a metal substrate; although the water film may perform as both a dielectric of high permittivity and a conducting substrate [99].

In this chapter, based on the experimental results presented in Chapters 4 and 5, physical explanation for observed phenomena during arc propagation will be proposed. Space charge distribution along the arc column and its sheath as well as in the arc foot will be explained. The results will be used to describe discharge propagation patterns, arc columns and foot geometries. Potential forces acting on the discharge column during the propagation will be discussed. The effect of water film thickness and conductivity on discharge initiation and propagation will also be discussed. The resulting effects of humidity, due to ambient relative humidity or water evaporation from discharge root, will be explained.

6.2. General appearance of arc column

6.2.1. Glow-to-arc transition threshold

The threshold current I_C could be considered as a transition current from glow-to-arc discharge. The sudden increment in the rate of variation of leakage current could also be due to a change in the ionization mechanism beyond the threshold level. At this current level, the arc channel becomes hot enough for thermal ionization to start. This accelerates the melting of ice in the vicinity of the arc root, thus increasing the surface conductivity, which in turn decreases the residual resistance and increases the leakage.

6.2.2. Arc radius and leakage current

According to the Bazelyan and Raizer's arc model [100], as the conductivity of the arc column is a definite function of temperature, the current may actually flow only inside a thin channel of radius $r_0<R$, where r_0 is the radius of the observed central core of high intensity light, and R is the radius of the total observed arc, including the weak intensity light zone.

6.2.3. Space charge distribution around the channel

The conductivity of the plasma channel is sensitive to the temperature, so that most of the current will flow within the high-temperature region. The radii of the current-carrying channel core and the corona sheath differ from each other. The radius of the

corona sheath may be estimated as the charge extends outwards, until the field at the outer boundary of the corona sheath equals the critical field necessary for streamer propagation.

The charge transported by discharge root and core is accumulated like a space charge cover around the channel. Similar to the leader cover, this sheath is not rigid, but there is continuous charge redistribution inside it, which may be accompanied by ionization events in the radial field at the channel surface [100]. To explain the process occurring in the sheath, the corona theory may be used, since all basic corona features are the same, except that we deal here with a plasma channel instead of an electrode. The sheath is dynamic and its linear charge varies with the arc evolution. Due to the similarities of this sheath to the observed leader cover [100], the same theory may be used to describe the charge distribution inside it. Only in the case of a rapid rise of voltage, the cover charge can be unipolar and have an increasing linear density (owing to the incorporation of charge of the same sign). This happens when the field near to the ice surface is positive and exceeds the corona ignition threshold. If the voltage decreases, remains constant or rises slowly, as observed in our case, the cover becomes two-layered: the outer layer charge has the same sign as the ionization zone at the tip of the arc on the ice surface and the inner layer charge polarity is opposite. The presence of two ion space charges in the case of both negative and positive corona around the cathode and anode has also been confirmed in [101].

6.2.4. Arc radius variation along the arc channel

At low current levels, i.e. less than 30 A in air, the controlling process is natural convection instead of magnetic forces [102]. When the arc is vertical, the input electrical energy produces arc plasma which is carried upward by natural convection. The integrated flow of enthalpy across any arc cross section is taken to be equal to the total input electrical energy upstream of the axial position being considered. Thus, the arc radius increases as a function of distance from the lower electrode.

6.2.5. Arc channel luminosity

The difference in the luminosity of positive and negative arcs may be related to the differences in sodium ion densities in the arc channel, as demonstrated by the existence of two bright sodium lines in the arc spectra [103]. There would be more Na in the partial arc extending from the electrode with positive voltage than in the arc originating from the negative electrode. Sodium atoms would be supplied from the arc roots and transported into the channel by diffusion. The numerous arc roots in the positive arc supply more sodium from the electrolyte forming on the ice surface to the arc channel. This will increase the luminosity of positive arcs.

6.3. Arc propagation pattern and features

6.3.1. General pattern

Regarding the repetitive pattern of arc re-ignition under dc voltage, this phenomenon is very similar to a gliding arc mounting up a Jacob's ladder [104]. The length of the arc increases together with its voltage; its power increases up to the maximum value depending on the source. During this quasi-equilibrium stage, the gas temperature does not change significantly. The non-equilibrium stage starts when the length of arc exceeds a critical value. Heat losses from the plasma column begin to exceed the energy supplied by the source, and it is not possible to sustain the plasma in quasi-equilibrium state. Then, the plasma rapidly cools down while conductivity is sustained by high electron temperature. After departure from non-equilibrium discharge, a new breakdown takes place at the shortest distance between the arc channel and ice surface, and the cycle repeats.

Convection heat transfer can be classified according to the nature of the flow as forced convection and free convection. A free convection flow field is a self-sustained flow driven by the presence of a temperature difference, which is opposed to a forced convection where external means are used to cause the flow [105]. Natural convection fluid motion is due solely to the buoyancy force caused by the density differences as a result of the temperature difference [105]. This force is a strong function of the temperature difference between two mediums. As such the buoyancy force will induce a flow current due to the gravitational field and the variation in the density field.

Arcs allowed to burn without constraint in open air are quite mobile and rarely exhibit steady-state behavior [93]. Electric arcs with currents of less than 20 A, which is the case in this study, generally have small self-magnetic fields, and if there is no imposed pressure gradient, the only term producing flow is gravity [106]. For horizontal arcs, gravity causes convective flow upward through buoyancy and natural convection, making the arc bow upward in the center, so that the discharge forms the shape of a circle's arc. Vertical arcs are also subject to buoyancy flow, driven by gravity, which is directed upward from the bottom electrode. The principal feature of such arcs is that their radius steadily increases from the bottom electrode.

6.3.2. Major and minor collapses

When arc length increases to more than the critical value beyond which the plasma cannot maintain its conductivity, the channel core cannot create enough electrical field of opposite sign at its surface. Therefore, the sheath of space charge cannot be removed from the channel; consequently for positive arcs, the positive charge increases. This may cause the field to increase between the arc column and the ice surface, which attracts the sheaths toward the surface. The question that may be raised after this discussion is: In major collapses, why is the arc column, and especially its sheath, attracted toward the ice surface, while in minor collapses the two arc columns do not show any considerable tendency to move toward each other? The answer may be found in the aspect of the space charge sheath around the arc core. In DC positive, the sheath carries positive charges. The electrostatic

force between the positive charges in two parts of the arc loop, which will be short-circuited later by a streamer starting from a more positive point (acting like the anode), prevents them from coming closer together. On the contrary, in the case of major collapses, the arc column, which is free to move, can be pulled toward the ice surface with no opposition.

In the case of a DC-positive major collapse, after the contact of the new streamer with the surface, the subsequent events could be explained as follows: The positive charges of the cover will be neutralized by electrons detached from the cathode (ice) surface. Following contact (Figure 4.11d), a neutralization wave passes along the channel. The strength of this wave depends on channel conductivity. Considering that the conductivity of the old arc channel has decreased greatly and this new path is also shorter, the current tends to divert to it. This causes an additional increase in conductivity, increasing the temperature and providing the conditions for thermal ionization to occur, which finally redirects the arc to this new shortcut.

The average voltage gradient required for the propagation of positive streamers is estimated to be about 5 kV/cm; it is in the order of 10 kV/cm to 15 kV/cm for negative streamers [107]. This is in agreement with the values reported by the Les Renardieres Group [108]. This may explain why the initiatory streamer of major and minor collapses under both positive and negative arcs in all cases starts from a more positive point, which acts like an anode whether it is located on the ice surface, HV electrode or along the arc column.

Let us consider a minor collapse where the distance between two edges which are going to join together was about 2 cm. Assuming the minimum required gradient for a positive streamer, the voltage difference between these two points should be about 10 kV (2 cm multiply 5 kV/cm). The loop length (i.e. the arc length which will be short-circuited by the new streamer) was about 5 cm. Thus, we could conclude that there is an average voltage gradient of 2000 V/cm (10 kV/5 cm). If we want to use the normal V-I characteristics of positive arcs on an ice surface from the results of [71] (considering the arc current which was about 100 mA), a value of about 588 V/cm is obtained. This is due to the fact that at this stage, the arc column is in a state of non-equilibrium, leading to lower conductivity and, consequently, a higher voltage gradient compared to the value reported in [71]. It also confirms the observation made in Section 4.8 and the necessity of using a critical V-I characteristic along with the standard static one.

In the case of a major collapse of a negative arc, the streamers initiate from regions of non-uniformity on the ice surface, and sometimes from the water drops acting like electrode points. The electric field in these regions is large enough to initiate positive streamers toward the arc channel. As mentioned above, the velocity of streamers decreases rapidly as they penetrate the low field region near the arc sheath.

A schematic diagram of the space charge distribution along the arc channel and in the new streamers initiated at the ice surface is depicted in Figure 6.1. We have already seen that the arc channel with negative voltage is surrounded by two space charge regions. The inner layer contains positive ions while the outer holds negative ions. The positive streamer initiated at the ice surface has a positive space charge at the tips of avalanches.

Upon the formation of this streamer, some parts of the leakage current will divert from the previous arc root to this new path. It will decrease the current through the old arc channel, decreasing the voltage gradient inside it. This will decrease the negative charge density in the outer layer of the arc sheath, which consequently weakens the electric field intensity in the gap. This could explain the large decrease in the streamer propagation velocity near the arc sheath, as shown in Figure 4.16.

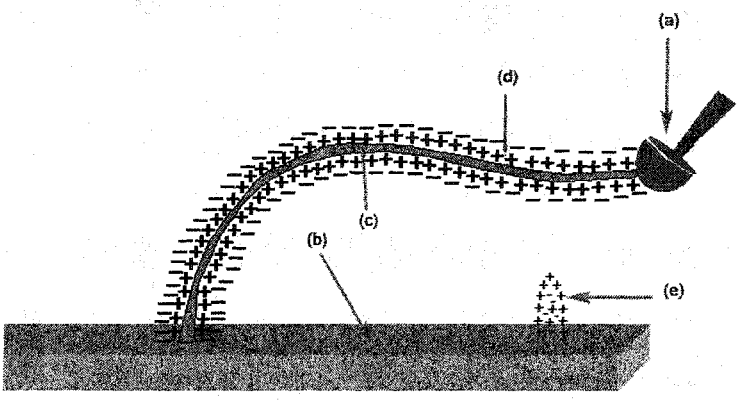

Figure 6.1. Space charge distribution during a major collapse in DC-negative: (a) HV electrode, (b) ice surface, (c) arc core, (d) arc sheath, (e) newly formed positive streamer from the ice surface

6.4. Anode and cathode current jumps

The differences observed in the current waveforms in Figures 4.21 and 4.22 could be explained as follows: While a cathode-directed streamer (positive streamer) is developing to cause a major collapse in DC-positive, the measured conduction current through the cathode remains unchanged until contact (Point b of Figure 4.21). Then, it suddenly increases, indicating the beginning of the charge neutralization process at the head

(Point c of Figure 4.21). On the other hand, for negative arcs, consequent to the initiation of a cathode-directed streamer (Point a in Figure 4.22), a sudden jump is detected in the current measured at the anode. This current is the sum of the conduction current flowing into the old arc channel, which continues to carry current to the high-voltage electrode, and the displacement current resulting from the newly developed streamers from the anode (ice surface).

6.5. Water film

It was observed that the thickness of the water film prior to the discharge inception is a determinant factor. This value along with the conductivity of the applied water and ice dimension determines the residual resistance of the ice. A linear relationship between the initiation current and the inverse of residual resistance has been established. It shows the important effect of water film thickness in the initiation of discharge. However, the results showed that in the later stages (after a few seconds from the discharge initiation) the melting effect generated by the arc results in reducing the importance of initial water film thickness. From the comparison of two cases with the same conditions, except for initial water film thickness, it was observed that although the current starts from a higher value when the initial water film is thicker, the rate of current increase is the same. This shows that if there is enough ice, the two cases behave similarly regarding flashover. But if the ice is too thin to produce more conductive layer, the result will be different. In the case of less

initial water film, the ice may melt down completely before the current can increase sufficiently to cause the arc to develop until flashover.

From the measurement results, it could be concluded that although water film thickness is mostly an important factor of discharge initiation, applied water conductivity also has a significant effect at all stages. Considering the same amount of water film, the higher the conductivity of applied water is, the lower is the residual resistance of the ice surface. This leads to higher current flow and, consequently, a higher ice melting rate leading to increased current as well. The current-time curves of different applied water conductivities showed that there is a direct relationship between the slope of current increase and water conductivity.

6.6. Effect of humidity

Regarding the effect of humidity on the inception voltage, two opposite influences were observed. The first is the same as that noted for air gap breakdown, which is the result of an increase in the attachment coefficient and a decrease of photoionization activity due to the presence of water molecules. The consequences are a decrease in corona activity, an increase in discharge inception voltage, and an increase in the streamer and leader voltage gradients.

The second effect is a consequence of the formation of a water film, or addition to it, on the ice surface. As this water film increases the surface conductivity, it causes a reduction in the residual ice resistance, thus decreasing the voltage drop along the ice

surface, and consequently increasing the voltage drop along the air gap. Additional effects may be due to changes in surface permittivity, and consequently in the secondary ionization processes along the surface.

Comparing the results for low and normal air humidity conditions showed that increasing the humidity level results in higher inception voltage. The difference in water contents in low and normal air humidity conditions was about 3.5 g/m^3 (from 6.9 to 10.4 g/m^3). The corresponding average increase in inception voltage was about 3.32 %. This increase is in the order of 1 % for a 1 g/m^3 increment of water content in air [74]. Thus, it can be concluded that in this region the first effect, decreased ionization activity in the presence of water molecules, is dominant.

The difference in absolute humidity between normal air with LWC of 10.4 g/m^3 and humid air with LWC of 15.6 g/m^3 resulted in an inception voltage increase of about 3.5 %. As previously mentioned, however, this increased humidity level causes a substantial decrease in ice surface resistance due to an increase in the water film thickness. This could explain the reverse effect of humidity from normal to humid air when the water film thickness is very low; an additional 0.08 mm in thickness could significantly change the ice resistance. However, when the water film thickness is too high, the additional water film due to humidity is negligible, and a direct increase in inception voltage can be observed by increasing the humidity level.

Concerning the effect of humidity on discharge propagation, it was observed that under the same applied voltage, the overall propagation velocity decreases with increasing humidity. Moreover, higher voltages are needed to support the development of discharge in

high humidity. This could be due to the larger voltage gradient in humid conditions. From the results reported in [34], the voltage gradient in a 100 mA arc in air is about 350 V/cm, while it is about 900 V/cm at the same current level for an arc burning in steam. This large difference, which is the result of the presence of water molecules, leads to higher voltage drops on the arc column. Considering the rough criterion of $E_{arc}<E_{residual}$ for arc propagation, increasing the arc voltage gradient provides less favorable conditions for its elongation.

The decrease in discharge channel luminosity with increasing humidity could also be a direct result of the lower ionization activity in humid air. However, this observation could not be quantified, as the available optical techniques may be misleading due to changes in luminosity proper to humidity.

As mentioned earlier, regarding the sudden displacement of discharge, no considerable influence was observed. However, the similarities in this sudden elongation of discharge channel with the restrikes in the long gap breakdown might be helpful in understanding the propagation mechanisms in our case.

During the discharge propagation on the ice, water vapor is present in the close vicinity of arc root due to heating effect. Because of the presence of water molecules in this region, a situation can be reached in which the streamer activities are so low that the discharge propagation practically halts. However, current will be supplied from the arc root to the channel. In this condition, the arc length is constant but the current increases due to the increase of ice surface conductivity and consequent decrease in residual resistance. This will decrease the voltage gradient in the arc column, resulting in an increase in the local

electric field at the arc root. When the electric field exceeds the necessary value for streamer inception, new discharges can start from the arc tip. This leads to the sudden elongation of the arc channel.

6.7. General discussion on the mechanisms of arc development

As noted earlier, mechanisms of discharge propagation over an ice surface differ from those of discharge over a dielectric, or electrolytes. Water has a significantly smaller secondary emission coefficient than most metals [88], leading to significantly different electrode properties.

In our experimental results, the development of an anode-directed streamer was invariably predominant, regardless of the polarity of applied voltage. Thus, the fact that the electric field is considerably enhanced ahead of the arc root may be considered as experimentally established. The origin of this enhancement is the transfer of the high-voltage electrode potential to the leading edge of the arc column due to its high conductivity. High electric conductivity of the arc channel at currents above the glow-to-arc transition threshold indicates that we are dealing with an arc discharge. Thermal ionization is responsible for the generation of charged particles in such a discharge. Propagation of the arc front is due to various mechanisms of energy transfer and ionization state from the arc column to nearby layers of unheated gas; these mechanisms include thermal conduction, shock wave, radiant heat exchange and diffusion of electrons.

In the early stages of arc propagation, the velocity of discharge advancement is low. Thus we may hypothesize that the main mechanism responsible for discharge propagation in this phase is related to thermal conduction transport of heat to the region of unheated gas with subsequent thermal ionization of this gas. However, even in this phase, small ionization avalanches were observed. They appeared either away from, or into, the moving tip of the discharge depending whether the high voltage electrode is positive or negative. The presence of these streamers shows the presence of collision ionization in this phase. A hypothesis that is also supported by observing the emission of high intensity light in the ultraviolet region from the tip of arc. High intensity light in this region is an indication of the existence of collision ionization. Hence, it is logical that the speed of propagation of the tip be expected to increase as the air above the unbridged surface became increasingly stressed since the individual avalanches would develop more quickly and extend further as the field became greater. Subsidiary branched and hair-like discharges would be expected to be generated for the same reason. The ionization activity in the discharge tip depend on the electric field strength and the rate of production of electrons which initiate the discharge in air in front of the tip. These electrons are produced mainly by photo-ionization of neutral molecules and photo-detachment of electrons from negative ions. In this phase, in addition to these forces, the rising of hot gas in the arc column due to buoyancy force is acting on the discharge.

The arc continues to propagate until the voltage drop in the channel reduces the root potential to a value insufficient to supply the necessary energy for ionization, dissociation and heating of the gas in the forward direction. It should be emphasized that, beyond a

certain value, the energy supplied from the unbridged section can no more support the voltage drop in the channel. The first reason for this halt in the propagation is to be related to this phenomenon. However, the presence of water molecules in the discharge tip, because of high humidity or direct evaporation of water from the heating effect of arc, could have an important impact. These water molecules cause a decrease in corona activity and photoionization, which could cause the discharge propagation to a pause. This halt, caused either by excess voltage drop in the channel or trapping in a humid area which reduces the activity at the discharge tip, may or may not resume. If the input energy increases the arc may continue to propagate forward. This increase in energy could be due to either an increase in applied voltage or a decrease in the resistance of the unbridged section. Current flow through the unbridged section is accompanied by melting ice that could result in an increase in surface conductivity, and consequently a reduction in the residual resistance.

Now, let us consider the instant before starting the final jump in which the propagation velocity increases suddenly to a very high value. As the total current increases, the temperature and electrical conduction of the channel rises. The effect of enhancement of the electric field strength ahead of the discharge root becomes more and more pronounced. In this case, a change of the discharge propagation mechanism could occur. Electrons in the channel diffuse into the region of heated gas and are subjected to a high electric field, where they ionize the gas. The propagation regime thus developed is similar to that occurring during corona discharge, but with efficient transfer of excess negative charge to the ice surface. As this takes place, the collision ionization process in the enhanced electric

field may become the main mechanism of discharge. This is the reason why in the last stage of flashover process (final jump) the propagation velocity increases suddenly in a non-reversible manner, leading to short-circuit.

6.8. Conclusion

The bright, highly conductive central core of the arc channel carries the current, while the arc sheath contains a corona-like weak ionization region. The radius of the central core increases with current. The arc sheath is two-layered: the outer layer charge has the same polarity as the ionization zone at the tip of the arc on the ice surface, and the charge polarity of the inner layer is opposite. As it propagates, the arc exhibits some types of decay resulting from space charge distribution in the arc channel and ice surface.

A linear relationship between the initiation current and the inverse of residual resistance was established. It shows the important effect of water film thickness on the initiation of discharge. A direct relationship between the slope of current increase and water conductivity was found.

Humidity will increase the discharge inception voltage and arc voltage gradient, and decrease the overall propagation. The presence of water molecules, originating either from ambient air humidity or water vaporization from the arc root, will cause strike-like propagation.

The conclusion drawn from the experimental observations was that during the early stages of arc propagation the mechanism related to thermal conductivity is responsible for

development. However, the buoyancy force, electrostatic force and collision ionization in front of arc root have considerable effect in the arc propagation pattern. The mechanism of flashover was related to the transfer of the electrode potential to the arc tip as a result of high conductance of the arc channel and the development of a region of high-strength electric field ahead of the discharge tip. As this takes place, the process of collision ionization in the enhanced electric field may become the main mechanism of arc propagation.

CHAPTER 7

CONCLUSIONS AND RECOMMENDATIONS

CHAPTER 7

CONCLUSIONS AND RECOMMENDATIONS

7.1. Conclusions and Contributions of the Thesis

1) An original test setup configuration was developed, allowing the recording of the optical parameters in the ultraviolet and/or visible region synchronized with electrical parameters, e.g. voltage and current. This was achieved using an ultra-high-speed camera and an image intensifier synchronized through a data acquisition system with electrical measurements.

2) Features of propagation of an arc over an ice surface were studied experimentally using the established methodology. The main findings are summarized below:

a) During the observation of the ultraviolet emission ahead of the principal discharge, bright spots with high ionization activity were detected. They might originate from corona activities near non-uniformities on the ice surface. When the main discharge reaches these zones, its velocity undergoes rapid and stepwise changes; hence it was concluded that ionization in these areas creates a space charge zone which governs and accelerates the growth of the main discharge. Such a

subsidiary discharge with this characteristic, and occurring far from the main discharge, has not been reported elsewhere for other surface materials.

b) From the comparison of the intensities of ultra violet emissions, it was concluded that the ionization occurring at the front of the discharge is collision ionization, whereas thermal ionization plays a larger role in ionization occurring in the channel.

c) The shape of the foot discharge was not found to be circular, as other researchers have pointed out. It consists of numerous branches that contribute to conducting the current to the ice surface.

d) Two different regions in the arc channel were detected. The interior one is a very bright core surrounded by an envelope which is not as bright as the core. The diameters of these regions were measured versus the variation of leakage current. The corona discharge around the current carrying part of the arc column was found to be responsible for the emission of a low-light-intensity envelope around the arc core. The presence of opposite space charge zones in this sheath could explain the differences in the behavior of newly formed streamers, their propagation velocity and the current jump in the leakage current measurements.

e) The effect of buoyancy force on the propagation pattern of the arc and the variation of arc diameter along the channel were observed and discussed.

f) The formation of the white arc begins with a remarkable change in discharge color: thin filamentary violet partial discharges suddenly transform into a thick white channel. This transition is also associated with an increase in the arc

current level and its rate of variation. From the data recorded from leakage current measurements through the data acquisition system, the threshold current was measured to be about 20 mA. Such glow to arc transition results from a change in the ionization mechanism. Below this threshold, collisional ionization takes place in the filamentary discharge channel, whereas above this value, thermal ionization could initiate and contribute to supplying energy to the arc column.

3) The arc propagation velocity during the whole process was measured. Under the experimental conditions of the present study, no minimum velocity similar to 10^6 cm/s [26] in air was observed. Generally, an arc requires a high ionization degree of the head gas, and enough energy to heat it to "arc temperature" and to compensate for heat losses. In the case of air, this energy is supplied by the total current from ionization activity at the front of the leader. In our case, when the arc develops along a conducting surface, the energy supply mechanism changes. The energy is supplied to the channel by leakage current through the contact surface between the arc and the electrolyte surface. Thus, the energy flow into the channel is determined by the resistance of the water film rather than by gas or plasma characteristics.

During the early stages of arc formation, the conductivity of the unbridged section is too low. The flow of leakage current through ice the surface is accompanied by Joule effect and the formation of a water film. This increases the surface conductivity and, consequently, the leakage current as well, thus supplying more energy to the arc channel and accelerating its development in the later stages. The study of the effect of conductivity

of the water utilized to form the ice also confirmed the proposed hypothesis. As conductivity is increased, more energy is supplied to the discharge channel, which accelerates propagation.

4) The final jump, the last stage of the flashover process, was studied experimentally. It is characterized by a rapid increase in current, a brighter arc channel and a greater propagation velocity, eventually leading to short-circuit. However, for flashover on ice surfaces, the velocity of the arc does not exceed a few thousand m/s even before the flashover. Based on the observations from high-speed imaging, it was proposed that at this stage, this is a result of propagation of a streamer-like discharge from the tip of the arc root. However, the necessary condition for continuous development is the existence of minimum electric field in the unbridged section. From the higher velocities noted at this stage, it was concluded that air breakdown in front of the arc foot is the dominant mechanism.

5) In order to study the effect of polarity on the propagation of discharges DC-positive and DC-negative arcs were closely observed using the high-speed camera. These results revealed many differences in the structure of DC-positive and DC-negative discharges, which may explain the effect of polarity in the DC withstand voltage of ice-covered insulators.

a) The arc exhibits a number of arcing modes dependent on the magnitude of current and length. Based on the analysis of leakage current measurements and arc elongation, it was concluded that to improve the modeling a mean gradient

curve should be considered, as well as a critical gradient curve instead of the customary V-I characteristics.

b) Close observation of negative and positive DC arcs showed differences in their appearance. The negative arc was relatively thick and had a thicker tip, while the positive arc was thinner and had some large branches at the tip. Furthermore, the positive discharge was brighter than that of negative polarity.

6) In the view of studying the effect of humidity, arc propagation was examined experimentally at three different humidity levels. It was observed that increasing the air humidity would cause the discharge inception voltage to increase and provide less favorable elongation conditions. If humidity significantly increases the water film thickness, it would decrease the inception voltage. But increasing the humidity generally decreases ionization activity, increases arc column voltage gradient, and reduces the propagation velocity and arc brightness.

7) Sudden elongation in the discharge development similar to restrikes has been noted. The presence of water molecules in close vicinity of the arc root has been considered to prevent discharges from elongating. However, this will cause the current to increase, leading the arc voltage gradient to decrease and, consequently, an increase in local electric field and initiation of new streamers which elongate forward rapidly.

8) Experimental studies were carried out to analyze the effect of water film thickness and applied water conductivity on arc propagation over an ice surface. The thickness of the water film was found to be a determinant factor for discharge initiation and initial current level. The conductivity of the water used for ice formation was found to be the decisive factor for the rate of current increase.

7.2. Recommendations for future work

1. Streamer propagation has already been studied [26, 87] at the CIGELE laboratory using the existing framing camera (IMACON200). The above research was performed to observe the visible discharge on an ice surface. Due to the limited sensitivity of the camera's photocathode, which is designed to work in the visible region, UV activity could not be observed. The available image intensifier (Invisible® Vision UVi) with a spectral range from UV to NIR could be mounted on the IMACON camera. This combination makes it possible to take the advantage of a wide spectral range of image intensifier as well as short exposure time, which can be set as low as 5 ns. It is recommended to use this system to observe streamer propagation on an ice surface, which is expected to result in valuable information. (Note: special attention should be paid to protecting the image intensifier from overexposure)
2. Using the results obtained during this research the effect of polarity was found to be very important. In a previous work [109] the identification

method was used to determine the residual voltage of an AC discharge on an ice surface. It is expected that if the acquired data for negative and positive half cycles were processed separately, more correlated results would be found. It is recommended to apply the developed artificial neural network to determine the residual voltage for positive and negative half cycles individually.

3. Using special image processing software, motion-analysis functions such as velocity and angular acceleration can be computed easily. It is suggested to use such software, which should also be compatible with the camera file (i.e. Photron Motion Tools TM). This allows for automatic tracking of the motion of any point within a recorded sequence. Using this method, the length velocity and discharge propagation pattern could be analyzed faster and with more precision, which could help to improve the existing dynamic models.
4. Adding a mirror in the view field of the camera, which makes it possible to observe the discharge from additional views, is also suggested. Using this method, it is possible to track the discharge propagation in three dimensions, which yields the correct value of discharge length.

REFERENCES

[1] Hydro-Québec Committee of Experts, "January 1998 ice storm", *Report for Hydro-Québec*, 1998.

[2] Joseph J. Barsugli, Jeffrey S. Whitaker, Andrew F. Loughe, Prashant D. Sardeshmukh, Zoltan Toth, "The Effect of the 1997/98 El Niño on Individual Large-Scale Weather Events", *Bulletin of the American Meteorological Society*, Volume 80, Issue 7, July 1999, pp. 1399-1411

[3] M. Farzaneh, "Ice accretion on high voltage conductors and insulators and related phenomena", *Phil. Trans. of the Royal Soc.*, vol. 358, No. 1776, pp. 2971-3005, 2000

[4] CIGRE Task Force 33.04.09, "Influence of ice and snow on the flashover performance of outdoor insulators, part I: Effects of Ice", *Electra*, No. 187, pp. 91-111, Dec. 1999.

[5] M. Farzaneh, *Atmospheric Icing of Power Networks*, Springer, Berlin, ISBN 9781402085307, August 2008, 381 p.

[6] Jones, K.F., "The Effect of Horizontal and Torsional Coupling on Vertical Galloping". 6th International Workshop on Atmospheric Icing on Structures, Budapest, Hungary 1993, 143-1 48

[7] Kiessling, F. and Ruhanau J. "Ice Loads on Overhead Power Lines in Germany and their Impact on Reliability and Design", 6th International Workshop on Atmospheric Icing on Structures, Budapest, Hungary, 1993, 127-132

[8] M. Kawai, "AC flashover tests at project UHV on ice- coated insulators", *IEEE Transactions on Power Apparatus and Systems*, Nov. 1970, Volume: PAS-89 , Issue 8, pp. 1800 - 1804

[9] O. T. Melo, Y.T. Tam and M. Farzaneh, "Freezing rain and fog events in southern Ontario: properties and effect on EHV transmission systems", Proc 4th Int. Wksp. Atm. Icing of Struct., IWAIS (Paris) pp 70-75, 1988

[10] A. Boyer and J. Meale, "Insulator flashovers under icing conditions on the Ontario Hydro 500 kV transmission lines system", CEA, Spring Meeting, Montreal, Canada, 1988

[11] A. Meier and W. M. Niggli, "The influence of snow and ice deposits on supertension transmission line insulator strings with special reference to high altitude operation" IEEE Conf Publ 44 London, 1968, pp 386-395

[12] S. M. Fikke, "Possible Effects of Contaminated Ice on Insulator Strength" Proc 5th Int. Wksp. Atmos. Icing of Struct., IWAIS (Tokyo) 1990, Paper No B4-2 pp 1-4

[13] F. Su and S. Hu, "Icing on overhead transmission lines in cold mountainous district of southwest China and its protection", Proc. 4th Int. Wksp. Atm. Icing of Struct., IWAIS (Paris) 1988, pp 354-357

[14] Makkonen H, Komuro H, and Takasu K, "Withstand voltage characteristics of insulator string covered with snow and ice" *IEEE Transactions on Power Delivery*, Jul 1991, Vol. 6 , Issue 3, pp 1243- 1250

[15] M. M. Khalifa, R. M. Morris, "Performance of Line Insulators under Rime Ice", *IEEE Transactions on Power Apparatus and Systems*, June 1967, Volume: PAS-86, Issue: 6, pp. 692 – 698

[16] W. A. Chisholm and J. Kuffel, "Performance of insulation coating under contamination and icing conditions", CEA, Spring Meeting (Vancouver), 1995

[17] M. Farzaneh, J. F. Drapeau, "AC Flashover Performance of Insulators Covered with Artificial Ice", *IEEE Transactions on Power Delivery*, Vol.10, No. 2, pp. 1038–1051, April 1995

[18] M. Farzaneh, J. Kiernicki, "Flashover problems caused by ice build-up on insulators" *IEEE Electrical Insulation Magazine*, Vol. 11, No. 4, pp. 5–17, 1995

[19] M. Farzaneh, I. Fofana, "Experimental study and analysis of corona discharge parameters on an ice surface", *Journal of Physics D: Applied Physics*, Volume 37, Number 5, pp. 721-729, March 2004

[20] IEEE standard 1783, M. Farzaneh (Chair), "Guide for Test Methods and Procedures to Evaluate the Electrical Performance of Insulators in Freezing Conditions"

[21] I. Fofana and M. Farzaneh, "Application of Dynamic Model to Flashover of Ice-Covered Insulators", I*EEE Transactions on Dielectrics and Electrical Insulation*, Special Issue on Ice-Covered Insulators, vol. 14, no. 6, December 2007, pp. 1410-1417

[22] M. Farzaneh and J. Zhang, "A Multi-Arc Model for Predicting AC Critical Flashover Voltage of Ice-Covered Insulators". *IEEE Transactions on Dielectrics and Electrical Insulation*, Special Issue on Ice-Covered Insulators, vol. 14, no. 6, December 2007, pp. 1401-1409

[23] J. Farzaneh-Dehkordi, J. Zhang and M. Farzaneh, "Experimental study mathematical modelling of flashover on extra-high voltage insulators covered with ice", *Hydrological Processes*, Vol. 18, 2004, pp. 3471-3480.

[24] M. Farzaneh, I. Fofana, C. Tavakoli and X. Chen, "Dynamic Modeling of DC Arc Discharge on Ice Surfaces", *IEEE Transactions on Dielectrics and Electrical Insulation*, Vol. 10, June 2003, pp. 463-474.

[25] S. Brettschneider, M. Farzaneh and K.D. Srivastava, "Nanoseconds Streak Photography of Discharge Initiation on Ice Surfaces", *IEEE Transactions on Dielectrics and Electrical Insulation*, Vol. 11, June 2004, pp. 450-460.

[26] I. Ndiaye, M. Farzaneh and I. Fofana, "Study of the Development of Positive Streamers Along an Ice Surface", *IEEE Transactions on Dielectrics and Electrical Insulation*, Special Issue on Ice-Covered Insulators, vol. 14, no. 6, December 2007, pp. 1436-1445

[27] D. Yu, M. Farzaneh, J. Zhang, L. Shu, W. Sima and C. Sun, "Effects of Space Charge on the Discharge Process in an Icicle/Iced-Plate Electrode System under Positive DC Voltage", *IEEE Transactions on Dielectrics and Electrical Insulation*, Special Issue on Ice-Covered Insulators, vol. 14, no. 6, December 2007, pp. 1427-1435

[28] D. A. Swift, "Flashover across the surface of an electrolyte: arresting arc propagation with narrow metal strips", *IEE Proc.*, Vol. 127, No. 8, November 1980.

[29] C. Volat and M. Farzaneh, "3D Modeling of Potential and Electric Field Distributions along an EHV Ceramic Post Insulator Covered with Ice. Part I: Effects of Air Gaps and Partial Arcs", *IEEE Transactions on Power Delivery*, vol.20, July 2005, pp. 2006-2013.

[30] M. Farzaneh and W.A. Chisholm, *Insulators for icing and polluted environments*, IEEE Press series on Power Engineering, IEEE/John Wiley, New York, ISBN 9780470282342, 680 p, October 2009

[31] N. Sugawara and M. Farzaneh, "On the Role of Water Film in the Mechanism of Flashover of Iced Insulator", Proceedings of IEEE Int. Symp. On Electrical Insulation, Washington, DC, June 1986

[32] K. Kannus, *Aspects of the electrical performance of high voltage insulators and metal oxide surge arresters under various environmental stresses*, Ph.D. Thesis, Tampere University of Technology 1998; Tampere, Finland.

[33] C. Volat , *Calcul de la distribution du potentiel du champ électrique le long des surfaces de glace recouvrant les isolateurs haute-tension et dans les intervalles d'air entre celles-ci*, Ph.D. Thesis, UQAC, 2002.

[34] B. F. Hampton, "Flashover mechanism of polluted insulation", *Proc. IEE*, No.111, pp. 985–998, 1964

[35] F. Obenaus, "Fremdschichtüberschlag und Kriechweglänge," *Deutsche Elektrotechnik,* Vol. 4, pp. 135-136, 1958

[36] G. Neumarker, "Verschmutzungszustand und Kriechweg," *Monatsber. D. Deut. Akad, Wiss., Berlin,* Vol. 1, pp. 352-359, 1959

[37] R. Wilkins., A. A. J. Al-Baghdadi, ''Arc propagation along an. electrolyte surface'', *Proc. IEE*, Vol. 118, pp. 1886-1892, 1971

[38] D. C. Jolly, "Contamination Flashover, Part I: Theoretical Aspects" *IEEE Transactions on Power Apparatus and Systems* Volume: PAS-91, pp. 2437-2442, Dec 1972

[39] A. Rahal, C. Huraux, "Flashover mechanism of high voltage insulators", *IEEE Transactions on Power Apparatus and Systems* 98 (6), pp.2223–2231, 1979

[40] T S Sudarshan, R. Dougal, "Mechanisms of surface flashover along solid dielectrics in compressed gases: A review" *IEEE Trans. Electrical Insulation.* Vol. 21, No. 5, pp.727–746, Oct. 1986

[41] S. Li, *The Mechanism of the Flashover on a Polluted Dielectric Surface under AC Voltage*, Dissertation of Ph. D., Tsinghua University, 1988

[42] N.L. Allen "Streamer propagation along insulating surfaces". *IEEE transactions on dielectrics and electrical insulation*, Vol. 6, No. 3, pp. 357–362, June 1999

[43] P. Claverie, "Predetermination of the Behavior of Polluted Insulators", *IEEE Transactions on Power Apparatus and Systems,* Vol. PAS-90, No. 4 P. 1902-1908, July 1971

[44] Matsuo H., Fujishima T., Yamashita T., Takenouchi O., "Propagation velocity and photoemission intensity of a local discharge on an electrolytic surface" *IEEE Transactions on Dielectrics and Electrical Insulation*, Jun 1996, Volume: 3 Issue: 3, pp. 444 – 449

[45] P. Bruggeman, J. Van Slycken, J. Degroote, J. Vierendeels, P. Verleysen, C. Leys, "DC Electrical Breakdown in a Metal Pin–Water Electrode System", *IEEE Transactions on Plasma Science,* Aug. 2008, Volume: 36 Issue:4 , 1138 – 1139

[46] A. Boudjella, H. Hadi, M. Yumoto, T. Sakai, T. Hosokawa, "Investigation on discharge development phenomena on D.C. high voltage insulator of two grooves", 2000 Annual Report Conference on Electrical Insulation and Dielectric Phenomena, 15-18 Oct. 2000, Volume: 2, pp. 804 - 807 vol.2

[47] H. P. Mercure and M. G. Drouet, "Dynamic Measurements of the Current Distribution in the Foot of an Arc Propagating Along the Surface of an Electrotype", *IEEE Transactions on Power Apparatus and Systems*, March 1982, Volume: PAS-101, Issue: 3, pp. 725 – 736

[48] C. T. Phelps and R. F. Griffiths, "Dependence of positive corona streamer propagation on air pressure and water vapor content", *J. Appl. Phys.* 47 2929 (1976)

[49] T. Yamashita, H. Matsuo, H. Fujiyama, T.Oshige, "Relationship between Photo-Emission and Propagation Velocity of Local Discharge on Electrolytic Surfaces", *IEEE Transactions on Electrical Insulation*, Dec. 1987, Volume: EI-22, Issue: 6, pp. 811 – 817

[50] T. Matsumoto, M. Ishii, T. Kawamura, "Optoelectronic Measurement of Partial Arcs on a Contaminated Surface", *IEEE Transactions on Electrical Insulation*, Dec. 1984, Volume: EI-19, Issue: 6, pp. 543 – 549

[51] F. D. A. Boylett and I. G. Maclean, "The Propagation of Electric Discharges Across the Surface of an Electrolyte", *Proceedings of the Royal Society of London. Series A, Mathematical and Physical Sciences*, Vol. 324, No. 1559 (Sep. 21, 1971), pp. 469-489

[52] D. C. Jolly and C. D. Poole "Flashover of Contaminated Insulators with Cylindrical Symmetry under DC Conditions", *IEEE Transactions on Electrical Insulation*, April 1979, Volume: EI-14, Issue: 2, pp. 77 – 84

[53] A. Rumeli, "Flashover along a water column" *IEEE Transactions on Electrical Insulation*, Vol, EI-11, No.4, December 1976 pp 115-120

[54] S. Flazi, A. Ouis, N. Boukhennoufa, "Resistance of pollution in equivalent electric circuit of flashover" *Generation, Transmission & Distribution, IET*, January 2007 Volume: 1 Issue: 1 pp. 183 – 188

[55] R. W. Flugum, A. J. Karcic, "Effect of Configuration on Contaminated Insulator String Performance", *IEEE Transactions on Power Apparatus and Systems*, Jan. 1972 Volume: PAS-91 Issue: 1, pp 336 – 344

[56] J. Johnson, R. T. Henderson, W.S. Price, D.E. Hedman, F. J. Turner, "Field and Laboratory Tests of Contaminated Insulators for the Design of the State Electricity Commission of Victoria's 500-kY System" *IEEE Transactions on Power Apparatus and Systems*, May 1968, Volume: PAS-87, Issue: 5, pp. 1216 – 1239

[57] M. Wien, "Über eine Abweichung vom Ohmschen Gesetze bei Elektrolyten", *Ann. Physik*, 1927, Volume 388 Issue 11, Pages 327 - 361

[58] Lars Onsager, Shoon Kyung Kim, "Wien Effect in Simple Strong Electrolytes", *J. Phys. Chem.*, 1957, 61 (2), pp 198–215

[59] Lars Onsager, "Deviations from Ohm's Law in Weak Electrolytes", *J. Chem. Phys.* 2, 599 (1934)

[60] T. Cserfalvi and P. Mezei , "Operating mechanism of the electrolyte cathode atmospheric glow discharge", *Fresenius J Anal Chem* (1996) 355 : 813–819, Springer-Verlag 1996

[61] A. I. Maksimov, V. A. Titov and A. V. Khlyustova "Electrolyte-as-Cathode Glow Discharge Emission and the Processes of Solution-to-Plasma Transport of Neutral and Charged Species", *High Energy Chemistry*, Volume 38, Number 3 / May, 2004, 196-199

[62] Park Yang, S., Ku Soo, H., Houng Sung, H., Kim Hyo, J., and Piepmeier, E.H., "Fundamental studies of electrolyte-as-cathode glow discharge-atomic emission spectrometry for the determination of trace metals in flowing water", *Spectrochimica Acta Part B: Atomic Spectroscopy,* Volume 53, August 1998, Pages 1167-1179

[63] Kutepov, A.M., Zakharov, A.G., and Maksimov, A.I., "Problems and Perspectives of Investigations of Plasma Activated Technological Processes", Dokl. Akad. Nauk, 1997, vol. 357, no. 6, p. 782

[64] P. Mezei, T. Cserfalvi, M. Janossy, "Pressure dependence of the atmospheric electrolyte cathode glow discharge spectrum", *J. Anal. At. Spectrom.* 12 (1997) 1203

[65] M. Farzaneh, Y. Li and J. Zhang, "Effect of high altitude on dc flashover process on an ice surface", *Int. J. of Offshore and Polar Eng.*, 2001, 11-4 304-09

[66] C. Sun, X. Jiang, S. Xie, L. Shu and W. Sima, "Ice flashover performance and process on three types of EHV DC insulators at low pressure" Proc. of 14th Int. Offshore and Polar Eng. Conf. ISOPE (Toulon), 2004, pp 933-937

[67] M. Farzaneh, S. Y. Li and K. D. Srivastava, "Flashover on ice surfaces", *Atmospheric Research* 46-1, 1998, 37-47

[68] Li P, Fan J, Li W, Su Z and Zhou J, "Flashover performance of HVDC iced insulator strings *IEEE Trans. on Diele. and Elec. Insul.* 14-6, 2007, 1334-38

[69] Zhang J, Shu L, Sun C and Gu L 1991, "DC flashover performance of iced insulators under pressure and pollution conditions", Proc. of the 3rd Int. Conf. on Properties and Applications of Dielectric Materials 2, pp 957-960

[70] M. Farzaneh, J. Zhang and X. Chen, "DC characteristics of local arc on ice surfaces", *Atmospheric Research*, Volume 46, Issues 1-2, April 1998, Pages 49-56

[71] M. Farzaneh and J. Zhang J "Modeling of dc arc discharge on ice surfaces" IEE Proc. Generation, Trans. and Distr., 2000, 147-2 81-86

[72] Yang Q, Sima W, Sun C, Shu L and Hu Q 2007 "Modeling of dc flashover on ice-covered HV insulators based on dynamic electric field analysis", *IEEE Trans. on Diele. and Elec. Insul.* 14-6 1418-1426

[73] Sima W, Feng J, Yu D, Zhang J, Yang Q, Lai X and Farzaneh M 2006 "DC corona discharge test and measurement in an icicle to iced-plate air gas system" High Voltage Eng. 32, no 5 pp 1-3,34

[74] Harada T, Aihara Y and Aoshima Y "Influence of Humidity on Lightning and Switching Impulse Flashover Voltages" *IEEE Transactions on Power Apparatus and Systems*, 1971 Vol. PAS-90, Issue: 4, pp. 1433-1442

[75] Kuffel E, "Electron attachment coefficient in Oxygen, Dry air, Humid Air and Water Vapour" Proc. Phys. Soc. 74 (1959), pp. 297-308

[76] Zheng J C, Wang Z and Liu Y W, "Influence of humidity on flashover in air in the presence of dielectric surfaces" TENCON '93. Proceeding of IEEE Region 10 Conference on Computer, Communication, Control and Power Engineering.1993 Oct vol.5 pp. 443-449

[77] Les Renardières Group, "Positive discharges in long air gaps at Les Renardières" – 1975 results and conclusions. *Electra* 53 (1977)

[78] Busch W, "Air Humidity: An Important Factor for UHV Design" *IEEE Transactions on Power Apparatus and Systems*, 1978, Vol. PAS-97, Issue: 6, pp. 2086-2093

[79] Krile J T, Neuber A A, Dickens J C and Krompholz H G, "DC flashover of a dielectric surface in atmospheric conditions", *IEEE Transactions on Plasma Science*, 2004 Vol. 32, Issue: 5, Part 1, pp. 1828 – 1834

[80] N. L. Allen, "Corona, breakdown and humidity in the rod-plane gap", IEE Proceedings Physical Science, Measurement and Instrumentation, Management and Education, Reviews, November 1986, Volume 133, Issue: 8, pp.562 – 568

[81] F. A. M. Rizk, "Influence of rain on switching impulse sparkover voltage of large-electrode air gaps", *IEEE Transactions on Power Apparatus and Systems*, Volume: 95, Issue: 4, Part: 1, 1976, pp. 1394 – 1402

[82] C. Tavakoli, *Dynamic Modeling of AC Arc Development on Ice Surfaces*, Ph.D. Thesis, UQAC, 2004

[83] M. Farzaneh, J. Zhang, X. Chen, "Modeling of the AC Discharge on Ice Surfaces", *IEEE Trans. on Power Delivery,* 1997, vol 12(1), pp. 325–338

[84] M. Farzaneh, J. Zhang and X. Chen, "DC characteristics of local arc on ice surfaces", *Atmospheric Research*, Volume 46, Issues 1-2, April 1998, Pages 49-56

[85] J. Zhang and M. Farzaneh, "Propagation of AC and DC Arcs on Ice Surfaces", *IEEE Transactions on Dielectrics and Electrical Insulation,* Vol. 7, No. 2, April 2000, pp. 269-276

[86] S. Brettschneider, *Contribution to study of visible discharge initiation and development on the ice surface*, Ph.D. Thesis, UQAC, 2000

[87] I. Ndiaye *Approche physique du développement de streamers positifs sur une surface de glace*, Ph.D. Thesis, UQAC, October 2007

[88] P. Bruggeman and C. Leys, "Non-thermal plasmas in and in contact with liquids", *Journal of Physics D: Applied Physics*, 2009, Volume 42, Number 5, doi: 10.1088/0022-3727/42/5/053001

[89] M. Farzaneh, *Atmospheric Icing of Power Networks*, Springer, 2008 chapter 7, pp. 269-325

[90] C.L. Phan, M. Hara, "Leakage current and flashover performance of iced insulators", *IEEE Transactions on Power Apparatus and Systems*, Vol.: PAS-98, Issue: 3, pp. 849-859, May 1979.

[91] F.A.M. Rizk, "Mathematical models for pollution flashover" *Electra,* Vol. 78, 1981, pp.71-103

[92] R. Wilkins, "Flashover Voltage of High Voltage Insulators with Uniform Surface Pollution Films", *Proc. of IEE,* Vol. 116, No. 3, pp. 457-465, 1969

[93] A.D. Stokes, W.T. Oppenlander, "Electric arcs in open air", *Journal of Physics D: Applied Physics*, Volume 24, Issue 1, pp. 26-35, 1991.

[94] F.D.A. Boylett, "Electric discharges on water surfaces", *Electronics Letters,* Volume: 5, Issue: 3, pp. 47-48, February 6 1969.

[95] Yamashita T, Matsuo H, Okuno Y, Oshige T 1990 Current density at the local discharge tip on an electrolytic surface *IEEE Trans. on Electr. Insul.* **25** Issue 6 pp 1104-1110

[96] Ishii M and Ohashi H 1988 Polarity effect in DC withstand voltages of contaminated surfaces *IEEE Trans. on Electr. Insul.* **23** Issue 6 pp 1033-1042

[97] D. F. Peelo, *Current interruption using high voltage air-break disconnectors*, Ph.D. Dissertation, Technische Universiteit Eindhoven, 2004

[98] Les Renardières Group, "Research on long air gap discharges at Les. Renardières 1973 results," *Electra*, no. 35, pp. 49–156, Jul. 1974.

[99] V. M. Shmelev and A. D. Margolin, "Propagation of an Electric Discharge over the Surface of Water and Semiconductor", *High temperature Journal*, 2003, vol. 41, no6, pp. 735-741

[100] E.M. Bazelyan and P.Y. Raizer, *Spark Discharge*, CRC Press, New York 1998

[101] Maruvada PS 2000 *Corona Performance of High-Voltage Transmission Lines* Research Studies Press Ltd London

[102] J.J. Lowke, "Simple theory of free-burning arcs", *J. Phys. D: Appl. Phys.* 12, pp. 1873-1886, 1979.

[103] Nekahi A, Farzaneh M, Mirzaei B and Kumar S 2009 "Time-resolved spectroscopic observation of surface flashover across an ice surface", Proc. of IEEE Conf. on Electr. Insul. and Diele. Phenomena CEIDP Virginia Beach

[104] A. Fridman, *Plasma Chemistry*, Cambridge University Press, New York, 2008

[105] K. Khanafer and K. Vafai, *Gas Transport in Porous Media*, Chapter 10, Natural Convection Gas Transport in Porous Media, pp.170-200, Springer Netherlands, 2006.

[106] R. W. Johnson, *The handbook of fluid dynamics*, pp.1522-1525, CRC Press, 1998

[107] Arora R and Mosch W 1995, *High Voltage Insulation Engineering: Behaviour of Dielectrics, Their Properties and Applications,* New Delhi New Age International Publishers Wiley Eastern

[108] Les Renardières Group 1981, "Negative discharges on long air gaps at Les Renardières", *Electra* **74** pp 67–216

[109] Y. Sabri, *Static modelling of AC flashover on contaminated insulators covered with ice using intelligent identification methods*, Ph.D. thesis, UQAC, December 2009